INVESTIGATION OF MARGINAL EXPLOSIBILITY OF ORGANIC DUSTS IN THE 20-L AND 1-m^3 EXPLOSION CHAMBERS

by

Albert Addo

Submitted in partial fulfilment of the requirements
for the degree of Master of Applied Science

at

Dalhousie University
Halifax, Nova Scotia
August 2018

DEDICATION

This thesis is dedicated to the loving memory of my late father, Emmanuel Kwaku Addo, my late sister Mrs. Franklina Afi Amponsah (whose demise occurred during the period of writing), my mother Mrs. Peace Akua Addo and my entire family back in Ghana.

Table of Contents

List of Tables

List of Figures

Abstract

Experimental investigation of a category of combustible dusts known as *marginally explosible* was conducted. While these dusts explode in smaller test apparatus, their explosibility in the intermediate test apparatus is not certain. These dusts have been defined based on a K_{St} value ≤ 45 bar·m/s. The question then is, whether these dusts would explode on the industrial scale or not. The materials tested were niacin, lycopodium, and polyethylene, all of which are well-known to be combustible. The concept of marginal explosibility was incorporated by testing fine and coarse fractions of polyethylene. Experiments were conducted in accordance with ASTM methodologies using calibrated standard equipment: (i) Siwek 20-L and 1-m^3 explosion chambers for determination of maximum explosion pressure (P_{max}), volume-normalized maximum rate of pressure rise (K_{St}), and minimum explosible concentration (MEC), (ii) MIKE-3 apparatus for determination of minimum ignition energy (MIE), and (iii) BAM oven for determination of minimum ignition temperature (MIT). The explosion data followed known trends, and P_{max}, K_{St} and MEC values compared well in the different size vessels. P_{max} was in the approximate range of 7 – 8 bar(g) for both chambers used; K_{St} values were in the approximate range of 80 – 230 bar·m/s for the 20-L chamber and 100 – 250 bar·m/s for the 1-m^3 chamber. The only exception to this conclusion was for the coarse polyethylene. This sample could not be classified as marginally explosible despite its low K_{St} (23 bar·m/s) in the 20-L, and being relatively insensitive to spark ignition as indicated by MIE values in the MIKE-3 apparatus. It was clearly explosible as confirmed by its K_{St} value (72 bar·m/s) in the 1-m^3 chamber, and measurable values of MEC (< 100 g/m^3), and MIT (420 °C). Thus, it was concluded that basing the definition of marginal explosibility on a K_{St} value from the 20-L may not be entirely accurate and that the explosibility behaviour differ from material to material.

For dust explosion testing facilities, it is important to continuously adhere to the recommendations by the ASTM standards when the 20-L results are in doubt, and strongly recommend testing in the 1-m^3 chamber.

List of Abbreviations and Symbols Used

BET	Brunauer-Emmett-Teller
CSB	U.S. Chemical Safety Board
CFD	Computational Fluid Dynamics
CRD	Collaboratives Research Development
Coarse PE	Coarse Polyethylene
FAI	Fauske and Associates Inc.
Fine PE	Fine Polyethylene
HOC	Heat of Combustion
IE	Ignition Energy
ISO	International Organization for Standardization
LOC	Limiting Oxygen Concentration
MAP	Monoammonium Phosphate
MEC	Minimum Explosible Concentration
MIE	Minimum Ignition Energy
MIT	Minimum Ignition Temperature
NFPA	National Fire Protection Association
PC	Personal Computer
PE	Polyethylene
SBC	Sodium Bicarbonate
SEM	Scanning Electron Microscopy
SSA	Specific Surface Area
TGA	Thermogravimetric Analysis
UHMWPE	Ultra-High Molecular Weight Polyethylene

VCE	Vapour Cloud Explosion

Symbols	**Representation**	**Units**
P_{max}	maximum explosion pressure of material	bar(g)
P_m	explosion pressure of a single concentration test	bar(g)
$(dP/dt)_m$	maximum rate of pressure rise for single test	bar/s
$(dP/dt)_{max}$	maximum rate of pressure rise for sample	bar/s
V	volume of explosion chamber vessel	m^3
$(dP/dt)_m.V^{1/3}$	size-normalized maximum rate of pressure rise for single test	bar·m/s
K_{St}	size-normalised maximum rate of pressure rise for sample	bar·m/s
P_s	particle size	μm
A	surface area	m^2
ρ	density	g/cm^3
E_s	statistic energy	mJ
E_{ign}	ignition energy	mJ
$E_{critical}$	critical ignition energy	mJ
δ	minimum flame thickness	m
V_{sc}	scoop or spatula volume	ml
m_T	total mass	g
m_s	mass of sample	g

Acknowledgement

First and foremost, I would like to express my sincere appreciation to my supervisor, Prof. Paul R. Amyotte, my master's committee and the entire CRD Project Team for their contribution, invaluable advice, constructive ideas, insightful discussion, and encouragement throughout this Master thesis. Their insights and guidance have been very useful indeed. I must say, it has been an excellent learning process and a great experience working in the research team.

I further gratefully acknowledge the financial contributions from (i) the Natural Sciences and Engineering Research Council of Canada (NSERC) in the form of a Collaborative Research & Development (CRD) Grant, (ii) Fauske & Associates, LLC, (iii) Fike Corporation, and (iv) PLC Fire Safety Solutions. I also gratefully acknowledge (i) Fauske for access to their 1-m^3 explosion chamber and the availability of personnel for testing purposes, and (ii) Jensen Hughes Canada for provision of material characterization data.

Humble thanks to my friend and brother, Dr. Ing. Emmanuel Kwasi Addai for his inspiration and encouragement given me throughout the course of this thesis. I will also like to express my sincere appreciation to all colleagues, friends and well-wishers whose expertise, resources, advice and efforts aided me to put together this work. Last but not least, my special appreciation goes to Miss. Georgina Ackah for her motivational support and endless caring throughout the years. Thank you very much.

CHAPTER 1: INTRODUCTION

Dust explosions have occurred in many process industries that handle, use, process, transport, or manufacture combustible dusts. These occurrences have caused and continue to cause harm to people, damage to equipment and buildings, and economic loss from process downtime and the ensuing interruption in business activities. As a result, several researchers have conducted studies throughout the world, including Canadian researchers with the aim of understanding in detail the mechanism or dynamics of this type of explosion, and preventing their occurrence and mitigating the consequences in situations where prevention is not possible.

Though the first dust explosion was reported in a Turin bakery in 1785, the study of dust explosions and their causes was initiated over a century ago, by John Hodgson in 1820 in the Felling coal-mine disaster, Britain [1]. In 1884, the Prussian Fire-Damp Commission in Prussia, Germany, also conducted a series of experiments with coal dust and coal dust with gas to determine their explosibility [2]. Since then, several studies have been conducted in this field. However, despite the extensive research and technological advancement in identification of combustible dust hazards, assessment as well as preventive and protective measures and strategies, the dust explosion problem still persists.

In recent years, the attention of combustible dust handling facilities and researchers in the dust explosion testing community has been directed to a particular class of dust referred to as “marginally explosible dusts”. These dusts present a distinct challenge to the community in the sense that whereas they explode or appear to explode in the laboratory-scale 20-L explosion vessel, they do not explode in the intermediate-scale 1-m^3 explosion chamber (which is considered as the standard chamber for testing dusts to determine whether they are explosible or not). Recent work by other researchers has also demonstrated that for some materials, the reverse occurs – i.e., values of explosion parameters are higher in a 1-m^3 chamber than one with a volume of 20 L. Uncertainties can therefore arise in the design of dust explosion risk reduction measures. However, one thing that is certain is that this class of dusts presents a flash fire hazard. Comprehensive investigation of this

uncertainty is therefore only possible by means of concurrent testing using well calibrated standard laboratory-scale equipment and specialized larger-scale test chambers.

1.1 Dust Explosion Incidents

A CSB (US Chemical Safety Board) report on combustible dust accidents in the United States found that from the year 1980 to 2005, 281 major accidents involving combustible dusts had been reported with 119 fatalities, 718 injuries and over hundreds of millions of US dollar losses in property damage [3]. Every year, an average of 10 dust explosion incidents were reported. The reports also found that the combustible dust accidents happened not only in chemical industries, but also in other industries such as food, metal and wood, as shown in Figure 1.1 [3].

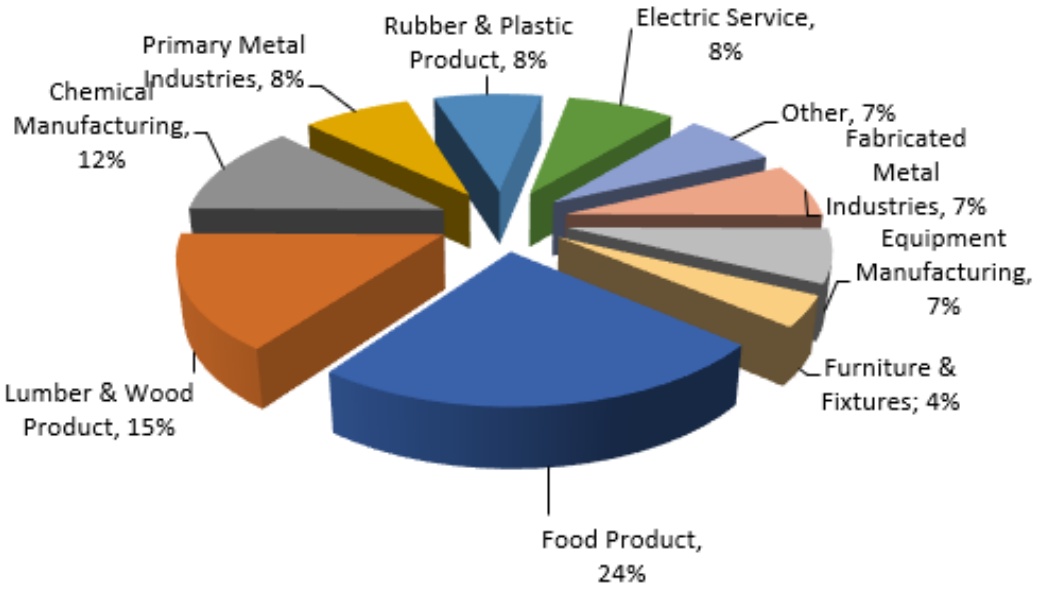

Figure 1.1: Distribution of combustible dust incidents by industry in USA [3].

Canada has also experienced its own share of dust explosions. Incidents such as the Westray Mine Explosion [4] on May 9, 1992 in Pictou, Nova Scotia, and its devastating outcomes such as the unfortunate loss of 26 mine workers and attendant effects on families and the community, the total collapse of the mine, and the enormous loss of investment, still remain on the minds of Canadians.

Table 1.1 shows some other combustible dust related incidents (flash fires and explosions) that occurred over the years. The occurrence of these incidents and many others has called for measures to prevent any recurrence, and heightened the interest of researchers in understanding the dynamics of the dust explosion problem.

Table 1.1: Some dust flash fires and explosions [5]

Date	**Facility**	**Fuel, Incident**	**Location**	**Loss**
September 14, 2016	Woodworks Facility	Wood dust, explosion	Abbotsford, British Columbia	Hopper Damaged
October 25, 2014	Veolia Environmental Services	Grain dust, explosion	Sarnia, Ontario	1 Fatality, 4 Injuries
April 24, 2012	Lakeland Sawmill	Sawdust, explosion	Prince George, British Columbia	2 Fatalities, 22 Injuries
January 20, 2012	Babine Forest Products	Sawdust, explosion	Burns Lake, British Columbia	2 Fatalities, 20 Injuries
May 27, 2011	Hoeganaes Corporation	$H_{2\,(g)}$ explosion, Iron dust, flash fire	Gallatin, Tennessee	3 Fatalities, 2 injuries [6]
March 29, 2011	Hoeganaes Corporation	Iron dust, flash fire	Gallatin, Tennessee	1 Injury [6]
January 21, 2011	Hoeganaes Corporation	Iron dust, flash fire	Gallatin, Tennessee	2 Fatalities [6]
January 29, 2003	West Pharmaceutical Services	Polyethylene dust, explosion	Kingston, North Carolina	6 Fatalities, 38 injuries, Facility Destroyed
October 3, 1975	Burrard Terminal Elevator	Grain dust, explosion	North Vancouver, British Columbia	5 Fatalities, Several Injuries, 8 Million Damages

1.2 Scope of Study

This research is an experimental campaign to identify and assess the hazards associated with a particular class of combustible dusts referred to as marginally explosible dusts. To achieve this, four organic dusts were selected for testing:

- Niacin
- Lycopodium
- Two different size fractions of ultra-high molecular weight polyethylene (UHMWPE) designated as:
    - Fine polyethylene (with size 40-48 μm according to supplier)
    - Coarse polyethylene (with size 125 μm according to supplier).

Two different testing scales (i.e., 20 L and 1 m^3) were employed to obtain data and make comparisons with the aim of achieving the research objectives (as stated in section 1.4). The study covered both explosion severity and likelihood parameters with their applicable apparatus.

1.3 Motivation for Current Research

Previous studies to investigate dusts considered to be marginally explosible have usually involved a lack of data on material characterization and information on how factors such as particle size distribution, moisture content and chemical composition affect the ignitability and explosibility of marginally explosible dusts. Thus, conclusions on what constitutes marginal explosibility have not been adequately investigated and validated. The literature also does not typically provide complete data sets on explosion likelihood parameters such as MIE, MIT and MEC for these materials.

This study focuses on investigating the potential for marginal explosibility of non-metallic dusts. Laboratory-scale testing of selected organic powders (niacin, lycopodium and polyethylene) was conducted at the Dust Explosion Laboratory of Dalhousie University located in Halifax, NS. These materials were also tested

using the 1-m^3 chamber at Fauske & Associates, LLC (Fauske) located in Burr Ridge, IL.

The behaviour of marginally explosible dusts needs thorough investigation to settle the ambiguity they present on the two test scales (20-L and 1-m^3). To do this, it is important to conduct extensive experiments to understand the underlying factors that come together to cause their explosibility. In addition, understanding of the explosibility parameters such as maximum explosion pressure (P_{max}), volume-normalised maximum rate of pressure rise (K_{St}), minimum explosible concentration (MEC), minimum ignition energy (MIE) and minimum ignition temperature (MIT) are essential for constituting prevention measures directed to the specific hazard (whether explosion or flash fire) posed by this class of dusts.

1.4 Objectives of Study

The objectives of this research are to:

- Develop and present comprehensive explosion data for inclusion in the dust explosion body of knowledge with full material characterization analyses.
- Determine whether the dusts selected will actually exhibit marginal explosibility on both testing scales
- Compare the explosibility results obtained on both testing scales and discuss the effect and limitations of scaling results from the 20-L explosion chamber to the larger setting.
- Investigate whether these dusts show low ignitability (as indicate by MEC, MIE and MIT).
- Investigate any possible correlation between marginal explosibility (as indicated by P_{max} and K_{St}) and dust ignitability as indicated by MIE, MIT, and MEC.

1.5 Thesis Overview

This thesis consists of six chapters and eight appendices.

Chapter 1 provides basic information about industrial dust explosions. It also includes examples of dust flash fires and dust explosion incidents. The chapter covers the scope of research, motivation and main objectives of this study.

Chapter 2 presents a literature review of explosions, dust explosions and marginal explosibility and its characteristics. It describes the explosion pentagon and discusses in general the important dust characteristics and their influence on the likelihood and severity of dust explosions as well as the main parameters affecting dust explosibility. The chapter also briefly discusses the phenomenon of dust flash fire and its characteristics, and possible control measures. Finally, a discussion of measures to control dust explosion risk is provided.

Chapter 3 provides information on the materials tested, material characterizations performed, description of apparatus and the experimental procedures employed in the determination of each explosion severity (i.e., P_{max}, $(dP/dt)_{max}$ and K_{St}) and explosion likelihood (i.e., MEC, MIT, and MIT) parameter in this study.

Chapter 4 presents the graphical representation of all experimental results.

Chapter 5 discusses the inferences of the results and observations of the experimental work, presents graphical comparisons, draws possible correlations, and offers scientific explanations for these observations.

Chapter 6 provides the conclusions and recommendations for future work regarding the subject discussed in this thesis.

CHAPTER 2: LITERATURE REVIEW

This chapter presents a literature review of explosions, dust explosions and marginal explosibility and its characteristics. The chapter also discusses the phenomenon of dust flash fire and its characteristics, and possible control measures. Finally, a discussion of measures to control dust explosion risk is provided.

2.1 Overview of Explosions

An explosion can be defined as "an exothermic chemical or physical process that when occurring at constant volume, results in a sudden and significant pressure rise" [7]. In general, there are three main types of explosions, namely; physical explosions, chemical explosions and nuclear explosions as illustrated in Figure 2.1. However, chemical and physical explosions are more often encountered in the process industries [8].

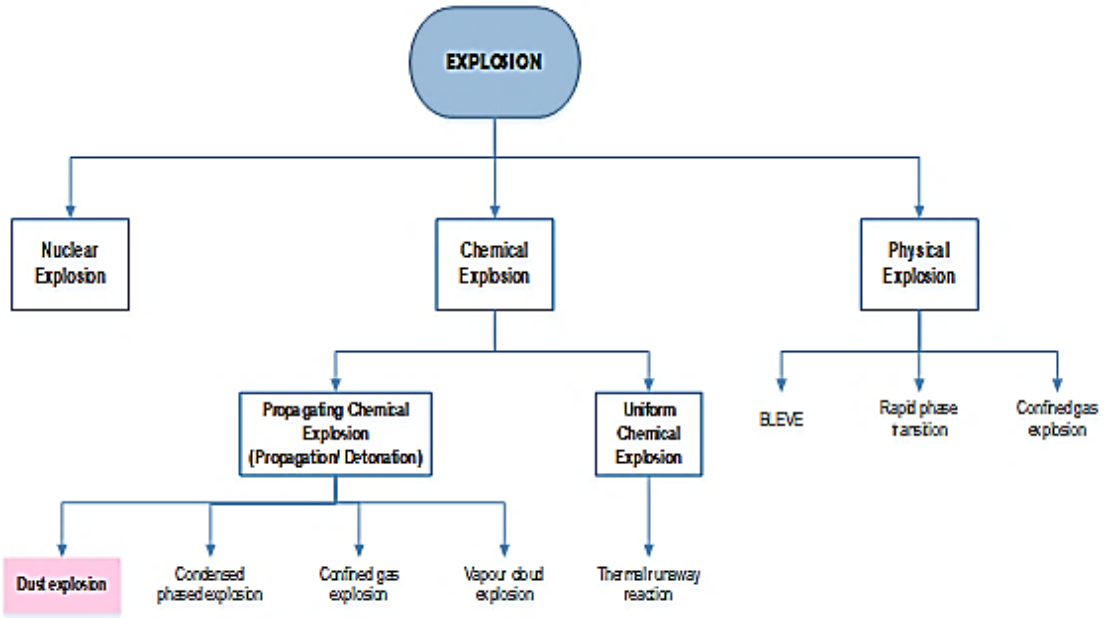

Figure 2.1: Types of explosions in general [8].

Physical explosions are those in which a high-pressure gas produces a physical reaction, that results in rupture of the container. These do not involve a chemical reaction. On the other hand, chemical explosions are usually associated with the

sudden generation and release of high pressure gas as a result of an exothermic chemical reaction. These reactions may include rapid combustion processes, decompositions or other rapid exothermic reactions. Chemical explosion reactions can occur in either the vapour, liquid or solid phases [9]. Propagating reactions are reactions that propagate spatially through a reaction mass, such as the combustion of a flammable vapour in a pipeline, a vapour cloud explosion or the decomposition of an unstable solid. In detonations, the reaction front moves at a speed equal to or faster than the speed of sound, whereas in deflagrations, it moves at a speed less than the speed of sound [10].

2.2 Dust Explosions

The National Fire Protection Association (NFPA) defined dust as a material 420 μm or less in diameter (capable of passing thorough a US No. 40 standard sieve) [11]. A combustible dust is defined as a combustible particulate solid that presents a flash fire or deflagration hazard when suspended in air or some other oxidizing medium over a range of concentrations, regardless of particle size or shape [12]. The materials that can cause dust explosion include [7]:

- Natural organic materials (grain, linen, starch, sugar, wood etc.);
- Synthetic organic materials (polymers, organic pigments, pesticides, etc.);
- Coal and peat;
- Metals (magnesium, aluminium, zinc, iron, etc.).

Dust explosions are exothermic combustion reactions and the heat of combustion determines the amount of heat that can be released in the explosion, and it is dependent on factors such as dust composition and the amount of oxygen consumed [7]. Fundamentally, with solid material as fuel, there are five requirements for an explosion to occur as shown in the explosion pentagon in Figure 2.2.

- Fuel – combustible solid (e.g. dust);
- Ignition source – examples: hot surface, sparks, naked flames, etc;
- Oxidant – typically oxygen in air;
- Confinement – to develop overpressure;
- Dispersion – mixing of the combustible dust in air to form a fuel-oxidant cloud.

Figure 2.2: Dust explosion pentagon [5].

In a dust-air mixture, the dust particles are strongly influenced by gravity; an essential pre-requisite for a dust explosion is therefore the formation of a dust/oxidant suspension. Once combustion of this mixture occurs, confinement (partial or complete) permits an overpressure to develop, thus enabling the transition of a fast burning flame to a dust explosion [13]. The explosion may result in a deflagration or detonation depending on the rate of reaction and resulting flame speed [14]. However, in the absence of confinement or a high enough dispersion of particles, only a flash fire may occur.

There are two important aspects of dust explosion parameters (each representing one risk component), namely: explosion likelihood (i.e., sensitivity) and explosion severity (i.e., consequence) as shown in Table 2.1 below. The explosion likelihood represents the ability of a fuel to cause an explosion, while the severity represents the ability of an airborne fuel mixture to propagate to result in a pressure rise after initiated by adequate ignition sources. The current study is focused on both the likelihood and severity characteristics of the dust materials, such as P_{max}, $(dP/dt)_{max}$, K_{St}, MEC, MIE and MIT.

Table 2.1: Important dust explosibility parameter [13] [15].

Explosion Parameters	**Typical units**	**Description**	**Risk Component Addressed**	**Examples of industrial applications**
P_{max}	bar (g)	Maximum explosion pressure in constant-volume explosion	Consequence severity	Isolation, partial inerting, pressure-resistant design
$(dP/dt)_{max}$	bar/s	Maximum rate of pressure rise in constant-volume explosion	Consequence severity	Venting, suppression
K_{St}	bar·m/s	Volume-normalised maximum rate of pressure rise	Consequence severity	Venting, suppression
MEC	g/m^3	Minimum explosible concentration of dust	Likelihood of occurrence	Control of fuel concentrations
LEL	Vol %	Lower explosion limits of gas or vapor	Likelihood of occurrence	Control of fuel concentrations
MIE	mJ	Minimum ignition energy of dust cloud (electric spark)	Likelihood of occurrence	Removal of ignition sources, grounding and bonding
MIT	°C	Minimum ignition temperature	Likelihood of occurrence	Control of process and surface temperatures
LOC	Vol%	Minimum (or limiting) oxygen concentration in the atmosphere for flame propagation.	Likelihood of occurrence	Inerting

2.3 Influence of Dust Properties on Ignitibility and Explosion Severity

Some properties that influence ignitibility and explosibility of dusts include but are not limited to the following [16]:

- Dust chemical composition
- Particle size and surface area
- Moisture content
- Oxygen concentration
- Initial pressure.

2.3.1 Chemical composition

Dust chemical composition (dust chemistry) influences both the thermodynamics and kinetics of dust explosions [7]. Thermodynamics relate to the amount of heat liberated during combustion, while the kinetics is the rate at which this heat is liberated [7]. As shown in Figure 2.3, metal dusts such as aluminium (Al) and magnesium (Mg) can generate higher maximum explosion pressures and higher maximum rates of pressure rise compared to organic materials, while other metals such as iron (Fe) and zinc (Zn) may produce lower P_{max} values than organics.

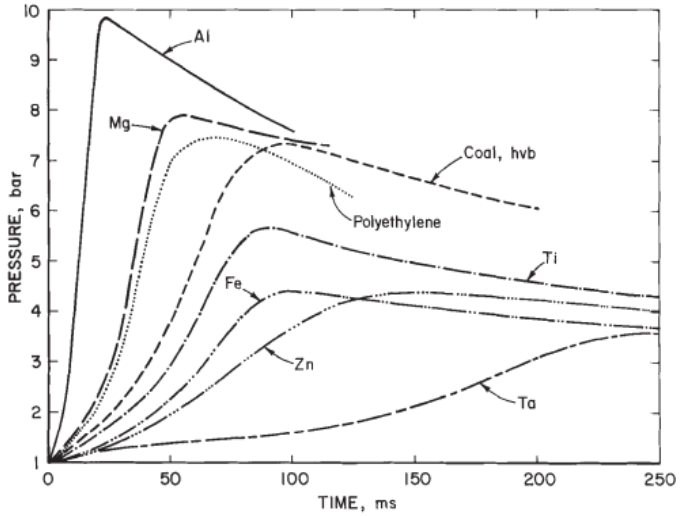

Figure 2.3: Explosion pressure for organic materials and metal dusts [16].

2.3.2 Particle size

Flame propagation in a dust cloud can occur in two different ways: (i) combustion of flammable gases emitted during pyrolysis or devolatilization of dust, or (ii) direct oxidation at the dust particle surface. In either case, the particle size of the sample plays an important role in the combustion process [17]. Abbasi and Abbasi [17] noted that finer dust particles provide higher surface area per mass, easily disperse in air, and stay airborne for a longer period. As shown in Figure 2.4, decreasing the particle size increases the surface area, thereby increasing the maximum rate of pressure rise.

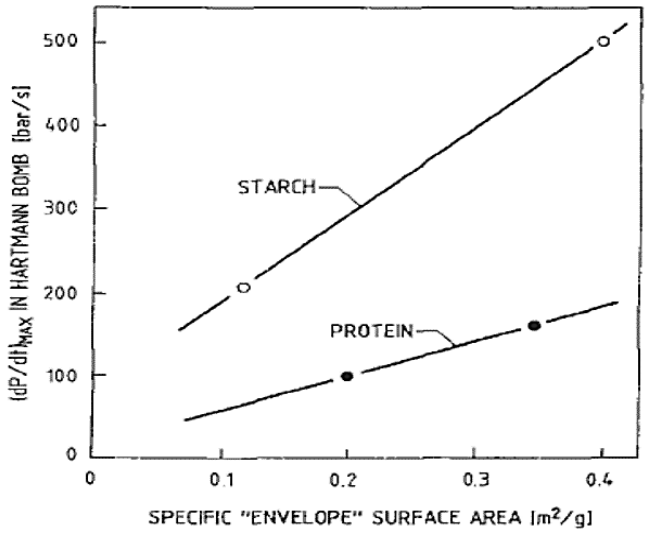

Figure 2.4: Influence of surface area on maximum rate of pressure rise [7].

However, the trend will not continue indefinitely as the particles get smaller. Eckhoff [7] explained that the limiting particle size, below which the combustion rate of the dust cloud cease to increase, depends on the ratios between the time constants of the three consecutive processes: devolatilization, gas-phase mixing and gas-phase combustion. The author further claims that particle size primarily influences the devolatilization rate. Hence, if gas-phase combustion is the rate determining step (slowest step) of the three, decreasing the particle size does not increase the overall combustion rate.

Mittal and Guha [18] conducted an experimental study on the MIT of polyethylene and found that the MIT is highly influenced by particle size at low dust concentrations. Thus, the MIT increases quite rapidly with an increase in particle size, whereas at high dust concentrations (such as 500 and 1000 g/m^3) the extent of the increase in the minimum ignition temperature was comparatively quite small as shown in Figure 2.5. The authors explain that at lower dust concentrations the finer particles volatize more rapidly, yielding an explosible volatile gaseous mixture at a concentration with high probability to ignite. On the contrary, at higher dust concentrations, the difference in the volatile yields for both smaller and larger particle sizes is not significant.

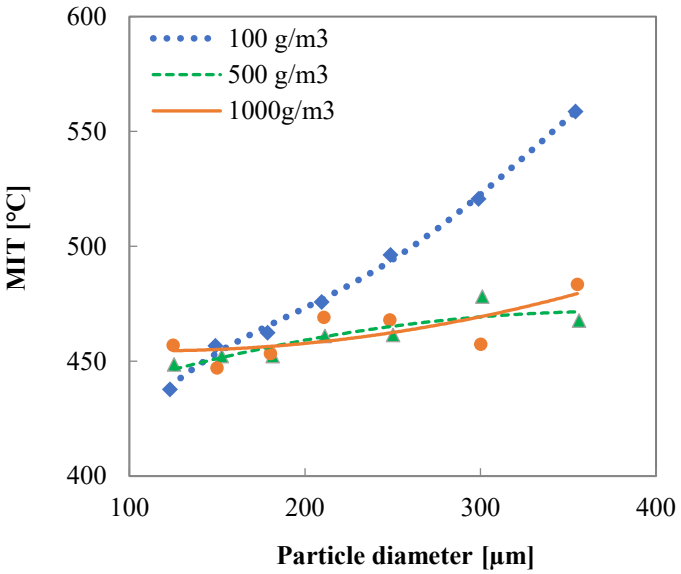

Figure 2.5: Influence of particle size diameter on MIT of polyethylene dust [18].

2.3.3 Moisture content

The presence of moisture in the dust reduces both the ignition sensitivity and explosion severity of the dust cloud. For instance, the minimum ignition temperature and minimum ignition energy of a dust cloud increases with increasing moisture content as illustrated in Figure 2.6 [7].

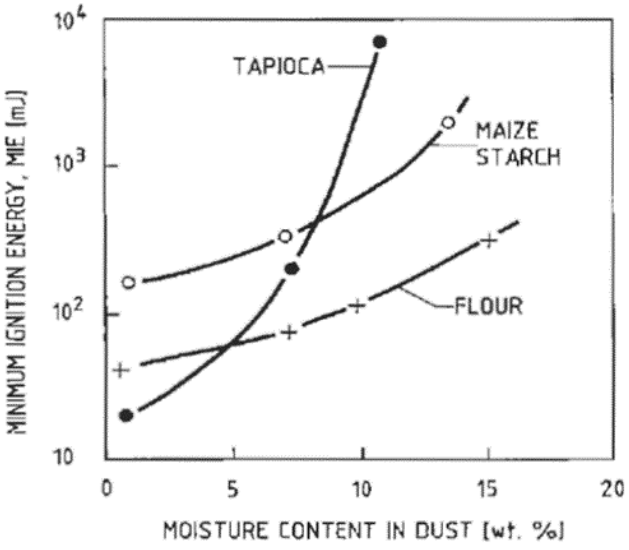

Figure 2.6: Influence of dust moisture content on dust MIE [7].

2.3.4 Oxygen content

The explosion violence and ignition sensitivity of dust clouds decrease with decreasing oxygen content of the gas in which the dust is suspended [7]. In addition, the influence of reducing the oxygen content becomes more significant with increasing particle size as shown in as shown in Figure 2.7.

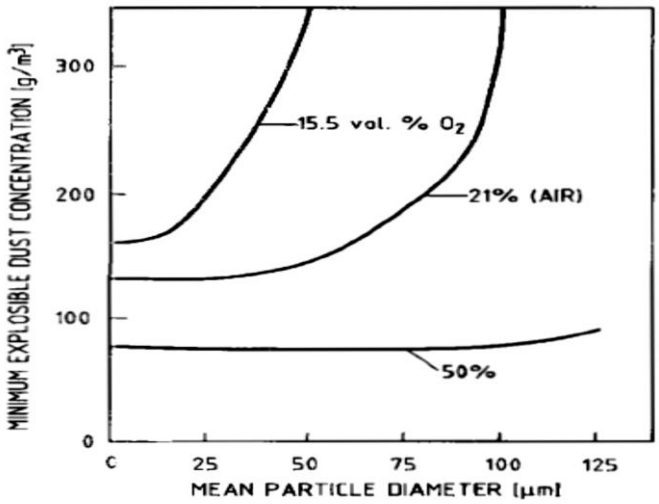

Figure 2.7: Influence of oxygen content on the MEC of coal dust [7].

2.3.5 Initial pressure

Increasing the initial pressure will increase the maximum explosion pressure and the maximum rate of pressure rise. However, Eckhoff noted that the initial pressure has no influence on the ratio of mass of the dust to mass of air (dust cloud concentration) that gives the most efficient combustion [7]. In addition, for the same initial pressure, reducing particle size results in more violent explosion as shown in Figure 2.8.

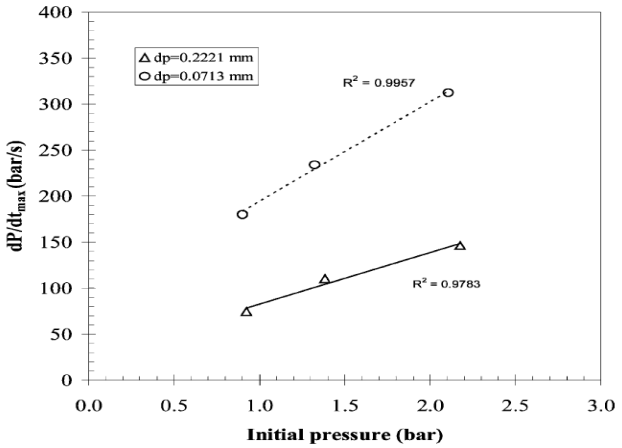

Figure 2.8: Influence of initial pressure on maximum rate of pressure rise on cork dust [19].

2.4 Dust Explosion Prevention and Mitigation

The prevention and mitigation (protection) measures of dust explosion are fashioned around the five basic components of the explosion pentagon and ensuring that they do not come together in a specific process. The principle is to eliminate or disable one or more elements to stop the explosion from occurring. The prevention measures are related to the total elimination (if possible) or reduction of the explosion likelihood occurrence, in which the aims are to avoid the conditions that allow the formation of dust explosion conditions and all the possible cause of ignition such as:

i. Elimination of dust deposits by cleaning of working environment.

ii. Elimination or reduction of oxidant (Inerting).

iii. Elimination of ignition source (avoid sparks, hot surface, mechanical or pneumatic elevator) etc.

The mitigation (protection) measures aim to reduce the consequence (or severity) of an explosion by:

- Containment of explosion: use of equipment suitably designed to withstand the maximum explosion overpressure potentially generated.

- Separation of equipment: installation of different process equipment at separate locations, or physical partition of the various operations with higher risks of explosion.

- Explosion suppression by using appropriate extinguishing substances: use of suppressants such as sodium bicarbonate (SBC), monoammonium phosphate (MAP), etc.

- Explosion venting: design of a suitably-sized relief panel or surface that raptures when an unacceptable pressure increase occurs. This method is more commonly used to mitigate dust explosions than inerting in the process industries [13]. The principle underlying vent systems is to prevent the generation of overpressures capable of causing an explosion from occurring in a closed vessel, by means of the rupture of a correctly sized disk.

2.5 Marginally Explosible Dusts

"Marginally explosible dusts" are primarily characterized by low values of explosion severity parameters P_{max} and K_{St}. These dusts present difficulties in the identification of hazards in industries that handle them. While they may be explosible using a standard laboratory-scale equipment and overpressure criterion, their explosibility in larger test chambers are not certain. Already, some studies have been conducted by researchers concerning this class of dusts to attempt to find a working definition within measurable contexts as well as provide explanations for their distinctive behaviour on both testing scales. This section reviews studies in the dust explosion literature related to these dusts.

For example, Palmer and Tonkin [20] tested phenol formaldehyde resin and magnesium oxide dusts, and their mixtures, in a vertical explosion tube and concluded that marginally explosible dusts have a comparatively narrow range of flammable concentrations, generate only moderate explosion pressures, and are unlikely to cause severe explosions. They also inferred that marginal dusts and their mixtures require a relatively high-energy ignition source in small-scale tests and will not propagate an explosion on a larger scale.

Proust et al. [21] conducted tests of 21 dusts (mostly organic) in both the 20-L explosion vessel and the intermediate-scale ISO 1-m^3 explosion chamber, using a 10-kJ ignition energy. The results from their experiments showed that a considerable number of dust samples (5 out of 21) exploded weakly in the 20-L sphere but did not explode at all in the ISO 1-m^3 explosion chamber. They also stated that dust samples having a volume-normalized maximum rate of pressure rise, K_{St}, of 45 bar·m/s or less in the standard 20-L vessel test might not explode in the 1-m^3 chamber and defined this value as the overdriving threshold in the 20-L sphere.

Rodgers and Ural [22] studied the explosion behaviour of various dust concentrations in the 20-L sphere using a single 2.5-kJ ignitor. They resolved that some dusts may well be considered as explosible when tested in the 20-L sphere with 2 × 5-kJ ignitors and with 1 × 2.5 kJ as per OSHA criteria, but at the same time do not fulfil the criteria of explosibility when tested in the larger 1-m^3 chamber. They further concluded that marginally explosible dusts could be defined as dusts that display weak K_{St} (< 50 bar·m/s) in the standard 20-L test with 1 × 2.5-kJ ignitors.

As more studies continue to be undertaken by researchers in the dust explosion community, some explanations have been given for the incongruities that characterize testing of marginally explosible dusts in the smaller 20-L chamber and the intermediate-scale 1-m^3 explosion chamber. Most of these studies have agreed in principle with respect to the potential effects of "preconditioning" which may be more profound when testing in the smaller chamber with a very strong ignition energy. Preconditioning occurs when the initial conditions of the system are altered significantly prior to flame propagation, with the more prominent effect being "overdriving". The phenomenon of overdriving is further attributed to differences in turbulence between the two chambers and pre-heating of the dust-air mixture by the ignitors in the 20-L vessel.

In their work, Cloney et al. [23] employed Computational Fluid Dynamics (CFD) to investigate the preconditioning aspect of ignitor overdriving in the 20-L and 1-m^3 dust explosion testing chambers and to quantify the fluid-particle state prior to flame propagation. They developed a 1-D spherical model which exhibited that preconditioning may significantly change the testing conditions in the 20-L chamber with polyethylene particles but may be negligible in the 1-m^3 vessel.

Kuai et al. [24] performed experimental studies of a typical metallic dust (magnesium) and non-metallic carbonaceous (sweet potato and bituminous coal) dusts in the 20-L vessel using ignition energies of 1, 2, 5, 7 and 10 kJ. The authors found that whereas weak or inadequate ignition energies would cause unrealistic explosion severity characteristics, overly strong ignitors would cause overestimated kinetic characteristics referred to as overdriving. They suggested that the most appropriate ignition energy (E_{ign}) in both thermodynamics and kinetic determinations is the "critical ignition energy" ($E_{critical}$), where the minimum flame thickness (δ) is attained. The $E_{critical}$ was found at the inflection point where rapid rise of $(dP/dt)_{max}$ shifts to a gentle linear increase. The authors highlighted that E_{ign} higher than 10 kJ must be excluded, because excessive energy will raise the initial temperature markedly and thereby yield unrealistic results (Kuai et al. [25]).

Gao et al. [26] conducted tests in the standard 20-L vessel to examine the effects of different energy ignitors on explosion overpressure behaviour during testing of 1-octadecanol ($CH_3(CH_2)_{16}CH_2OH$) dust using four different ignitors: chemical ignitor (10 kJ), chemical ignitor (2.5 kJ), electrostatic ignitor (10 kJ; actual energy, 1.86 kJ), and electrostatic ignitor (2.5 kJ; actual energy, 0.53 kJ). They observed that varying the ignition energy influenced both P_{max} and K_{St}, and concluded that as the ignition energy increased from 2.5 kJ to 10 kJ, the apparent P_{max} and K_{St} values increased significantly.

Thomas et al. [27] undertook an experimental investigation of the anomalies that characterize marginally explosible dusts by performing standard testing of urea dust in both the 20-L and 1-m^3 explosion chambers. They observed that although ignition occurred in the 20-L sphere using two 5-kJ ignitors (i.e., 10 kJ), ignition did not occur with one 5-kJ ignitor in the 20-L sphere, or with two 10-kJ ignitors in the 1-m^3 chamber. They also concluded that explosion of marginal dusts in the 20-L chamber may be as a result of overdriving yielding a "false positive" result. The authors suggest that this false positive result could be avoided by testing such a dust in a larger vessel (such as the 1-m^3 chamber) where the flame must propagate over a more reasonable distance in order to develop a maximum pressure sufficient to classify the dust as explosible.

Rodgers and Ural [22] recognized that a combustible dust may be non-explosible, marginally explosible or severely explosible. Their work demonstrates how some non-explosible dusts are erroneously classified as explosible as a result of false positives,

and highlights that overdriving in the 20-L explosion chamber may also contribute to this erroneous classification. They further pointed out that despite the differences between marginally and severely explosible dusts, most safety standards and regulations do not specify these differences, and both classes of combustible dusts continue to trigger the same legal and technical burden or consequence on the users.

A parallel situation arises from the ASTM E1226-12a [28] standard where a dust that exhibits a measurable K_{St} with ignitor energies of 5 kJ and 10 kJ, but produces a non-measurable K_{St} with 2.5 kJ in a 20-L chamber, may infer that an overdriven explosion has occurred. In such a case, the standard recommends that the dust be tested in the 1-m^3 chamber to establish whether it is indeed explosible.

The work of Cashdollar and Chatrathi [29] measured the minimum explosible concentration (MEC) of dusts in the U.S. Bureau of Mines 20-L chamber (Pittsburgh, PA) and Fike Cooperation's (Blue Springs, MO) 1-m^3 chamber with varying ignition energies of 0.5 kJ to 10 kJ. They concluded from their studies that MEC values measured in the 20-L chamber with 2.5-kJ ignitors were comparable to those in the 1-m^3 chamber, and that there was evidence of overdriving at higher ignition energies in the 20-L chamber which was absent in the larger volume.

Going et al. [30] compared results from measurement of the MEC and limiting oxygen concentration (LOC) of dusts in the Pittsburgh Research Laboratory (PRL) 20-L chamber (formerly known as the U.S. Bureau of Mines 20-L chamber) and the Fike Cooperation (who are in the business of providing fire and explosion solutions and partners of this project) 1-m^3 chamber with varying ignition energies and made conclusions similar to those in the work of Cashdollar and Chatrathi [29]. The authors additionally recommended that a lower ignition energy of 2.5 kJ in the 20-L vessel would yield results comparable to those in the 1-m^3 chamber using standard 10-kJ ignitors.

Another complication associated with marginally explosible dusts is the difference in behaviour of metallic marginally explosible dusts relative to non-metallic marginally explosible dusts. This has been demonstrated in the dust explosion literature ([21] [31] [32]). Whereas the behaviour of the non-metallic marginally explosible dust from the work of Proust et al. [21] correlates with the non-metallic samples in the work of Bucher et al. [31], the latter authors concluded from their study that metallic marginally

explosible dusts may behave differently from non-metallic marginally explosible dusts. Out of the 13 metallic dust samples tested, a significant majority of 12 dusts that tested to be explosible in the 20-L chamber with K_{St} values below 50 bar·m/s, were found to have greater values of both P_{max} and K_{St} in the 1-m^3 vessel.

Myers et al. [32] experimentally studied and compared explosion pressures of 20 dusts comprising 7 non-metallic and 13 metallic dusts in the 1-m^3 chamber according to the procedure given in ISO 6184-1 [33], and in the Siwek 20-L chamber according to the procedure outlined in ASTM E1226-12a [28]. Only one out of the 13 metallic samples tested was found to be non-explosible in the 1-m^3 chamber and this sample had tested as very weakly explosible in the 20-L chamber. Similar to Bucher et al. [31], the remaining majority of metallic dust samples (12), produced P_{max} and K_{St} values that were higher in the 1-m^3 chamber than in the 20-L chamber. Additionally, six out of the seven non-metallic dusts were found to be non-explosible with P_{max} values ranging from 2.6 to 5.4 bar(g) and K_{St} values ranging from 2 to 39 bar·m/s. In these studies, however, the particle size distribution, material analysed, and full-testing concentrations were not completely characterized, thus making it difficult to offer further clarification for these results. The findings of Bucher et al. [31] and Myers et al. [32] were confirmed in a recent investigation by Marmo et al. [34] who conducted an experimental study of fourteen metallic waste dusts.

The main conclusions from the discussion of the above literature on the testing of marginally explosible dusts in the 20-L and 1-m^3 explosion chambers is summarized as follows:

1. There is uncertainty in the explosibility test results for marginally explosible dusts between the two vessels ([21],[29],[27],[23]) as determined in accordance with standardized test protocols, yet the literature does not provide a path towards resolving the issue for those responsible for the development and implementation of testing standards.

2. The current ASTM standard [28] does not differentiate between marginally explosible dust and severely explosible dusts; both dust categories continue to trigger the same explosion prevention and mitigation measures, which may place a potential financial burden on dust-handling facilities [22].

3. There is a marked difference with respect to the behaviour of metallic marginally explosible dusts relative to their non-metallic counterparts during testing at laboratory- and larger-scales ([21][31] [32][35]).
4. There is a lack of data on material characterization and how factors such as particle size distribution, moisture content and chemical composition affect the explosibility of marginally explosible dusts [31] [32].

Although some of the literature ([20][21][22][31]) suggest that marginally explosion dusts have low explosion likelihood, these conclusions have not been adequately investigated and validated. The literature does not provide adequate data on explosion sensitivity parameters such as MEC, MIE and MIT.

2.6 Dust Flash Fires

One thing that is certain about the so-called marginally explosible dusts is that they indeed pose a flash fire hazard. A flash fire is said to have occurred when a dust deflagration does not generate significant overpressure. The distinction between a flash fire and explosion is usually based on whether the overpressure produced by the deflagration was sufficiently large to cause structural or mechanical damage. In a closed space, any deflagration releases heat into that space raising its average temperature, and hence, the ambient pressure.

Ogle [36] identifies two circumstances, either one of which occurs to create a flash fire: (i) either the space is not truly closed; or (ii) only a fraction of the space has been filled with an ignitable dust concentration. If the space is not truly closed, then there are openings in the enclosure that can vent the rising pressure and hot gases formed by the deflagration. If the space is indeed closed, then the confinement volume must be much larger than the volume of the unburnt dust cloud [36].

2.6.1 Characteristics of dust flash fires

Typically for flash fires, the flame front spreads at velocities less than that of sound (i.e., subsonic), hence the overpressure damage is usually negligible, and the bulk of the damage comes from the thermal radiation and secondary fires [37]. In addition to the requirements of any fire event (i.e., the fire triangle), there should

be dispersion of a dust deposit in order to meet the requirements of a flash fire hazard (as seen in Figure 2.9). The magnitude and consequence of a flash fire hazard are strongly influenced by factors such as the size of the dust deposit, its location, the potential for dispersal, the location and frequency of occupation of an area by personnel, and by the nature of the work activities in the area [36]. Among all these factors, the elevation of the dust deposit is critical. The reason is that dust deposits located above the occupants of the work space (i.e., on beams, ceiling, ducts, overhead frames, fans, pipes, etc.) offers a greater level of the hazard. This is because of the high probability of forming a suspended dust cloud should the dust deposits be disturbed [36].

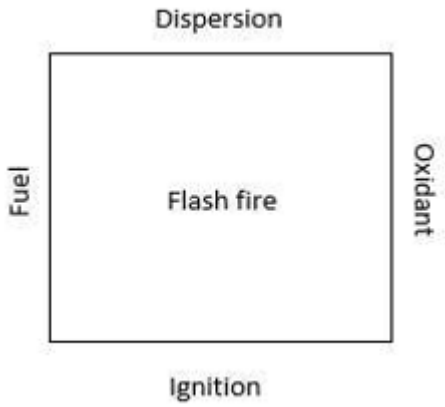

Figure 2.9: Flash fire square [36].

Flame engulfment, radiant heat, and direct contact with burning particles are the main hazards of a combustible dust flash fire. Flash fire is a particular danger in enclosed spaces, as even a relatively small fire can consume enough oxygen and produce enough smoke to cause death of persons present, whether by asphyxiation or smoke inhalation [37].

2.6.2 Control of dust flash fire

Current editions of combustible dust standards (such as NFPA 654 [12], and ASTM E1226 [28]) do not offer a graduated approach towards combustible dust hazards. That is, the standards do not differentiate between dusts which present explosion and flash fire hazards, and dusts which only present flash fire hazards. Similarly, the frameworks that exist for prevention and mitigation of combustible dust fire and explosion hazards do not distinguish between marginally and non-marginally

explosible dusts. Although there is uncertainty of the explosion hazards presented by marginally explosible dusts, this is not the case with respect to flash fire hazards associated with the same materials. In view of the lack of distinction between dusts which present explosion hazards and those that present only flash fire hazards, measures employed for the prevention and mitigation of dust flash fires largely follow those for dust explosions as outlined in the standard NFPA 654 [12] and summarised in section 2.3. The principle here also, is to eliminate or disable one or more elements to prevent the flash fire event. Industries that handle so-called marginally explosible dusts are therefore faced with legal and technical requirements for explosion protection for cases in which it may be more appropriate to focus on flash fire hazards. Additionally, the use of fire clothing made of fire-retardant materials (e.g. Nomex) may prevent or mitigate the harmful effect of a flash fire in the body areas that are covered by the personal protective equipment (PPE) [37].

2.6.3 Application of inherent safety for dust explosion and fire control

In addressing the problem of dust explosions and dust fires, it is essential to establish a framework in order to make suitable choices. A well studied approach is the application of inherent safety as exemplified below by the four principles; minimization, substitution, moderation and simplification [38].

1. Minimize: Whether dust exists as desired product or unwanted by-product of the process undertaken, it is critical to minimize, whenever possible, the amount of dust available to participate in an explosion arising from normal operating conditions or an upset event. This is to ensure that both dust clouds and dust layers of explosible concentrations are not formed [38].
2. Substitute: Replace one work procedure for another that reduces dust production and accumulation. Substitute a process route that produces large amounts of dust for one that produces lesser amount of dust. Where possible, replace the more combustible, reactive and hazardous material with a less combustible, less reactive, or less hazardous material [38].
3. Moderation: Process dust material in its less hazardous form by means of any of the following [38]:

- altering the composition of a dust by admixture of solid inertant to reduce its hazardous nature.
- increasing the dust particle size resulting in decreased reactivity as well as dustiness.
- avoiding the formation of hybrid mixtures of explosible dusts and flammable gases.

4. Simplify: Complex and unnecessary add-ons that results in further reduction of size and subsequent dispersion must be avoided. Possibly, processing must be through the simplest of processes. Additionally, information on the hazardous properties of combustible dusts should be clear and easily understandable by all [38].

CHAPTER 3: MATERIALS CHARACTERISTICS AND PRELIMINARY ANALYSES

This chapter provides information on the materials tested, various material characterizations performed, and a description of all apparatus used in this experimental investigation including schematics and photos. It also gives a brief overview of the various experimental parameters determined in the study.

3.1 Materials

Information about all materials used in the current project are provided in this section.

3.1.1 Niacin

Niacin has the molecular formula, C_5H_4NCOOH (or $C_6H_5NO_2$). It is also known as nicotinic acid or pyridine-3-carboxylic acid is in the vitamin B family of medications specifically the vitamin B3 complex and may be used as dietary supplement, and as a medication. Though it occurs naturally in foods such as yeast, milk, meat, and green vegetables, it can also be synthesized for commercial use from the hydrolysis of 3-cyanopyridine (nicotinonitrile). Niacin powder finds a variety of applications in the pharmaceutical industry such as for treatment of niacin deficiency (pellagra), acne, inflammatory skin conditions, and is present in many multivitamins [39]. It has been used widely as a reference dust in many other experimental studies. In this current work, niacin served two purposes: first as a calibration standard and then as one of the four organic samples tested. Figure 3.1 shows photos of the niacin dust used.

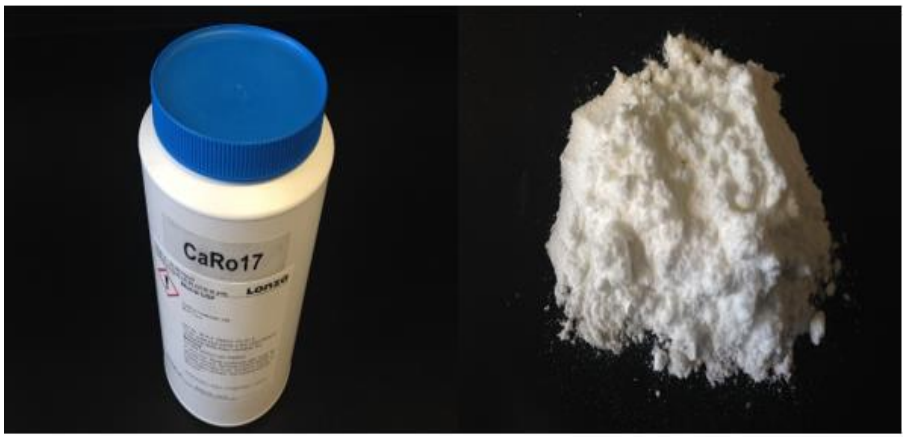

Figure 3.1: Photos of niacin dust

3.1.2 Lycopodium clavatum

Lycopodium clavatum is the most widespread species in the genus lycopodium in the clubmoss family [39]. Though its molecular mass has not been confirmed, a few studies have determined it. For instance, Addai et al. [40] determined in their work that the molecular mass of lycopodium is $C_{5.77}H_{9.59}O_{1.23}S_{0.001}N_{0.08}$. It consists of the dry spores of clubmoss plants. Lycopodium powder is a yellow-tan powder used in the past as a flash powder. When mixed with air in high enough concentrations, these spores become highly flammable due to their high fat content and their large area per unit volume. It has been used in the production of fireworks and explosives, covering pills, as fingerprint powder, and as a stabilizing agent in ice-cream [39]. In this work, lycopodium powder was used as a reference dust for equipment calibration and as one of the selected organic dust samples. Figure 3.2 display photos of lycopodium.

Figure 3.2: Photos of lycopodium clavatum dust

3.1.3 Polyethylene

The type of polyethylene samples used in this work were ultra-high molecular weight polyethylene (UHMWPE). UHMWPE is a polyethylene thermoplastic with extremely long chains and a molecular mass usually between 3.5 – 7.5 million amu. It has the basic (monomer) unit $–(CH_2\text{-}CH_2)_n—$ (where n > 100000) [41]. The UHMWPE dust used in this work is laboratory grade and procured from Sigma Aldrich Chemicals, USA. Its properties include high resistance to corrosive chemicals, extremely low moisture absorption and a very low coefficient of friction. Due to its outstanding toughness and cut, wear, and excellent chemical resistance, UHMWPE is used in a diverse range of applications such as coatings, machine moving parts, bearings, gears, artificial joints, and butchers' chopping boards. As fibre, it competes with aramid in bulletproof vests [41]. Figure 3.3 below shows photos of the fine size UHMWPE powder. Figure 3.4 also shows photos of the coarse size UHMWPE powder.

Many studies have been conducted on polyethylene dust explosion and there are evidence to conclude that polyethylene dust is explosible. The choice to use this dust material was based on the established principle that a change in particle size influences both the likelihood and severity of explosion, thus there could be a particle size range of the material where it may show marginal explosibility. For the purpose of this current work, fine UHMWPE will be hereafter designated as fine polyethylene or abbreviated as Fine PE, whereas the coarse UHMWPE will be designated as coarse polyethylene or simply Coarse PE.

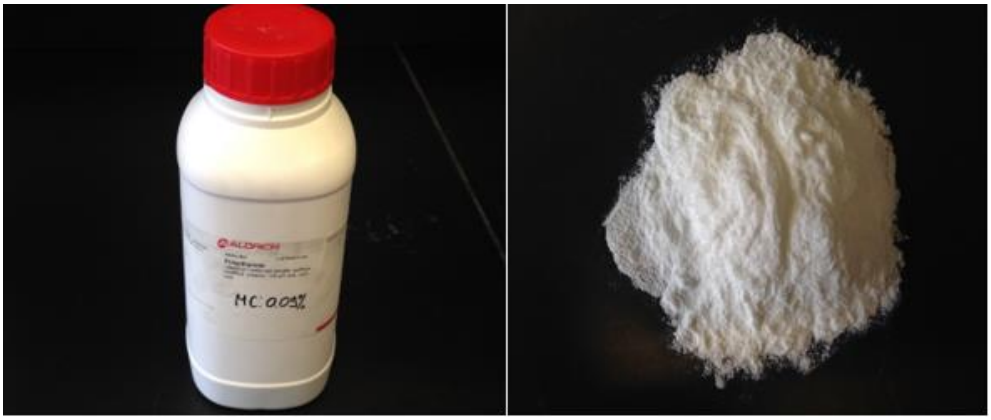

Figure 3.3: Photos of fine polyethylene dust

Figure 3.4: Photos of coarse polyethylene dust

3.2 Sample Characterization Analysis

This section presents the various characterization analyses performed on each of the dust materials to understand the physical and chemical properties. Knowledge of these characteristics help to make good predictions of the explosibility behaviour of the particular material. The selected properties to be analysed were those established in literature to have the strongest influence on dust material ignition and explosibility.

3.2.1 Sample preparation

Prior to all preliminary analyses described in this section, all dust samples were prepared in accordance with requirements stipulated in the applicable standards. This was to ensure accurate response to the equipment and apparatus used for the analyses.

3.2.2 Particle size distribution (laser diffraction spectroscopy)

The particle size distribution of all dusts was determined using a laser diffraction particle size analyser (Mastersizer v3.50) applying standard procedures outlined in ASTM D4464 [42]. Measurements were done by passing a laser beam through a sample pre-dispersed in water or other compatible organic liquid. The resulting scattering was then collected by a photodetector array and converted to electrical signals which were then analysed using Fraunhofer Diffraction. The median diameter D_{50} (defined as the diameter where 50% by weight of the dust sample is finer and 50 wt% is coarser) was determined. Also, the 10% and 90% boundaries (D_{10} and D_{90}, respectively) were

determined. Figure H.1 to Figure H.4 (in Appendix H) show the particle size distribution graphs for each sample tested as received.

3.2.3 Moisture content analysis (% wt)

Moisture content is the amount of moisture absorbed within a dust particle or adhering to the particle's surface. The moisture content is a factor that can greatly influence a dust materials ability to form a dust cloud, ignite and its ability to sustain an explosion. In addition, the degree of wetness of a particle's surface can increase the particle's electrical conductivity and reduce its propensity to create and retain electrostatic charge. Surface moisture can also facilitate agglomeration of fine particles and thereby increase the dust suspension's apparent average particle size. The ASTM standards [28], [43], [44], [45] for dust ignitability and explosibility testing stipulates that moisture content of dust sample should be less than 5 % prior to testing. This is because materials with moisture content below 5 wt% are considered "dry" and are able to exhibit high ignition sensitivity and explosion severity. Prior to testing of the materials in the current work, moisture analysis was performed for all dust samples in accordance with ASTM 3173 [46] using a moisture analyser (Sartorius MA37-1).

3.2.4 Heat of combustion (BTU analysis)

The heat of combustion of a substance is the total energy released as heat by a complete combustion of the material. It is usually expressed with the quantities, energy per amount of fuel (i.e., kJ/kg or Btu/lb). The heat of combustion of a dust sample has a direct influence on the explosion severity. A dust with a high calorific or heating value has a high tendency to release large amounts of energy (as heat) during combustion, hence increasing the explosion severity. In the current study, the heat of combustion of the all dusts was determined by the adiabatic bomb calorimetric method according to ASTM D5865 [47].

3.2.5 Scanning electron microscopy (SEM)

Dust particles may have different particle shape, agglomeration behaviours, and porosity. These factors may influence significantly the dust's ability to be dispersed

(i.e., dustiness), ease of volatilization, ignition ability and explosibility. It is therefore important to obtain information about these properties to further understand the hazards they pose. For each dust sample tested, SEM analyses to visualize the particle properties aforementioned were obtained. The SEM is a powerful magnification tool that utilizes focused beams of electrons to obtain high-resolution three-dimensional images. These give a qualitative picture of the powdered samples. Figure 3.5 shows SEM images of the organic dusts.

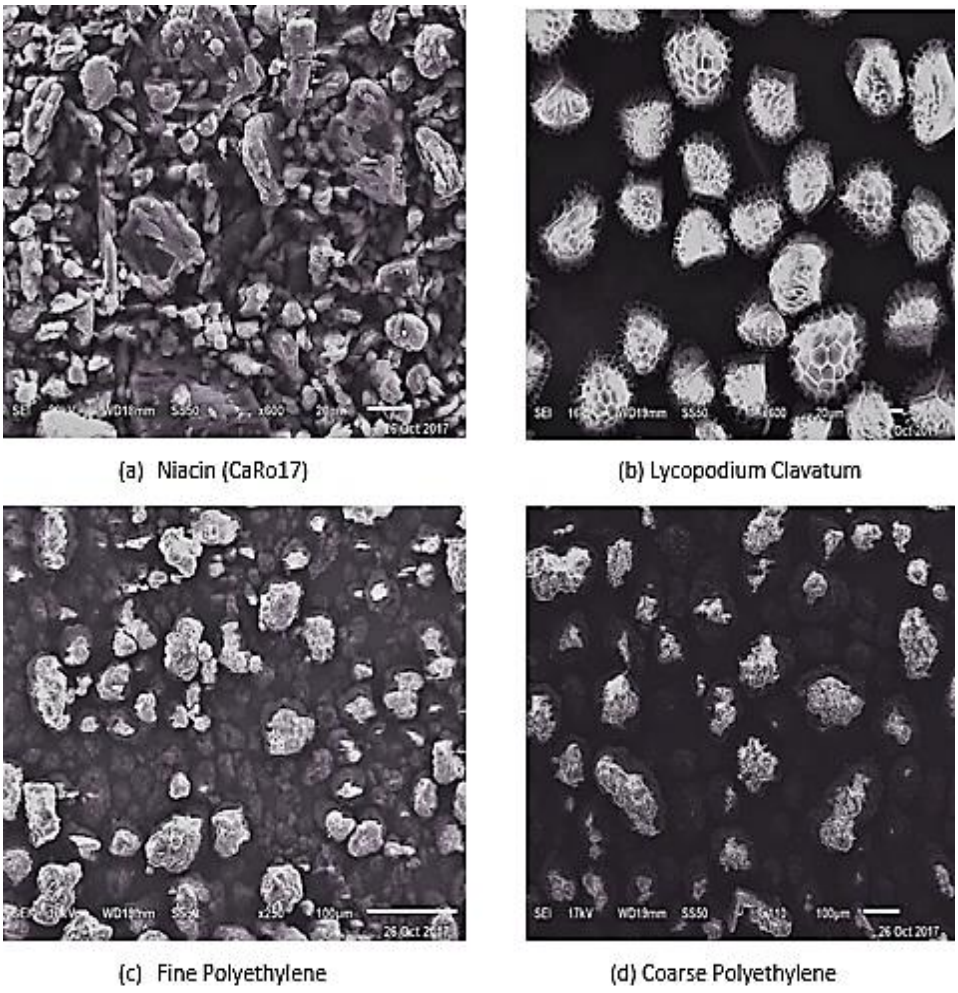

Figure 3.5: SEM images for all organic samples

3.2.6 Specific surface area (BET)

The specific surface area (SSA) of a solid material (e.g. dust) is the total surface area of that material per unit mass. The specific surface area of all dusts were determined

based on the Brunauer–Emmett–Teller (BET) multilayer gas adsorption theory (which is currently the most accurate means of measuring the SSA), using single-point, multi-point, and Langmuir methods in agreement with the applicable standard ASTM D6556-16 [48]. The BET theory is used to evaluate the gas adsorption data of powdered samples and generate a specific surface area result expressed in units of area per mass of sample (m^2/kg or m^2/g). Prior to analysis, the dust samples were preconditioned to remove physically bonded impurities from the surface in a process called degassing or outgassing. The SSA of the dust was then determined by the physical adsorption of nitrogen gas onto the surface of the sample at cryogenic temperatures (typically liquid nitrogen temperatures). Once the amount of adsorbate gas has been measured, the specific surface area is automatically calculated using an in-built algorithm by assuming adsorption of a monomolecular layer of the known gas.

3.2.7 Density

The densities of the four dust samples were determined prior to testing in the 1-m^3 chamber using the simple scoop method. A scoop or spatula of known volume (V_{sc}) was used to scoop a quantity of sample onto a weighing plate (with known mass, m_p) and placed onto an analytical balance to determine the total mass (m_T) of sample and weighing plate. The mass of sample (m_s) only is obtained by subtracting the mass of weighing plate from the total mass (i.e., $m_s = m_T - m_p$). The density (ρ) is then calculated using the relationship:

$$\rho = m_s/V_{sc} \quad (1)$$

The results for all material characterisation analyses conducted for this work can be seen in Table 3.1 below.

Table 3.1: Summary of material characteristics

Material	Particle Size			Moisture Content	Heat of Combustion	Single point BET (SSA)	Multi point BET (SSA)	Langmuir (SSA)	Density
	[µm]			[wt %]	[kJ/kg]	[m^2/g]	[m^2/g]	[m^2/g]	[g/cm^3]
	D_{10}	D_{50}	D_{90}						
Niacin	5	20	66	1.1	22,420	0.65	0.74	0.60	0.41
Lycopodium	23	31	42	4.3	31,330	1.07	1.30	1.00	0.36
Fine polyethylene	21	42	69	0.2	45,750	1.48	1.66	1.37	0.41
Coarse polyethylene	78	131	210	0.2	45,810	2.71	2.94	2.79	0.41

3.3 Apparatus and Experimental Procedures

This section presents calibration information, a description of all apparatus used for the determination of the explosion severity and explosion likelihood parameters essential for the current study and the standard test procedures used.

3.3.1 Equipment calibration

Prior to testing, all apparatus at the Dalhousie Dust Explosion Laboratory were calibrated with three reference dusts: niacin (by participating in the 2017 calibration round-robin (CaRo17) coordinated by Cesana AG), lycopodium, and Pittsburgh coal. The results obtained during calibration were within acceptable limits relative to all reference samples. The results from all dust testing equipment used to determine applicable explosion parameter(s) could be found in Table A.1 to Table A.20 (in Appendix A). For the current experimental work, the pieces of apparatus used for determining explosion severity parameters (P_{max} and K_{St}) included the standard Siwek 20-L explosion chamber and the 1-m^3 explosion chamber. The two explosion chambers were also used to determine one of the likelihood parameters, the minimum explosible concentration (MEC). The MIKE-3 apparatus, and BAM oven were used to determine the likelihood parameters, MIE and MIT respectively. The following section gives a description of all experimental apparatus.

3.3.2 Siwek 20-L explosion chamber

The standard Siwek 20-L explosion vessel, manufactured in Switzerland by Kühner A.G, is used to determine various explosion parameters, such as maximum explosion pressure (P_{max}), maximum rate of pressure rise ($(dP/dt)_{max}$), and minimum explosible concentration (MEC) in accordance with ASTM E1226 [28] and ASTM E1515 [43]. The test apparatus comprises of an explosion chamber, a jacketed cooling system, a vacuum pump for evacuating the chamber, an external dispersion system for dusts, an ignition source located at the centre of the sphere, pressure measurement system, and a data recording system (Kuhner KSEP-Software). Together, these function to disperse, ignite, contain, and record the properties of the dust explosion. Figure 3.6 and Figure 3.7 show a schematic diagram, and picture of the Siwek 20-L explosion chamber.

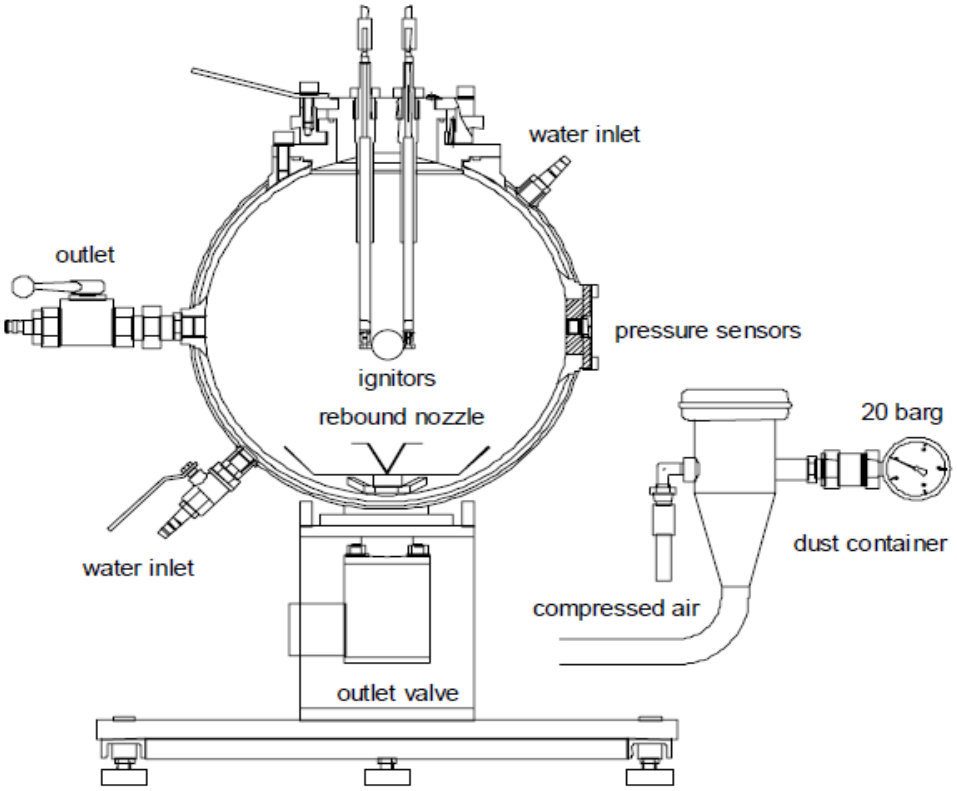

Figure 3.6: Schematic of the 20-L explosion chamber

Figure 3.7: Photo of Siwek 20-L explosion chamber

The test apparatus consists of a hollow sphere made of stainless steel with an internal volume of 20 L. The bayonet ring seals a 94-mm opening at the top of the sphere when in use. Situated through the bayonet ring are two ignitor posts that hold the pyrotechnic ignitors (which cause the explosion during a test). The bayonet ring can be removed between tests to allow access into the chamber for cleaning and to mount new ignitors. A solenoid valve positioned at the bottom of the chamber separates the explosion chamber from a 0.6-L external dispersion reservoir (that holds the dust during the dispersion sequence). Two valves, one connected to a vacuum, and the other for venting combustion products, are located on the side of the sphere.

Ignition of the dust cloud is achieved by chemical ignitors with specific ignition energies. An electrical current is sent through the ignitor post and ignites the Sobbe ignitors. The ignitors comprises 40% zirconium, 30% barium nitrate and 30% barium peroxide. Ignition of the dust cloud occurs 60 ms after the dispersion sequence. Also, two Kistler piezoelectric pressure transducers that measure pressure changes are held in a 30-mm flange on the side of the chamber. They measure the pressure difference as a result of deformation of a quartz crystal by pressure wave from an explosion. The pressure difference is directly proportional to the deformation.

3.3.3 Test procedure in 20-L chamber

Dust explosion severity testing on the small scale was carried out using the 20-L explosion chamber in accordance with applicable ASTM standards [28] [43]. To start testing, a defined amount of combustible dust was placed into the dust container. The explosion chamber which was initially filled with air at atmospheric pressure, was then evacuated to 300-torr (0.4-bar absolute). An automatic test sequence was initiated to pressurize the dust container to 20-bar(g). The fast-actuating valve on the dust container outlet was then opened to inject the dust into the explosion chamber through a rebound nozzle. The rebound nozzle ensured an even distribution of dust within the explosion chamber. The control system activated the ignitor(s) positioned at the centre of the sphere at an ignition delay time of 60 ms after the dust was dispersed.

Explosion pressures (P_m) and maximum rate of pressure rise $(dP/dt)_m$ were measured for each dust concentration tested via two piezoelectric pressure transducers. For the current experimental work, testing of all dusts samples was conducted in the 20-L

vessel with three different ignition energies (i.e., 2.5, 5, and 10 (2×5 kJ)). On the other hand, an ignition energy of 2.5 kJ was used for MEC determinations in the same chamber.

3.3.4 Explosibility parameters tested in 20-L chamber

This section describes how the explosibility parameters such as maximum explosion pressure (P_{max}), the maximum rate of pressure rise $(dP/dt)_{max}$ and the minimum explosible concentration (MEC) were determined in the standard 20-L sphere.

3.3.5 Maximum explosion pressure (P_{max}) and maximum rate of pressure rise $(dP/dt)_{max}$

P_{max} and $(dP/dt)_{max}$ were determined using the 20-L spherical explosion test chamber, then the K_{St} value was calculated from the $(dP/dt)_{max}$ value using the cubic relationship:

$$K_{St} = (dP/dt)_m \cdot V^{1/3} \quad (2)$$

The test commenced by using a low dust concentration and continued over a range of fuel concentrations (typically 50 – 3000 g/m^3). P_{max} and K_{St} were obtained as the arithmetic means of the P_m and $(dP/dt)_m$ respectively over at least three test series. According to the standard [28] ignition should be provided by 2×5-kJ chemical ignitors. However, for this present study, tests were also conducted with two additional ignition energies (i.e., 2.5 and 5 kJ) to investigate their effect on the P_{max} and K_{St} values. The pressure-time graph for each explosion and at each ignition energy used was recorded.

A typical pressure evolution curve resulting from an experiment where an explosion occurred is shown in Figure 3.8. The injection of the dust occurred after a delay t_d (in the range of 30 to 50 ms). A pressure rise, P_d occurred due to the injection of dust using pressurized air. A chemical ignitor energy discharge is initiated after a delay time of t_v = 60 ms. If explosion occurred, a rapid increase in pressure was observed. The time between ignition and the occurrence of P_{max}, t_1, is considered as the duration of combustion. The induction time, t_2, is the time between ignition and the intercept of a line drawn tangent to the pressure curve at (dP/dt).

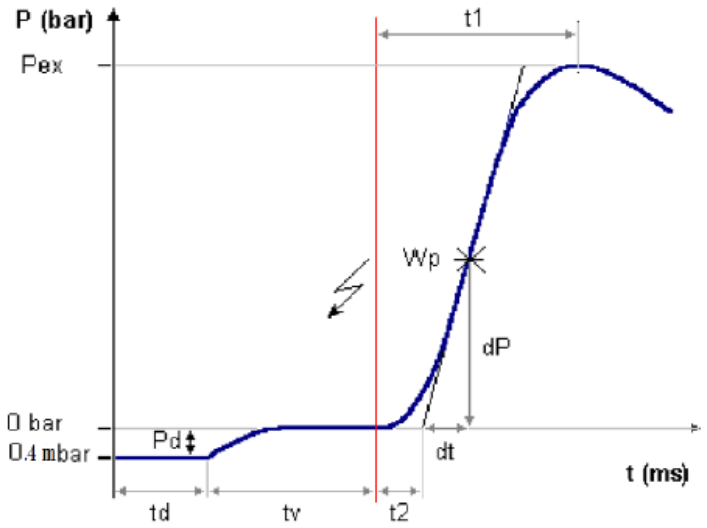

Figure 3.8: Pressure-time diagram of a fuel explosion.

3.3.6 Minimum explosible concentration (MEC)

The test to determine the MEC was performed in the standard 20-L sphere in accordance with the standard testing method ASTM E1515 [43]. The test procedure involved dispersing the dust sample into a sphere and attempting to ignite the resulting dust cloud with an ignition source of 2.5 kJ. To begin, an arbitrary concentration of the fuel (with high probability of explosion) was chosen and tested to check if an explosion would occur or not. In the case where no explosion was observed, the concentration of the dust was increased until the dust/air mixture exploded. If an explosion occurred, testing was continued, and the concentration further reduced until a point where no explosion of the dust cloud was observed in two successive tests. The lowest concentration where last an explosion was observed was recorded to be the MEC of the fuel.

3.3.7 1-m^3 explosion chamber

The 1-m^3 explosion chamber is considered to be the international benchmark for dust testing, and it is useful for providing data whenever the results from the 20-L test chamber raise questions about the explosion characteristics of a dust. The 20-L sphere is a practical substitute for the 1-m^3 chamber, as it requires significantly less sample and labour to conduct testing. Figure 3.9 and Figure 3.10 show a general schematic diagram, and a photograph of the 1-m^3 chamber respectively. The 1-m^3 vessel is a

spherical explosion chamber designed to gather explosion severity and explosion protection testing data. Both combustible dust mixtures and combustible gas can be introduced into the vessel. The 1-m^3 chamber used in this work is located at one of the industrial partners' (Fauske and Associates Inc.) facility in the United States of America (where I spent three weeks to conduct tests). The chamber has a design pressure of about 40 bar(g) and can contain most explosions. The chamber consists of a complete spherical structure with hydraulically operated thick steel gates that can be opened after each test to access the interior to clean and fit new ignitor(s).

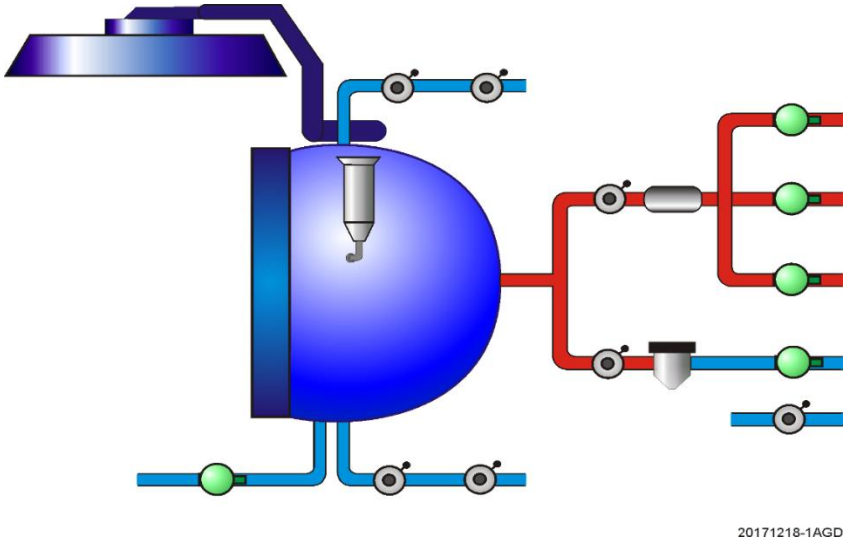

Figure 3.9: Schematic of the Fauske 1-m^3 Explosion Chamber [49]

Figure 3.10: Photo of the Fauske and Associates Inc. 1-m^3 Explosion Chamber [50]

The dust injection system consists of two 5-liter dispersion reservoirs, two dust dispersion (or rebound) nozzles positioned at the outlet of each dispersion system in the chamber, and a ball valve each between the dispersers and the nozzle. A vacuum pump is used to evacuate a given amount of air from the chamber before dust dispersion. Two ignitor poles around which chemical ignitors are wound extend from approximately the top-middle part of the chamber into the chamber. The chamber is also equipped with two highly sensitive pressure transducers that detect and measure pressure rise after an ignition process. The outlet (exhaust) valve opens to depressurize and exhaust burnt gases after an explosion event, while the inlet valve allows air into the chamber to purge the interior of any product gases. The entire apparatus is connected to a control and data acquisition system that initiates the test and records the explosion characteristics of the test sample.

3.3.8 Experimental procedure in the 1-m^3

The experimental procedures in the 1-m^3 explosion chamber were conducted in accordance with ISO 6184/1 [33]. Prior to start of testing, an ignitor check without dust is done to ensure that any residual dust from previous testing is burnt-off and that all units of the apparatus are functioning effectively. The chamber is cleaned thoroughly afterwards and made ready for testing with dust. The dispersion reservoir(s) or disperser(s) were then charged with a weighed amount of dust sample. Depending on the amount of sample and the explosion parameter (P_{max} and K_{St}, or MEC) being measured, one or both dispersers were utilized. The disperser(s) were then closed tightly, and the chemical ignitors fitted on the well-cleaned ignitor leads. The chamber gate was closed with the aid of a hydraulic system and the lock-switch engaged. After the chamber was closed, the testing process was initiated from a central control and data acquisition system. There are three main steps involved in a complete test cycle: stabilization, actuation, and ventilation.

At the stabilization stage, the resistance (in ohms) offered by the ignitor wires to the current flowing through the ignitor leads is automatically calculated. Testing only proceeds when the resistance calculated is less than 10 ohms (Ω). If the resistance is greater than 10 Ω, an alarm is triggered and does not allow testing to proceed until

ignitor/ignitor-leads contacts are well cleaned to allow enough current flow to trigger the ignitors.

After the ignitor resistance has been stabilized (i.e., below 10 Ω), the actuation process starts. The process commences by evacuating air from the chamber. The amount of air evacuated by the vacuum pump is based on the density of the dust and the head-space in the dispersion reservoirs so that the total pressure in the chamber prior to explosion will be 1 bar(g).

The next step that follows is the disperser pressurization step. At this step, the dispersers are pressurized with dry air to a pressure of 20 bar(g). When the pressure in the dispersers has stabilized at 20 bar(g), the "IGNITE" button on the control system software is highlighted indicating that the dust dispersion and ignition steps can proceed. The dust-air mixture is discharged into the 1-m^3 chamber through the rebound nozzle(s) and creates a combustible dust cloud. The dust cloud is then ignited by the chemical ignitor(s) located approximately in the middle of the chamber after a set delay time (usually 500 to 700 ms) is reached. The pressure that results from an explosion is measured with pressure transducers located in a flange on the side of the chamber and displayed digitally on the connected PC. An explosion is said to have occurred if the dust is able to propagate a deflagration by itself to produce an explosion overpressure equal or greater than 1 bar(g) (i.e., according to the ASTM standard [28]).

The ignition step brings an end to the actuation process and gives way for the ventilation process to begin. During the ventilation stage, the dispersers and the chamber are depressurized by the opening of the outlet (exhaust) valve. Product gases from the burning process exhaust through the outlet valve. The purging step then ensures that air is allowed into the chamber through the inlet valve, circulates and then exhausts through the outlet valve to the duct work. When purging is completed, the system software then allows access the chamber for more cleaning by vacuuming. The chamber is then prepared for subsequent testing.

3.3.9 Experimental parameters determined in the 1-m^3 chamber

This section describes the explosion parameters determined and procedures used for their determinations in the 1-m^3 explosion chamber.

3.3.10 Maximum explosion pressure (P_{max}) and maximum rate of pressure rise $(dP/dt)_{max}$

Following their determinations in the 20-L chamber, companion P_{max} and $(dP/dt)_{max}$ values were obtained using the in accordance with ASTM 1226-12a [28] and ISO 6184/1 [33]. In the 1-m^3 chamber, the $(dP/dt)_{max}$ is equal in magnitude to the K_{St} value using the relation in equation (2). The procedure for testing was similar to that for determining the same parameters in the 20-L chamber. The source of ignition was provided by 2×5-kJ chemical ignitors. For effective comparison, the explosion criterion was kept the same for determinations in the 1-m^3 and 20-L chambers. An explosion in the chamber produces a pressure-time curve similar to Figure 3.8. For this work, P_{max} and $(dP/dt)_{max}$ were determined at two different ignition set delay times of 550 and 600 ms.

3.3.11 Minimum explosible concentration (MEC)

Determination of the minimum explosible concentration of dusts in the 1-m^3 chamber also followed standard procedures outlined in ASTM E1515 [43]. The determination of MEC followed similar steps as outlined in section 3.3.6 for the 20-L chamber. The difference here was that the ignition source used was 10 kJ. Also, MEC determinations in the 1-m^3 was conducted at a delay time of 550 ms for all dust.

3.3.12 MIKE-3 apparatus

The MIKE-3 apparatus was manufactured by Kühner and is a modified Hartman tube used to measure the dust's minimum ignition energy (MIE). The apparatus is made-up of a glass tube (combustion chamber), a dispersion system, and an electrode assembly. Schematic and photo of the MIKE-3 apparatus are shown in Figure 3.11 and Figure 3.12 below. The glass tube, which serves as the combustion chamber is a vertical cylindrical tube with volume of 1.2 L, a height of 300 mm, and diameter of 68 mm. It has two holes approximately 120 mm from its bottom part to accommodate the electrodes when fitted. The dispersion system comprises a mushroom-shaped nozzle in a dispersion cup as part of the bottom assembly, and compressed air supply. The mushroom cap forces high velocity air down to disperse the dust into a uniform dust cloud within the combustion chamber. The air pressure used for dispersion is 7 bar(g).

The MIKE-3 Apparatus uses high-voltage electric spark produced by two electrodes to initiate an ignition. The spark energy for a particular series of test is determined by the operator. Energies available for testing in the apparatus are 1000, 300, 100, 30, 10, 3, and 1 mJ. Each energy setting is controlled through switches that complete different circuits for the specified energy level. Compressed air also controls the movement of the electrodes. When the circuit is closed, the selected energy is discharged through the high-voltage electrodes across a 6 mm gap, causing the spark.

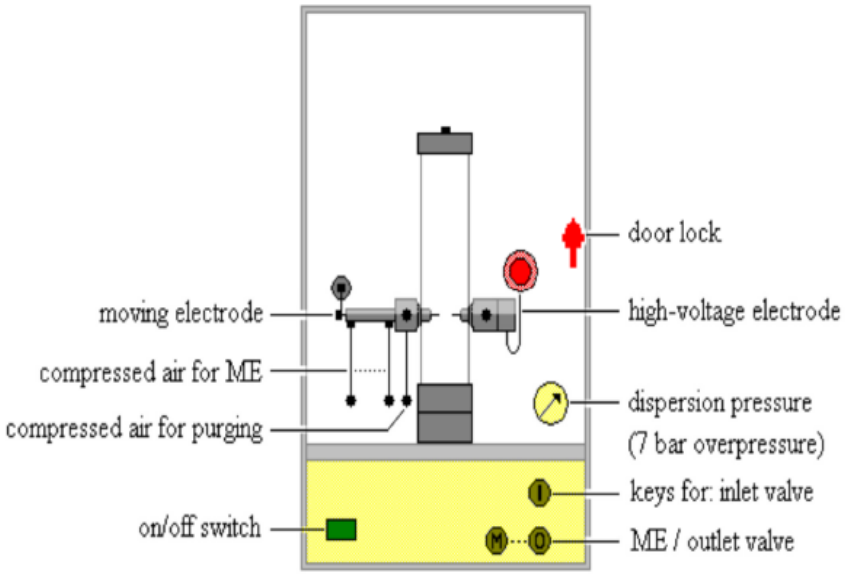

Front view

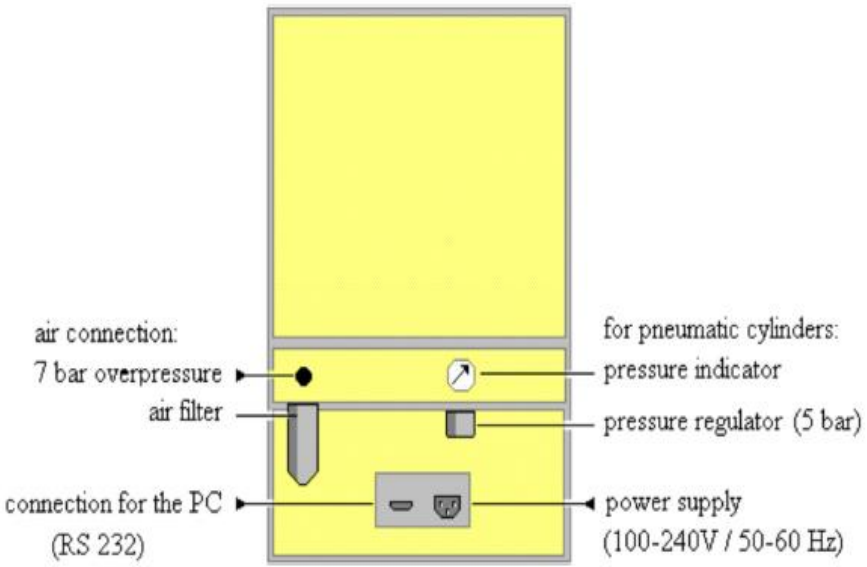

Back view

Figure 3.11: Schematic of the MIKE-3 apparatus showing both front and back views

Figure 3.12: Photo of MIKE-3 apparatus

The apparatus also has different delay-time settings which allow the dust ignition to occur at varying turbulence levels. The typical delay-times settings for the apparatus are 60, 90,120, 150, and 180 ms. Tests can be conducted either with inductance (1 mH) or without inductance (0 mH). The apparatus is automated and controlled with the MIKE-3.3f software from Kühner which initiates the test and ensures that the correct ignition energy, delay time, and inductance are applied.

3.3.13 Experimental procedure to determine MIE in the MIKE-3 apparatus

Experimental procedures for all dusts in this work (i.e., niacin, lycopodium, fine PE and coarse PE) were conducted in accordance with ASTM E2019-03 [44]. Prior to testing, both the glass tube and dispersion system were visually inspected to certify that they are clean. A test check without dust was initiated to ensure accurate dispersion pressure, spark discharge, and the dispersion system was free of any previous dust. With the use of a glass rod the electrode spacing was set to 6 mm.

The test was initiated at conditions where there was high probability of an ignition. Usually, an initial sample mass of 900 g was weighed and placed into the dispersion cup. Testing was conducted with dust amounts typically in the range from 300 to 3600 mg. The dust concentration (g/m^3), ignition energy (mJ), delay time (ms), and inductance (mH) were all set into the MIKE-3.3f software. The testing sequence was then initiated using the software. The dust was dispersed to create a dust cloud, then a spark is generated after the initial delay time (120 ms) to ignite the cloud and create an explosion. Determining whether there was an explosion or not was by visual observation. An explosion was said to have occurred when flame propagation was more than 6 cm from the electrodes. If an ignition occurred, it was confirmed by choosing 'YES' in the software and the test was deemed complete for that set conditions. Testing was continued at the same dust concentration but with a lower ignition energy. If on the other hand, no ignition occurred, it was also confirmed by choosing 'NO' in the software and more trials were required.

For lower dust concentration, the sample was changed after three consecutive, non-ignitable trials. For a given test to be considered non-ignitable at that specific energy and concentration, a total of ten consecutive non-ignitions were required. The procedure was repeated at higher and lower dust concentrations at the ignition energy of no ignition to confirm non-ignition at that ignition energy. The MIE lies between the lowest energy value at which there was ignition (E2) and the energy at which no ignition (E1) was observed (i.e., E1<MIE<E2). An in-built algorithm in the MIKE 3.3f software was able to extrapolate the MIE and give a single value referred to as the "Statistic Energy" (E_S). Once the MIE was found, the test was repeated at varying delay times. The delay times chosen for the testing in the current study were 90, 120, and 150 ms. Following testing at different delay times, the procedure was repeated by changing the inductance setting. The MIE for the dust cloud without inductance was also determined for all dust samples and was in many instances different from that obtained with inductance.

3.3.14 BAM oven

At the Dalhousie University Dust Explosion Laboratory, tests to determine minimum autoignition temperature were conducted using a BAM oven in accordance with ASTM

E1491 [45]. The purpose of this test is to find the lowest temperature at which the dust cloud will ignite when in contact with a heated surface. The furnace was designed in Berlin, Germany by Bundesanstalt für Materialforschung und prüfung (BAM). A schematic and photo of the BAM oven can be seen in Figure 3.13 and Figure 3.14 respectively.

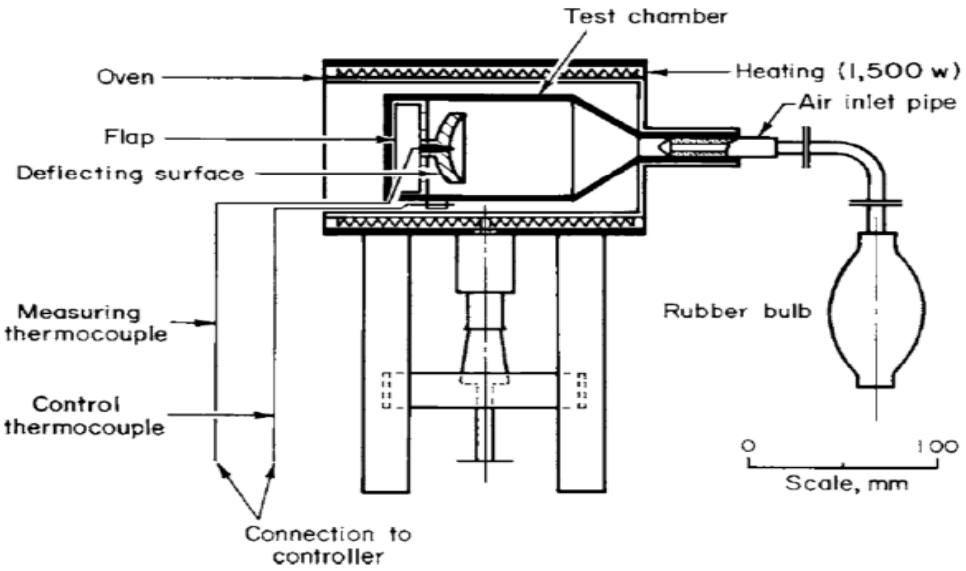

Figure 3.13: Schematic of the BAM oven

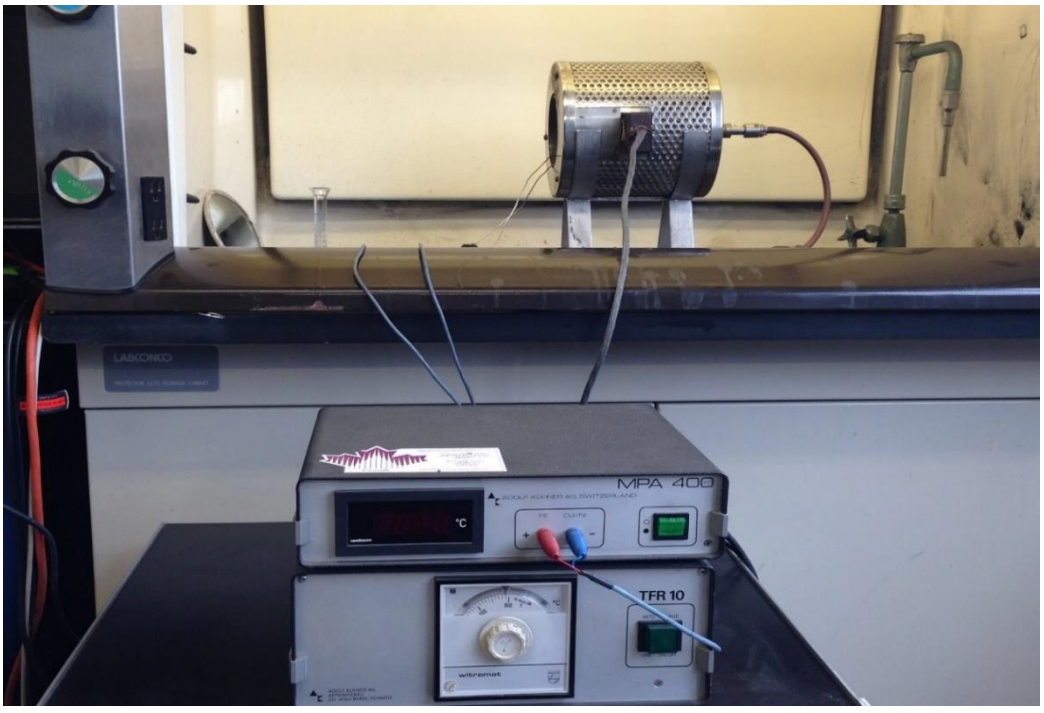

Figure 3.14: Photo of BAM Oven and electricals

3.3.15 Equipment description

The BAM oven is a 170 mm long electrically heated pipe-oven, which is horizontally arranged. Approximately in the centre of the oven there is a vertical impact plate which is shaped like a calotte (with diameter 48 mm and surface area 2000 mm^2) at which the temperature is measured. The apparatus has a chamber volume of 0.35 L which is approximated by a cylinder with a diameter (D) of 0.06 m and length (L) of 0.125 m. The test chamber was surrounded by a 1500 W heater enabling the BAM oven walls to reach temperatures up to 600 ºC. Heater temperature was controlled externally, and the temperature was monitored using two thermocouples with an accuracy of +/- 1 ºC. A rubber bulb connected to a nozzle is used to disperse the dust into the furnace. The dust sample is placed in the nozzle, then with the rubber bulb connected, it is squeezed to disperse the dust and create a dust cloud which is ignited by the heated impact plate or the walls.

3.3.16 Test procedure to determine minimum ignition temperature in the BAM oven

The test procedure for determining the minimum ignition temperature of all dust samples in this work was in accordance with ASTM E1491 [45]. The oven was thoroughly cleaned to ensure that there was no residue of the previous material left as this may influence current test results. The oven was then heated to a temperature of 600 ºC and then the heating is stopped at this temperature and allowed to fall. The test is initiated when the temperature drops to 590 ºC.

Once this desired starting temperature was reached, a premeasured dust of 1 ml of was placed in the dispersion nozzle and then connected to the rubber bulb. A dust cloud was then generated by squeezing the rubber bulb which directed the dust against the circular concave impact plate. The dust cloud upon contact with the plate and the walls of the chamber heats up rapidly. A strategically placed mirror observes the production of a flame from the chamber. Observation of a flame exiting the flap at the rear of oven within 5 seconds of dust dispersion was considered an ignition event.

If an ignition occurred, the oven temperature was recorded and then reduced by 10 ºC followed by re-testing the same dust concentration at the new lower temperature. This procedure is repeated until no ignition was observed. The oven was then cooled and

cleaned for a subsequent testing series. To confirm test results, the non-ignition point was then confirmed similarly with 0.5 and 2 ml of dust. If both volumes resulted in a non-ignition point, the MIT was recorded as the last ignition temperature. If ignition occurred at any of the volumes, then the temperature was further reduced by 10 ºC and testing continued until there was no ignition to ensure that the MIT was recorded at the lowest ignition temperature as possible. The MIT of the dust cloud was then reported as the lowest temperature at which flame was observed exiting the oven's flap. The apparatus was then allowed to cool to room temperature and cleaned thoroughly for subsequent testing with other dust samples.

CHAPTER 4: RESULTS

This chapter gives a graphical representation of the all results for explosion severity and explosion likelihood obtained during the current experimental campaign, including calibration results. These include all P_{max}, $(dP/dt)_{max}$, and MEC results gathered in both the 20-L and the 1-m^3 explosion chambers, MIE results from the MIKE-3 apparatus, and MIT results gathered from the BAM oven. The complete numerical data are found in tabular form in the Appendix A to Appendix G.

4.1 Calibration Results

This section presents calibration results obtained for all parameters and all test apparatus using the three reference dust samples mentioned in section 3.3.1. The explosion severity results obtained in the 20-L chamber are given in Figure 4.1 to Figure 4.3 (and the data tables are provided in Appendix A.1 to A.20). The MEC results obtained during calibration of the 20-L vessel can be seen in Figure 4.4 to Figure 4.6. Also, calibration MIE results for the MIKE-3 apparatus are presented in Figure 4.7 to 4.9. The calibration results obtained in the BAM oven can also be found in Figures 4.10 to 4.12.

4.1.1 Results of 20-L chamber calibration

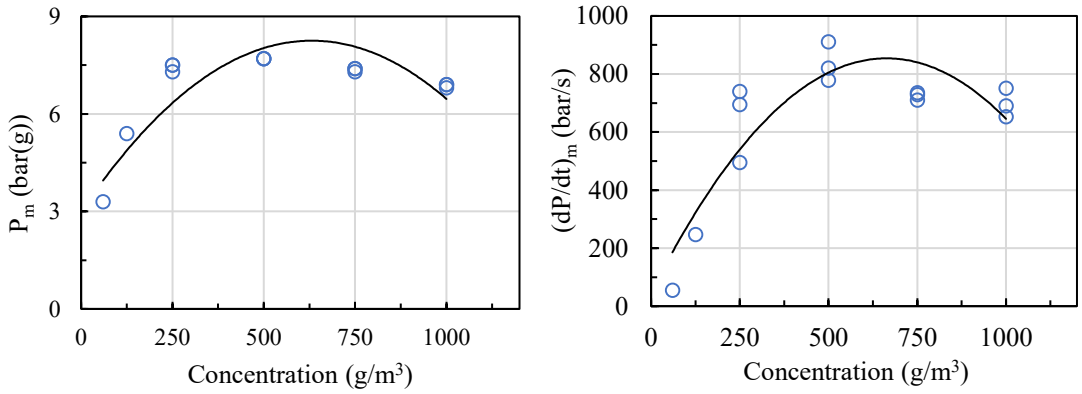

Figure 4.1: 20-L chamber calibration plots of P_m and $(dP/dt)_m$ with niacin using 10-kJ ignition energy

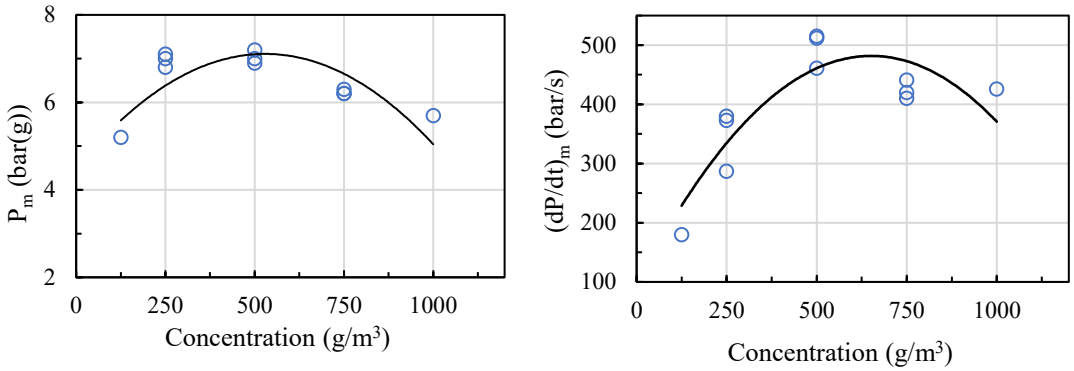

Figure 4.2: 20-L chamber calibration plots of P_m and $(dP/dt)_m$ with lycopodium using 10-kJ ignition energy

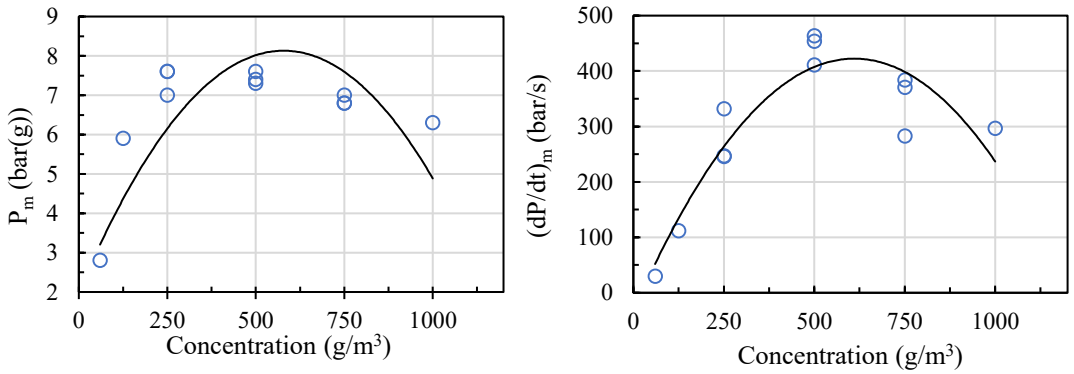

Figure 4.3: 20-L chamber calibration plots of P_m and $(dP/dt)_m$ with Pittsburgh coal using 10-kJ ignition energy

4.1.2 Calibration results for MEC in the 20-L chamber

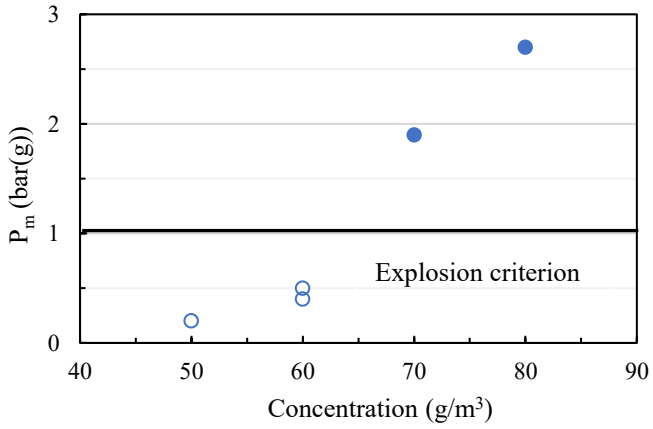

Figure 4.4: 20-L chamber calibration MEC results with niacin using 2.5-kJ ignitor

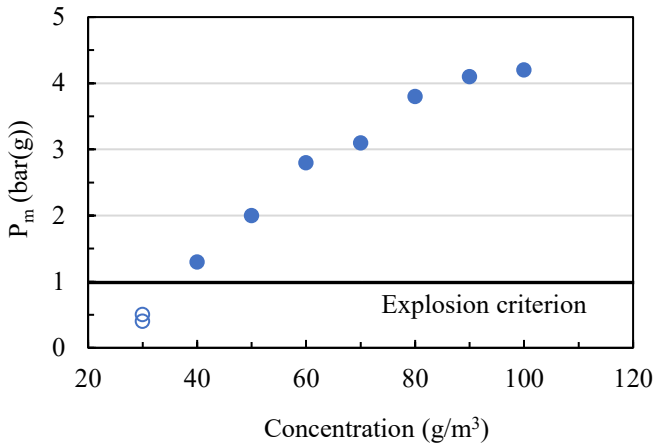

Figure 4.5: 20-L chamber calibration MEC results with lycopodium using 2.5-kJ ignitor

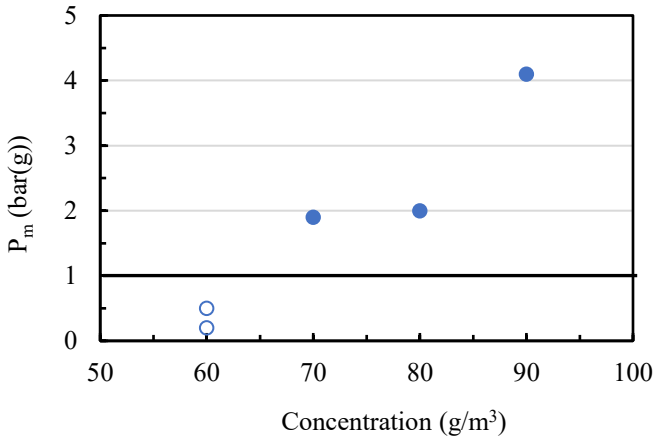

Figure 4.6: 20-L chamber calibration MEC results with Pittsburgh coal using 2.5-kJ ignitor

4.1.3 Calibration results in MIKE-3 apparatus

The MIE results were obtained in the MIKE-3 apparatus with varying concentration of the dust samples. Testing was done at three ignition delay times (i.e., 90, 120 and 150 ms). In the graph, an ignition is indicated by a filled data point while an unfilled data point represents non-ignition at the selected conditions. The test was also conducted with and without the application of inductance. Tests with inductance could be seen on the left while those without inductance could be seen on the right.

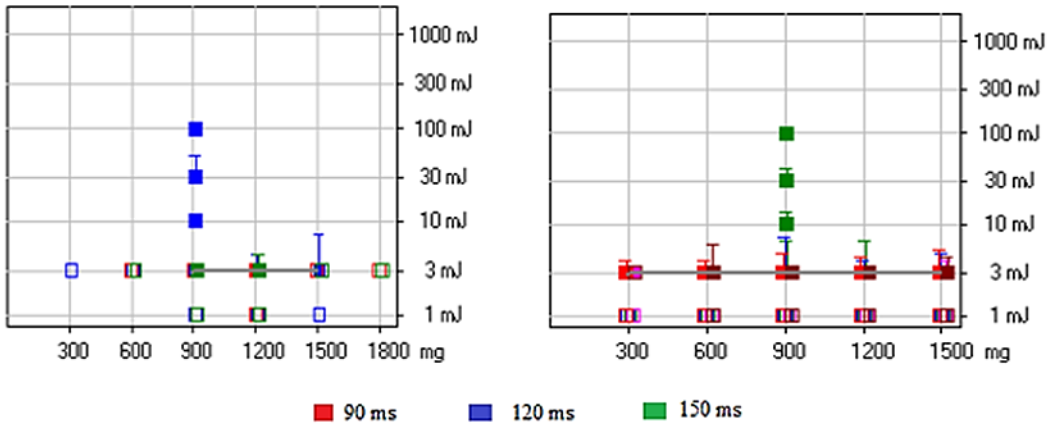

Figure 4.7: Calibration MIE of niacin with (left) and without (right) inductance at different delay times

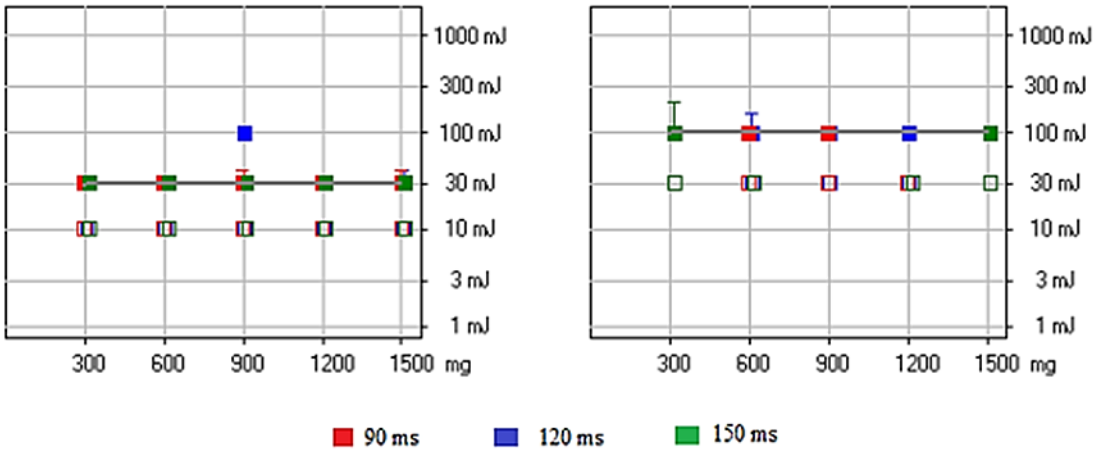

Figure 4.8: Calibration MIE of lycopodium with (left) and without (right) inductance at different delay times

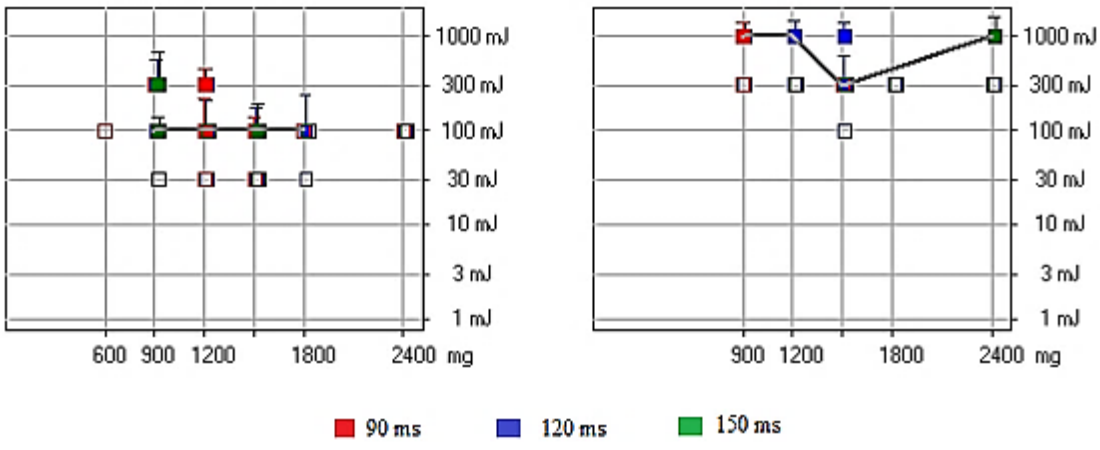

Figure 4.9: Calibration MIE of Pittsburgh coal with (left) and without (right) inductance at different delay times

4.1.4 Calibration results for MIT in BAM oven

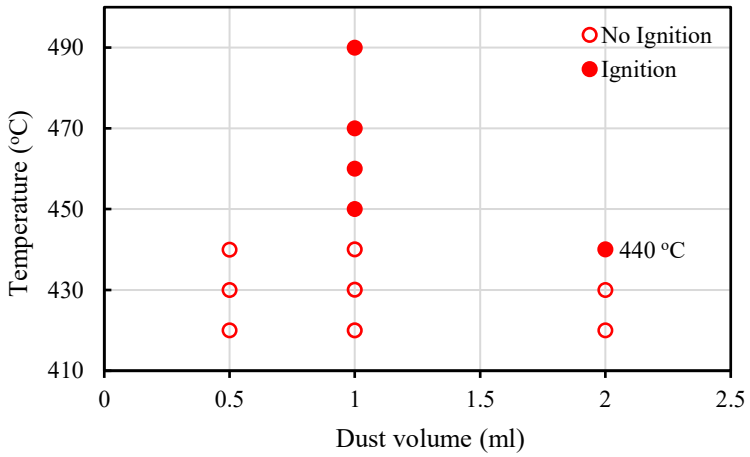

Figure 4.10: Calibration of the BAM oven with niacin dust

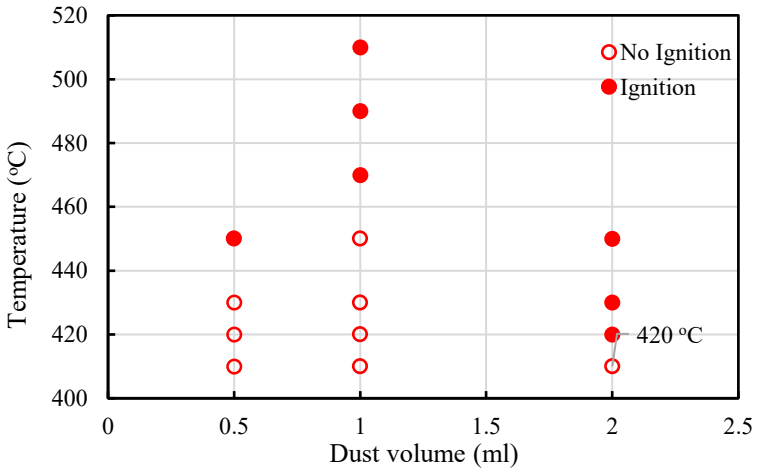

Figure 4.11: Calibration of BAM oven with lycopodium

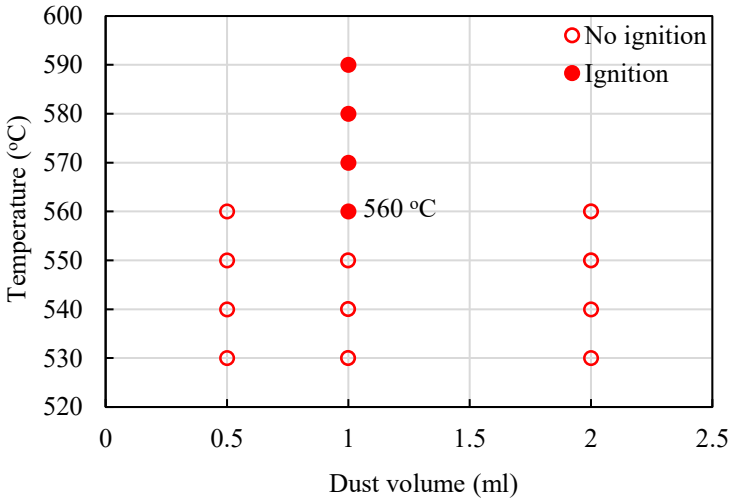

Figure 4.12: Calibration of BAM oven with Pittsburgh coal

4.2 Explosion Severity Results in the Siwek 20-L Explosion Chamber

This section presents the explosion severity data obtained from the 20-L chamber with three different ignition energies for all four dust samples. For each sample, the explosion pressure (P_m) and maximum rate of pressure rise $(dP/dt)_m$ over a range of concentrations were recorded. Tests were repeated at the concentration(s) where the maximum (or highest P_m and $(dP/dt)_m$) values were obtained. A third series was obtained by following the preceding step based on where the maxima values occurred in series two. The detailed severity results (indicating each trial) for all samples at different ignition energies can be seen in Figure 4.13 to Figure 4.24. The data tables for these results are also presented in Appendix B (i.e., Table B.1 to B.27).

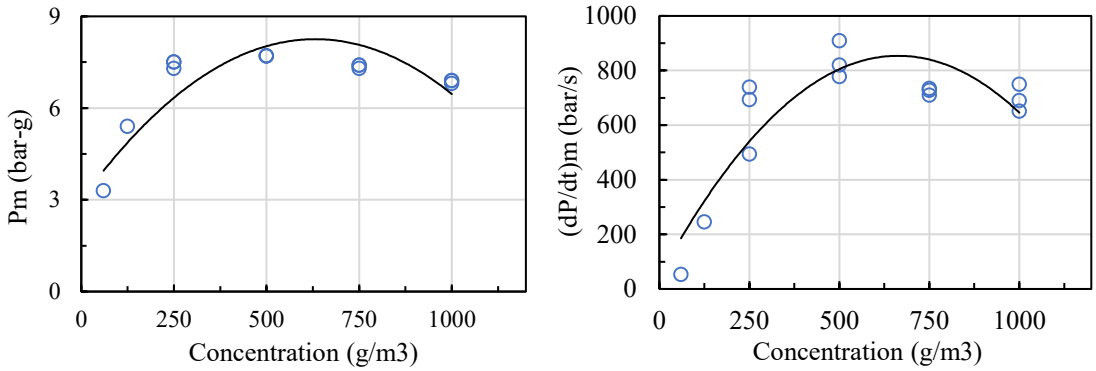

Figure 4.13: Plots of explosion pressure (P_m) and rate of pressure rise $(dP/dt)_m$ at various niacin dust concentrations in the 20-L chamber with 10-kJ ignition energy

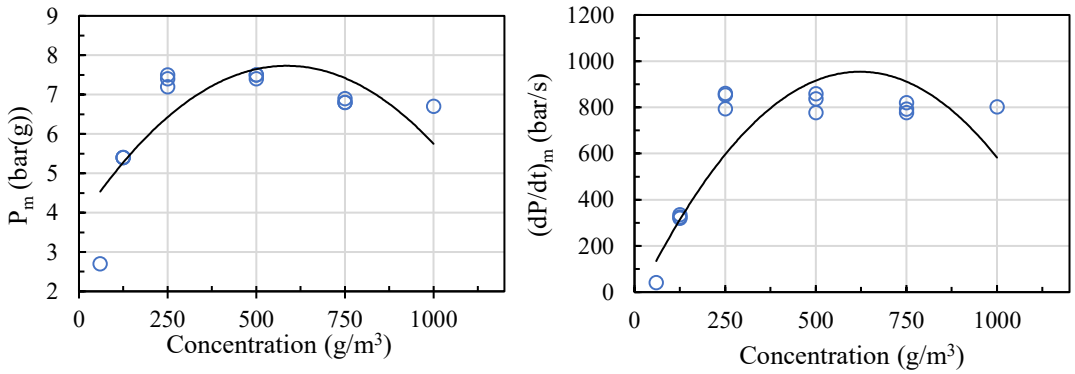

Figure 4.14: Plots of explosion pressure (P_m) and rate of pressure rise $(dP/dt)_m$ at various niacin dust concentrations with 5-kJ ignition energy in the 20-L chamber

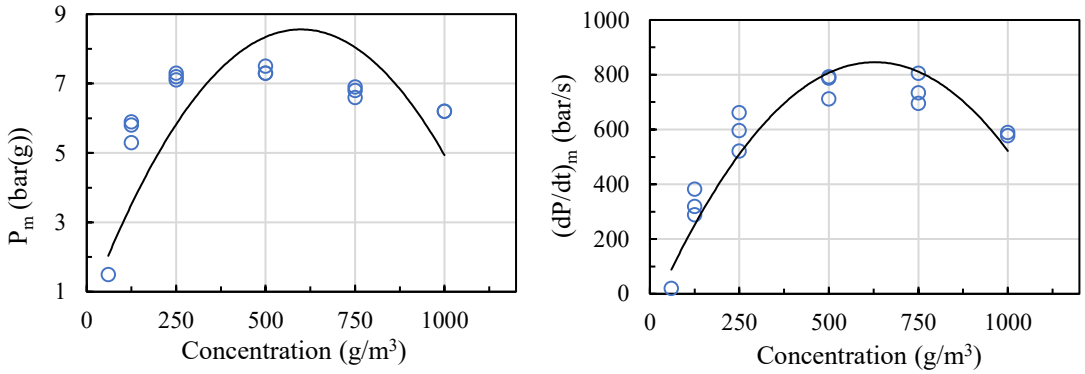

Figure 4.15: Plots of explosion pressure (P_m) and rate of pressure rise $(dP/dt)_m$ at various niacin dust concentrations with 2.5-kJ ignition energy in the 20-L chamber

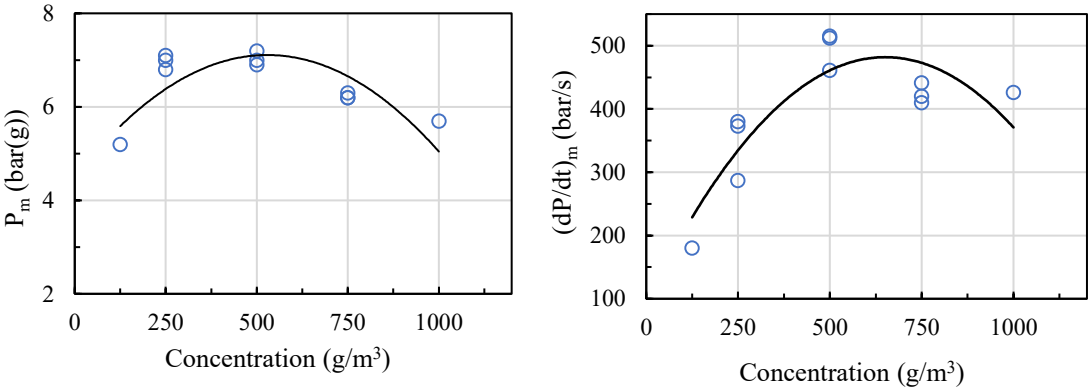

Figure 4.16: Plots of explosion pressure (P_m) and rate of pressure rise $(dP/dt)_m$ at various lycopodium dust concentrations with 10-kJ ignition energy in the 20-L chamber

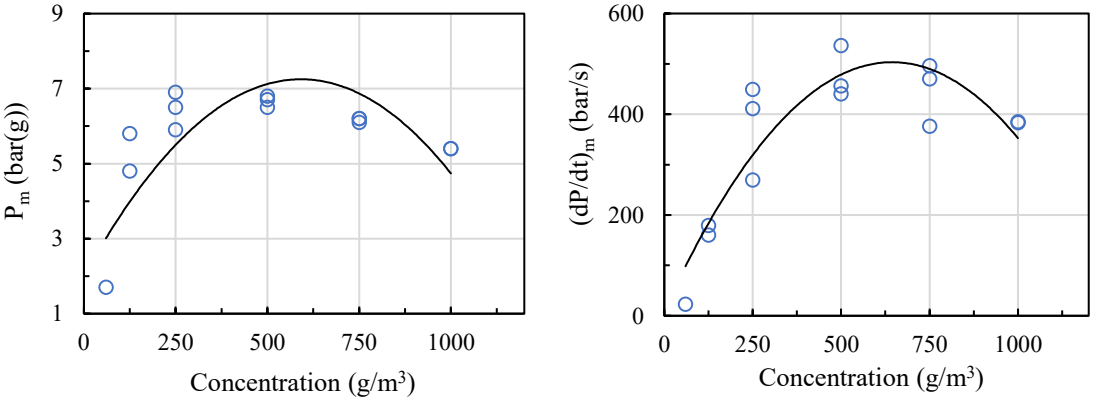

Figure 4.17: Plots of explosion pressure (P_m) and rate of pressure rise $(dP/dt)_m$ at various lycopodium dust concentrations with 5-kJ ignition energy in the 20-L chamber

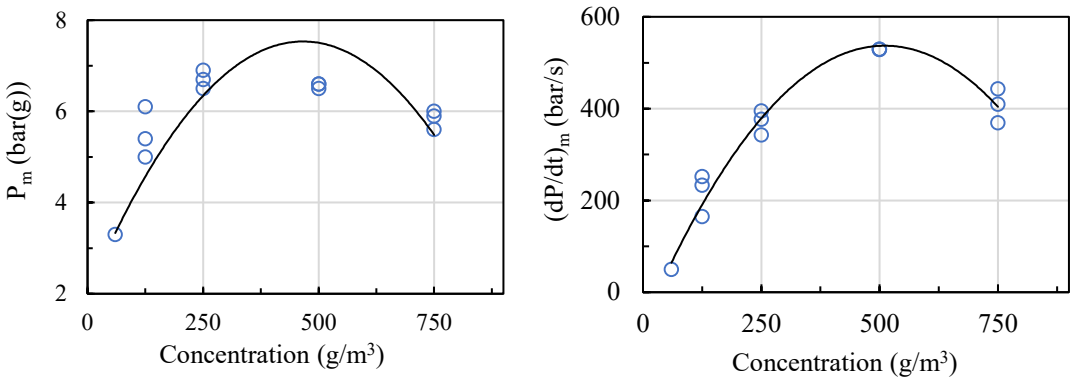

Figure 4.18: Plots of explosion pressure (P_m) and rate of pressure rise $(dP/dt)_m$ at various lycopodium dust concentrations with 2.5-kJ ignition energy in the 20-L chamber

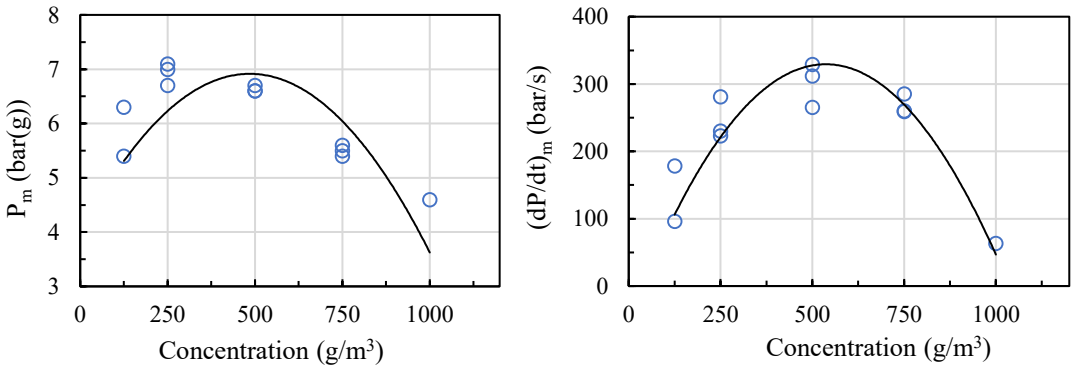

Figure 4.19: Plots of explosion pressure (P_m) and rate of pressure rise $(dP/dt)_m$ at various fine polyethylene dust concentrations with 10-kJignition energy in the 20-L chamber

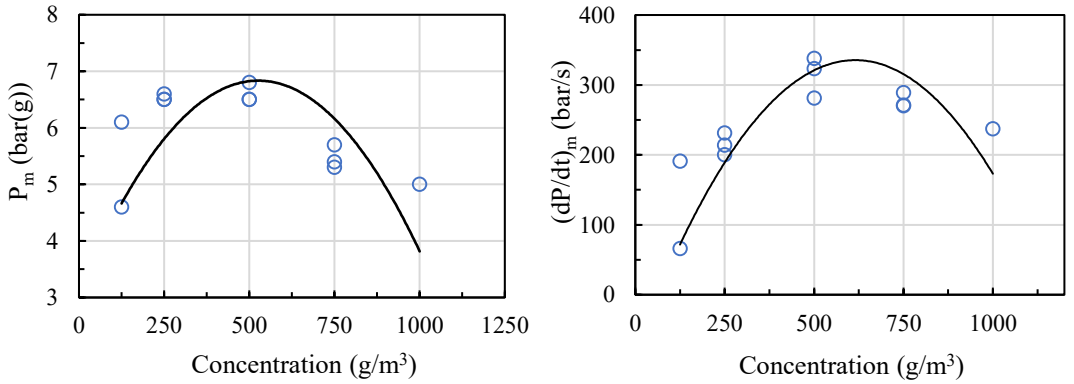

Figure 4.20: Plots of explosion pressure (P_m) and rate of pressure rise $(dP/dt)_m$ at various fine polyethylene dust concentrations with 5-kJ ignition energy in the 20-L chamber

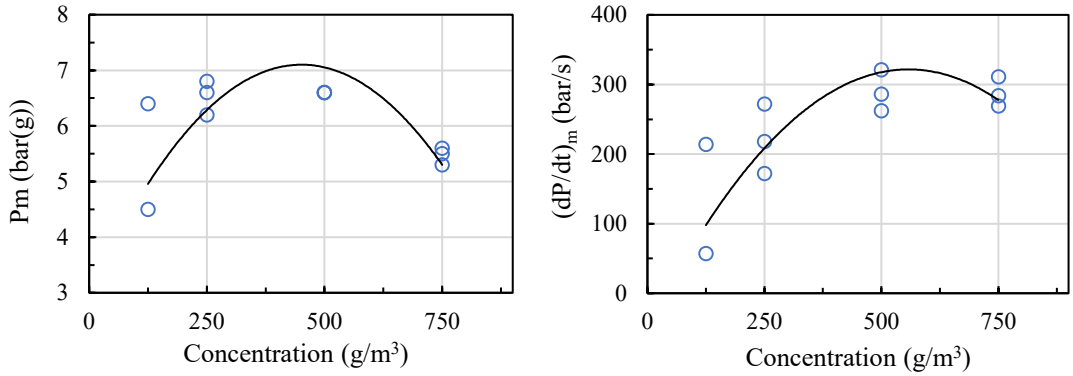

Figure 4.21: Plots of explosion pressure (P_m) and rate of pressure rise $(dP/dt)_m$ at various fine polyethylene dust concentrations with 2.5-kJ ignition energy in the 20-L chamber

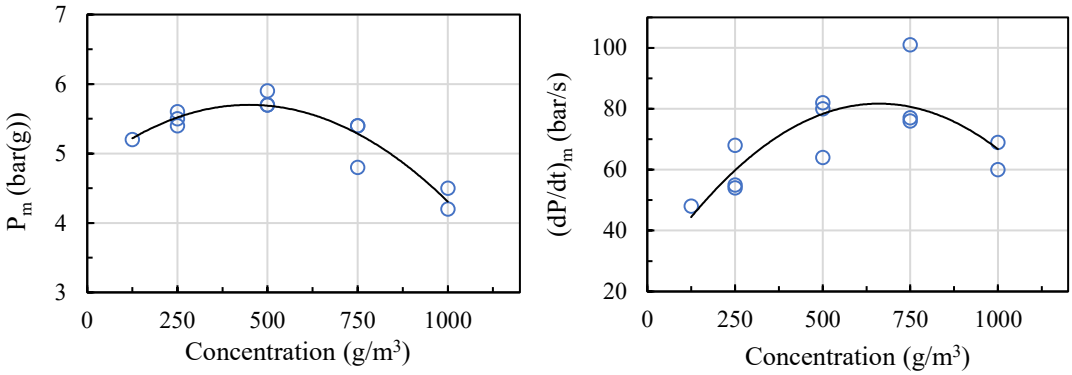

Figure 4.22: Plots of explosion pressure (P_m) and rate of pressure rise $(dP/dt)_m$ at various coarse polyethylene dust concentrations with 10-kJ ignition energy in the 20-L chamber

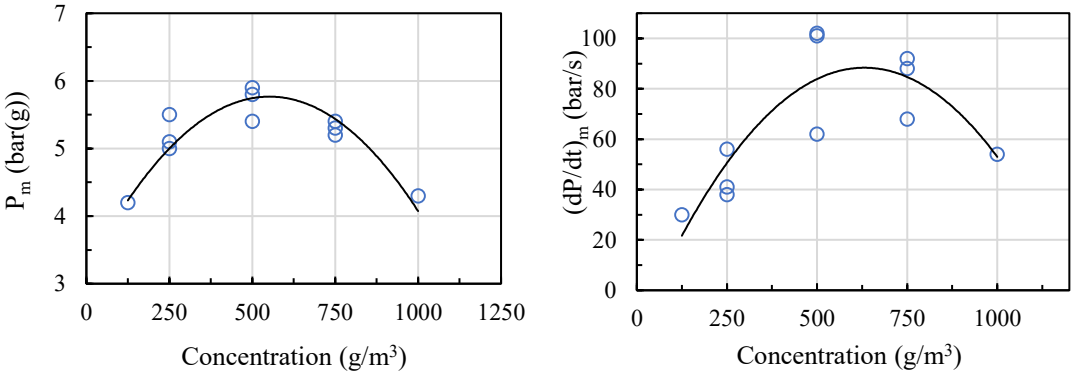

Figure 4.23: Plots of explosion pressure (P_m) and rate of pressure rise $(dP/dt)_m$ at various coarse polyethylene dust concentrations with 5-kJ ignition energy in the 20-L chamber

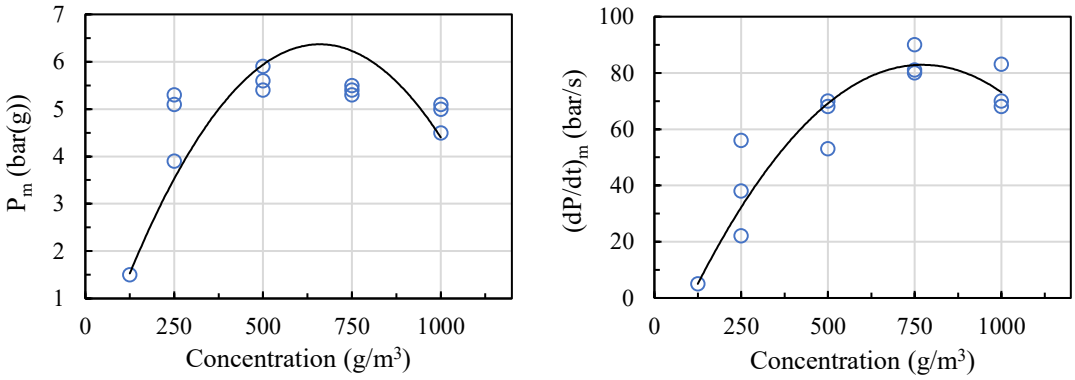

Figure 4.24: Plots of explosion pressure (P_m) and rate of pressure rise $(dP/dt)_m$ at various coarse polyethylene dust concentrations with 2.5-kJ ignition energy in the 20-L chamber

4.3 Explosion Severity Results in the 1-m³ Chamber at Time Ignition Delay Time of 550 ms

Following tests in the 20-L chamber, companion tests were conducted with all dust samples in the 1-m³ chamber using 10-kJ ignition energy at 550 ms. The P_m and $(dP/dt)_m$ at each concentration was recorded and are presented in graphical form in Figure 4.25 to Figure 4.28. These results can be found in tabular form in Table C.1 to Table C.4 (in Appendix C).

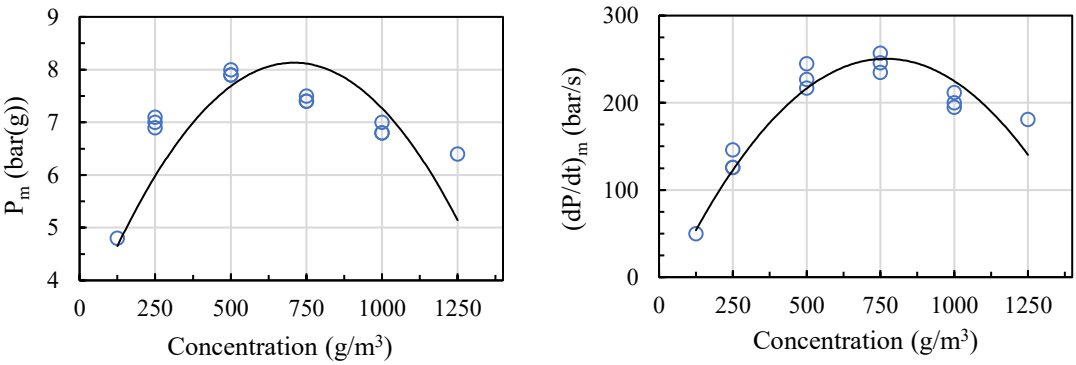

Figure 4.25: Plots of explosion pressure (P_m) and rate of pressure rise $(dP/dt)_m$ at various niacin dust concentrations with 10-kJ ignition energy in the 1-m³ chamber at 550 ms

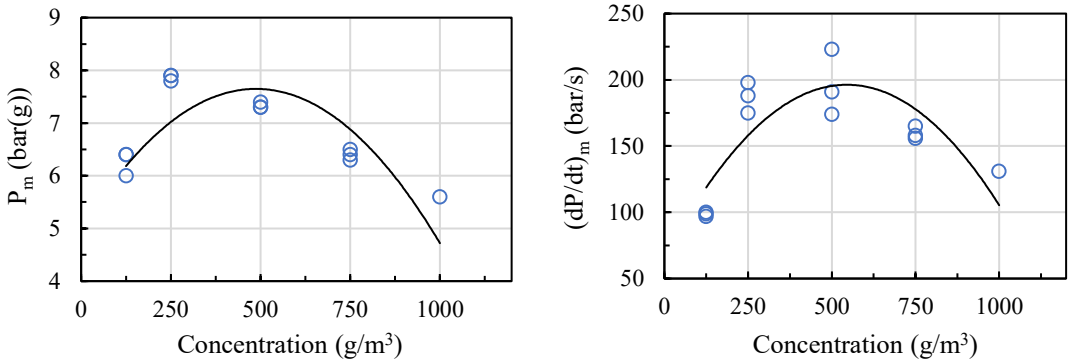

Figure 4.26: Plots of explosion pressure (P_m) and rate of pressure rise $(dP/dt)_m$ at various lycopodium dust concentrations with 10-kJ ignition energy in the 1-m^3 chamber at 550 ms

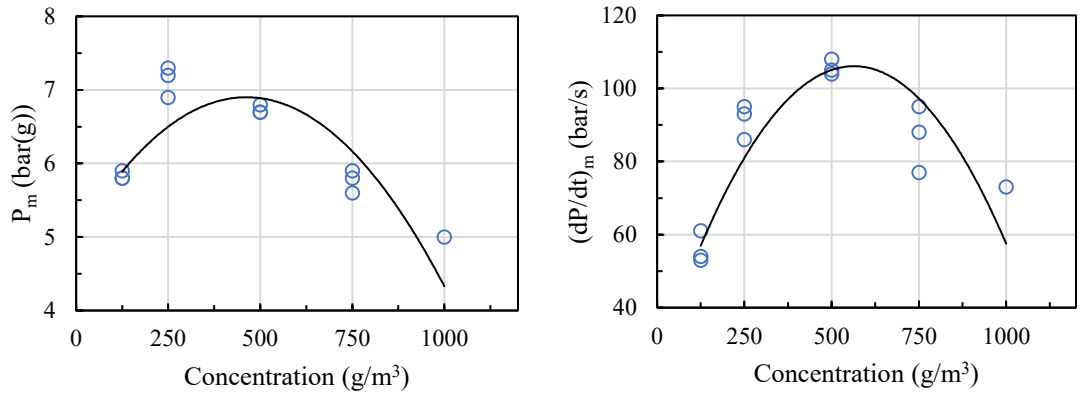

Figure 4.27: Plots of explosion pressure (P_m) and rate of pressure rise $(dP/dt)_m$ at various fine polyethylene dust concentrations with 10-kJ ignition energy in the 1-m^3 chamber at 550 ms

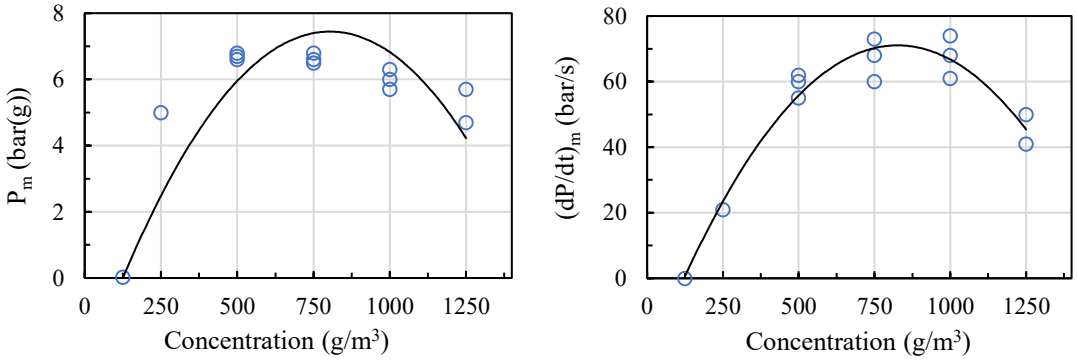

Figure 4.28: Plots of explosion pressure (P_m) and rate of pressure rise $(dP/dt)_m$ at various coarse polyethylene dust concentrations with 10-kJ ignition energy in the 1-m^3 chamber at 550 ms

4.4 Explosion Severity Results in the 1-m^3 Chamber at Time Delay of 600 ms

This section presents explosion severity results obtained from the 1-m^3 chamber but with a longer ignition delay time of 600 ms. Further discussion of these results are presented in the next chapter. The data tables for each explosion severity test at 600 ms can be found in Table C.5 to Table C.7 (in Appendix C). Figure 4.29 to 4.31 are graphical representations of the explosion severity of the samples tested.

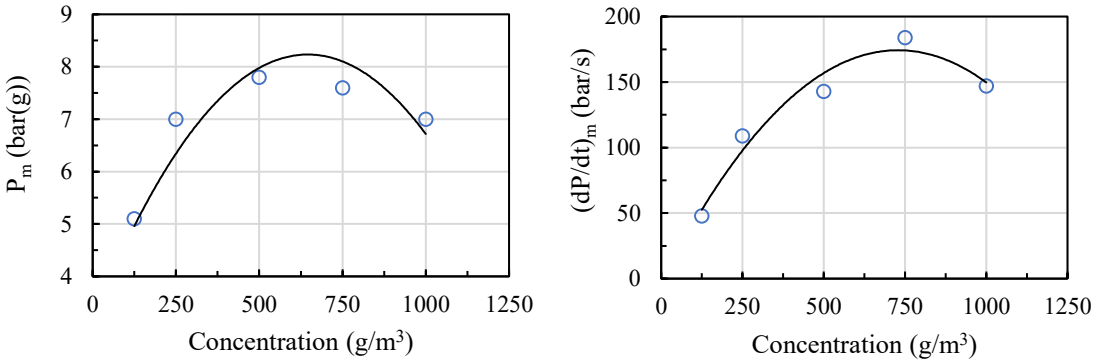

Figure 4.29: Plots of explosion pressure (P_m) and rate of pressure rise $(dP/dt)_m$ at various niacin dust concentrations with 10-kJ ignition energy in the 1-m^3 chamber at 600 ms

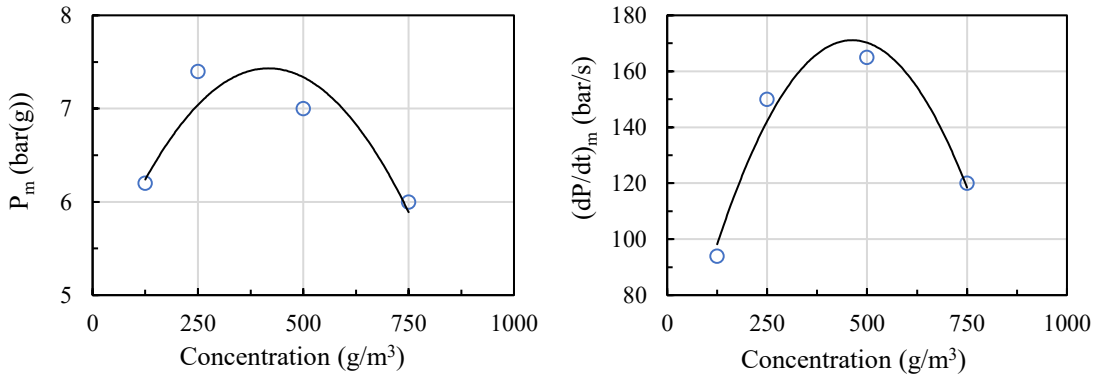

Figure 4.30: Plots of explosion pressure (P_m) and rate of pressure rise $(dP/dt)_m$ at various lycopodium dust concentrations with 10-kJ ignition energy in the 1-m^3 chamber at 600 ms

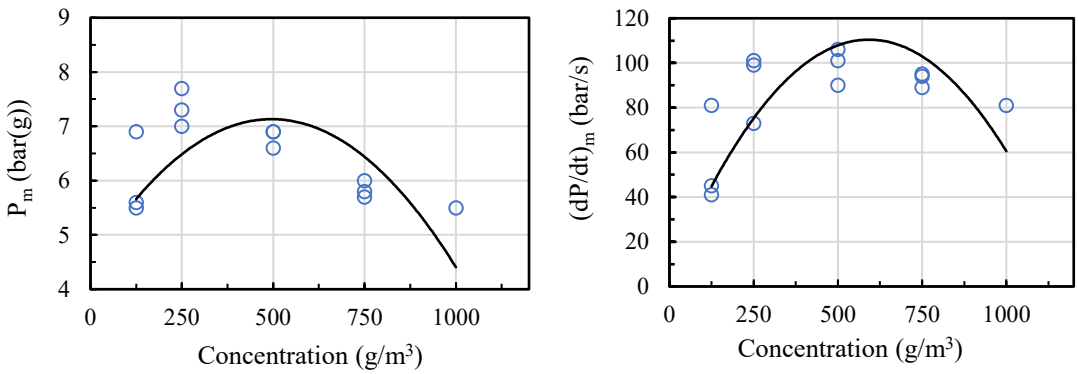

Figure 4.31: Plots of explosion pressure (P_m) and rate of pressure rise $(dP/dt)_m$ at various fine polyethylene dust concentrations with 10-kJ ignition energy in the 1-m^3 chamber at 600 ms

4.5 MEC Results in the 20-L Chamber

This section presents the results for minimum explosible concentration of all dust samples determined in the 20-L chamber using 2.5-kJ ignition source. An explosion criterion of 1 bar was used and indicated on each plot as the bold line. Data points above the bold line (and also unfilled) indicates explosion while those below (and also filled) indicate non-explosible. The MEC of each test is the lowest concentration where last ignition occurred. Further discussions are presented in the next chapter. Figure 4.32 to Figure 4.35 show results for the dust samples in the 20-L chamber. Data tables can be found in Tables D.1 to D.4 (in Appendix D).

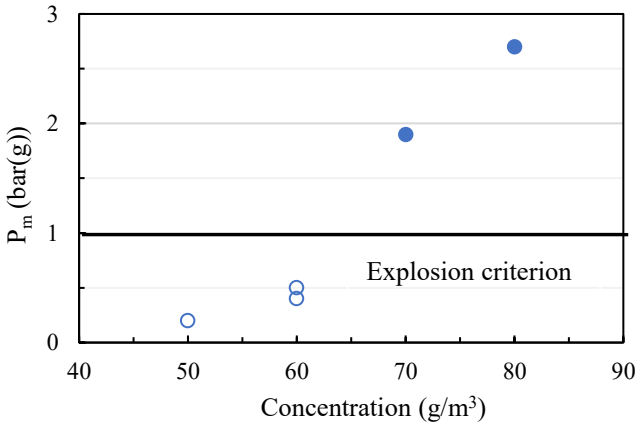

Figure 4.32: MEC of niacin in 20-L chamber with 2.5-kJ ignitor

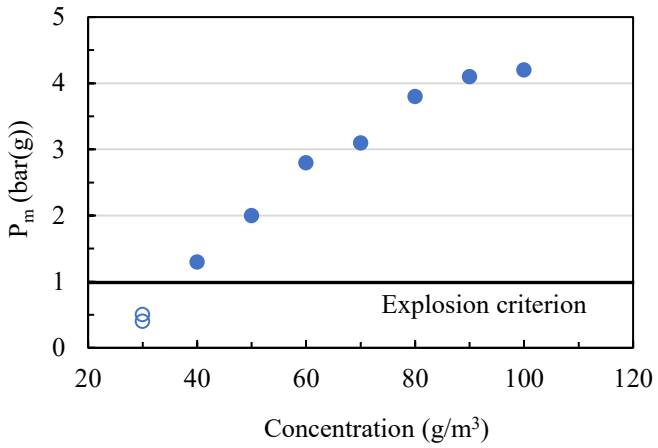

Figure 4.33: MEC of lycopodium in 20-L chamber with 2.5-kJ ignitor

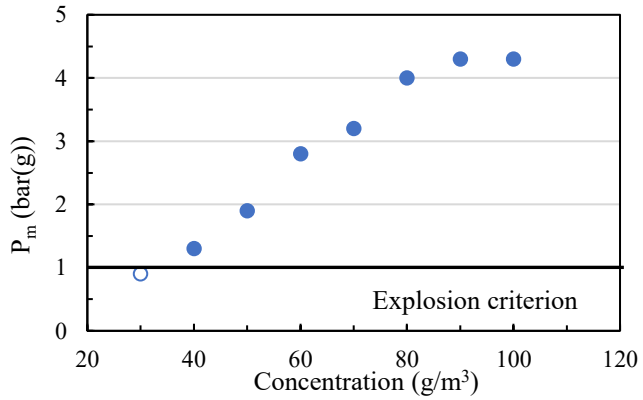

Figure 4.34: MEC of fine polyethylene in 20-L chamber with 2.5-kJ ignitor

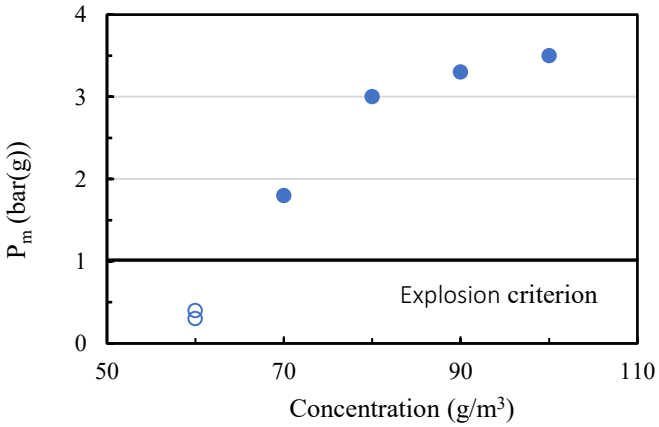

Figure 4.35: MEC of coarse polyethylene in 20-L chamber with 2.5-kJ ignitor

4.6 MEC Results in the 1-m^3 Chamber at Delay Time of 550 ms Using 10-kJ Ignition Energy

The minimum explosible concentration of all samples was also determined in the 1-m^3 using 10-kJ ignition energy at a time delay of 550 ms. The results can be seen graphically in Figure 4.36 to Figure 4.39. Results are also presented in tabular form in Table E.1 to Table E.4 (in Appendix E). The hollow data points indicate non-ignition while the solid points represent ignition.

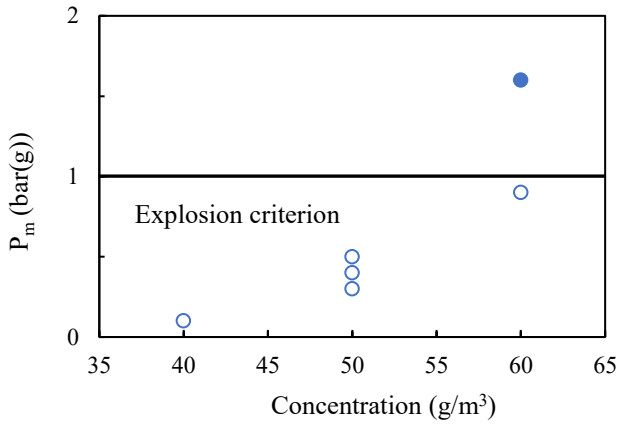

Figure 4.36: MEC of niacin in 1-m^3 chamber using 10-kJ ignition energy at delay time of 550 ms

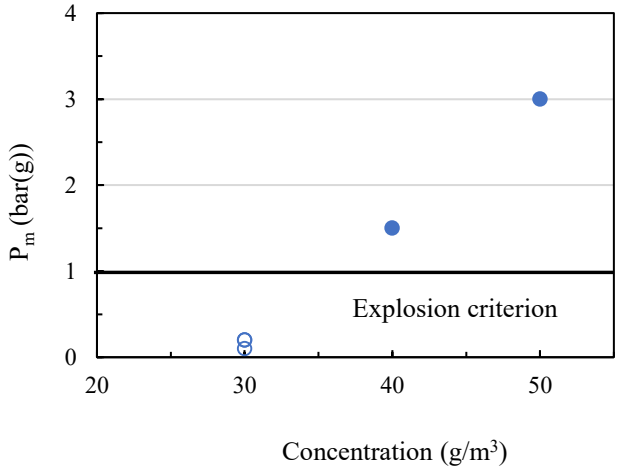

Figure 4.37: MEC of lycopodium in 1-m^3 chamber using 10-kJ ignition energy at delay time of 550 ms

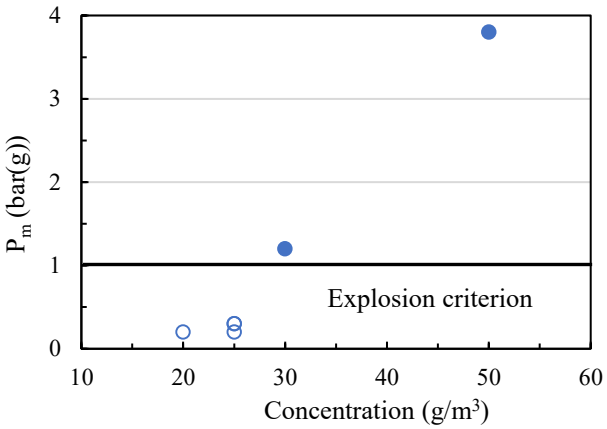

Figure 4.38: MEC of fine polyethylene in 1-m^3 chamber using 10-kJ ignition energy at delay time of 550 ms

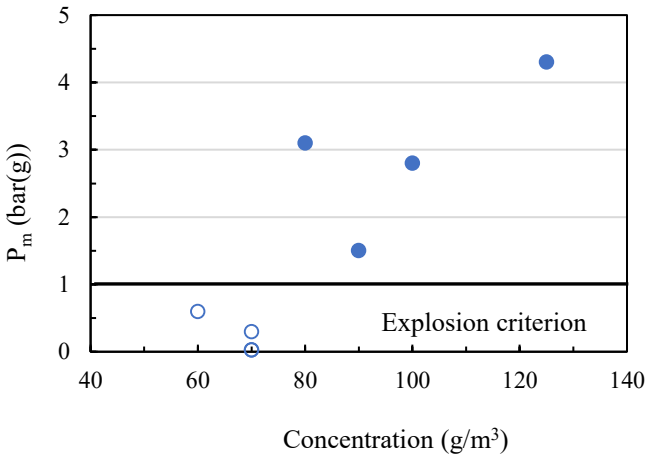

Figure 4.39: MEC of Coarse polyethylene in 1-m^3 chamber using 10-kJ ignition energy at delay time of 550 ms

4.7 MIE Results in the MIKE-3 Apparatus

This section presents all results of minimum ignition energy obtained from the MIKE-3 apparatus. For each dust sample, results are presented with inductance (left) and without inductance (right). Filled data points show ignition at a particular ignition energy and dust concentration while unfilled markers indicate non-ignition at the given conditions. The different data points represent different ignition delay times. The results can be seen in Figure 4.40 to Figure 4.43 in graphical form. Data in Table F.1 to Table F.20 (in Appendix F) represent the MIE data obtained for both non-metallic and metallic samples in the MIKE-3 apparatus with 0-mH and 1-mH inductance.

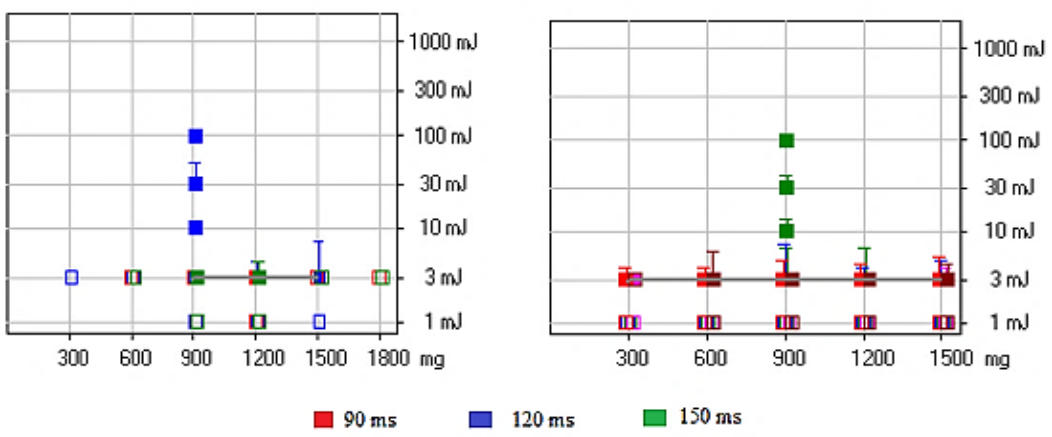

Figure 4.40: MIE of niacin with (left) and without (right) inductance at different delay times

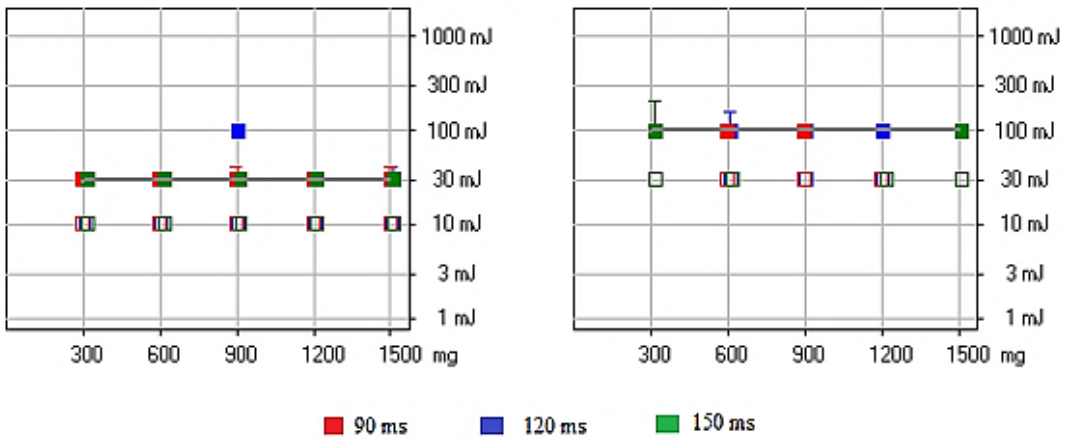

Figure 4.41: MIE of lycopodium with (left) and without (right) inductance at different delay times

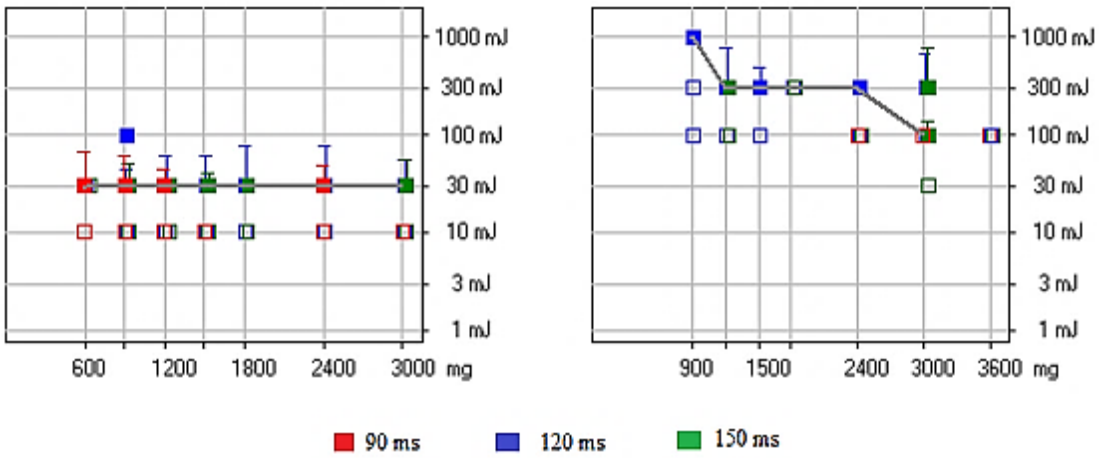

Figure 4.42: MIE of fine polyethylene with (left) and without (right) inductance at different delay times

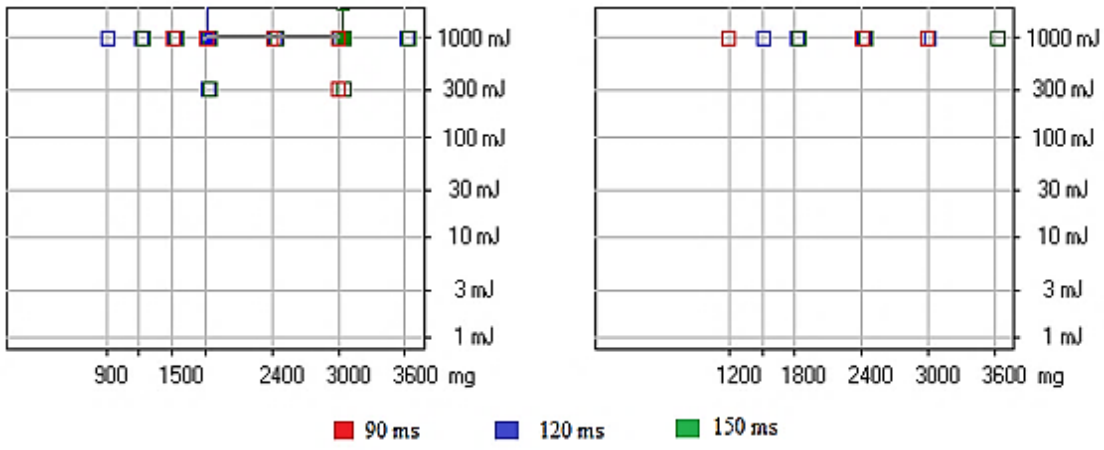

Figure 4.43: MIE of coarse polyethylene with (left) and without (right) inductance at different delay times

4.8 MIT Results in the BAM Oven

The minimum ignition temperature of the four dust samples were determined in the BAM oven and the results presented in this section. A filled data point indicates ignition whiles an unfilled ones mean there was no ignition at that temperature. Discussion of these results are discussed in detail in the next chapter of this thesis. The MIT results are presented in Figure 4.44 to 4.47. Tabulated form of the results (including for metallic samples) can be found in Appendix G in Tables G.1 to G.10.

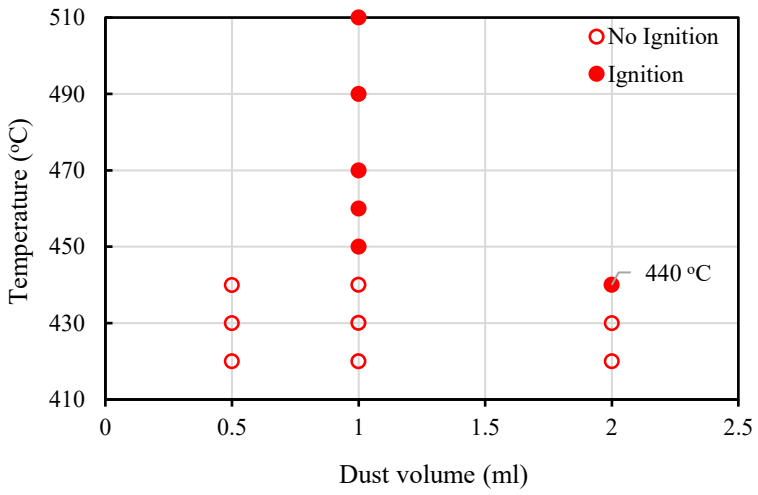

Figure 4.44: MIT of niacin in the BAM oven

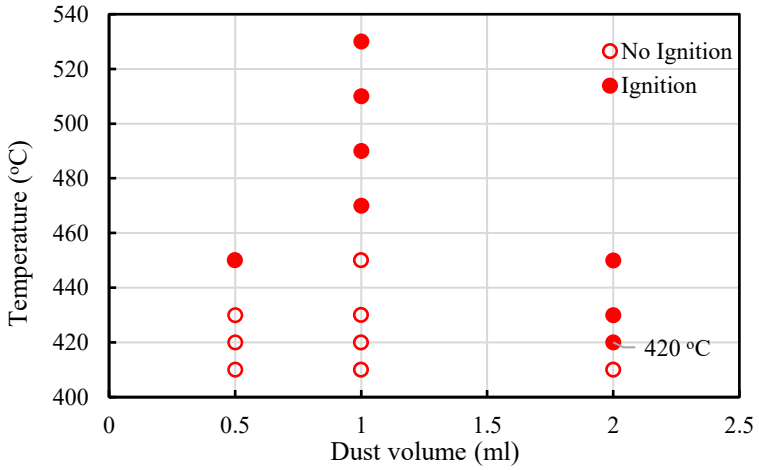

Figure 4.45: MIT of lycopodium in the BAM oven

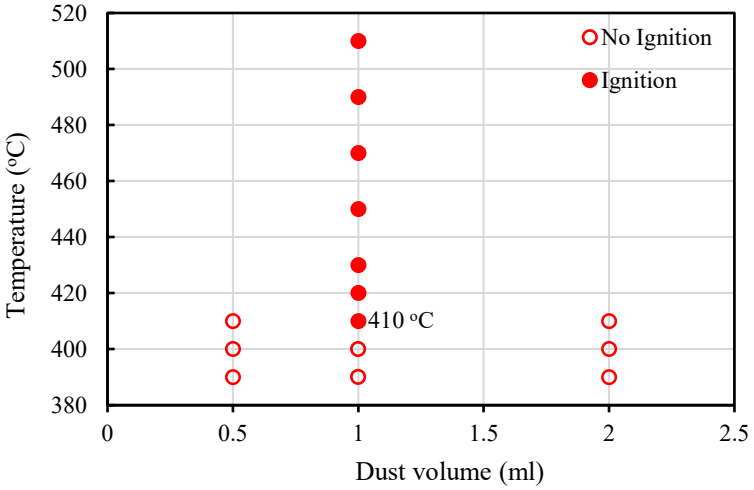

Figure 4.46: MIT of fine polyethylene in the BAM oven

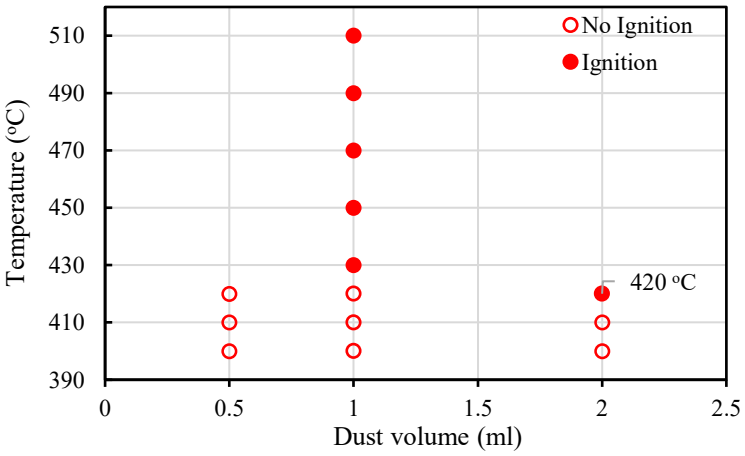

Figure 4.47: MIT of coarse polyethylene

CHAPTER 5: DISCUSSION

The current chapter discusses the inferences of the results and observations of the experimental work, presents graphical comparisons, draws possible correlations, and offers scientific explanations for these observations. Summary graphs of the results presented in Chapter 4 are presented in this current chapter, comparisons made, and explanations provided.

5.1 Explosion Severity

In assessing the explosion severity of combustible dusts, knowledge about parameters such as the P_{max}, $(dP/dt)_{max}$ and the K_{St} is imperative. Detailed information about these parameters is vital for the establishment of safety boundaries of any type of equipment used during processing, handling, storing, and transporting of combustible dusts. Specifically, the information obtained from these parameters is utilized by process equipment manufacturers to corroborate the strategies of dust explosion protection systems such as explosion containment, explosion venting, explosion suppression and isolation.

This section presents a detailed discussion of the results obtained for the explosion severity parameters ((P_{max}), $(dP/dt)_{max}$ and K_{St}) of all four organic dusts: niacin, lycopodium, fine polyethylene and coarse polyethylene, on the two test scales (i.e., 20-L and 1-m^3 chambers). In the 20-L chamber, experiments were conducted with three different ignition energies (i.e., 2.5, 5, 10 (2×5 kJ)), at the same set ignition delay time of 60 ms. In the 1-m^3 explosion chamber, experiments were conducted only with 10-kJ (i.e., 2×5-kJ) "Sobbe" chemical ignitors at two different ignition delay times (of 550 ms and 600 ms).

5.1.1 Explosion severity (P_{max}, $(dP/dt)_{max}$ and K_{St}) in the 20-L chamber

Figure 5.1 shows the summary of results obtained (from Figure 4.13 to 4.24) in the 20-L explosion chamber for the explosion pressure (P_m) and volume-normalized maximum rate of pressure rise ($(dP/dt)_m \cdot V^{1/3}$) values at the different concentrations tested for all four dusts. The data points are averages of the data points presented in section 4.2 for

each sample. The maximum or highest P_m and $(dP/dt)_m \cdot V^{1/3}$ values are the maximum explosion pressure (P_{max}) and volume-normalized maximum rate of pressure rise (K_{St}) respectively for the particular sample. That is, the highest P_m is the P_{max} while the highest $(dP/dt)_m \cdot V^{1/3}$ is the K_{St} of the sample obtained over a series of tests. Only tests with ignition energy of 10 kJ are presented in Figure 5.1. The P_{max} and K_{St} values determined with 5-kJ and 2.5-kJ ignition energies were solely included in the experimental work for comparison purposes, whereas those determined with 10 kJ were considered for actual comparison with the 1-m^3 results and other analyses. This is because only values determined with an ignition energy of 10 kJ are considered as suitable for the design of explosion prevention and protection measures. From the graph, it can be deduced that niacin recorded the highest values in terms of both P_{max} and K_{St} while coarse polyethylene recorded the lowest values. This behavior is consistent with known trends in accordance with relevant physical and chemical properties of the materials used.

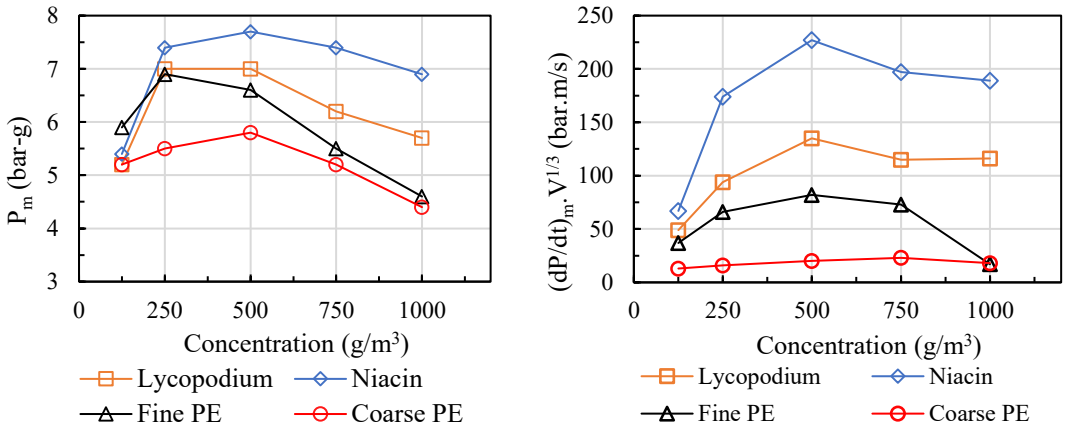

Figure 5.1: Summary of explosion parameters (P_m and $(dP/dt)_m \cdot V^{1/3}$) in the 20-L chamber using 10-kJ ignition energy

The explosion severity parameters are influenced by physical factors such as the particle size, density, specific surface area, moisture content, etc. They are also influenced by the chemical composition of the material, volatile content, heat of combustion (or calorific value), ash content, etc. For instance, the results displayed expected trends with respect to composition, with P_{max} and K_{St} increasing in moving from polyethylene → lycopodium → niacin (which is a refined chemical). Further, a similar trend was seen in terms of particle size, with P_{max} and K_{St} increasing in moving from coarse polyethylene → fine polyethylene.

P_{max} and K_{St} values were also determined in the 20-L chamber using 5-kJ and 2.5-kJ chemical ignitors. Figure 5.2 to 5.5 shows the explosion severity of all four dusts at the different ignition energies. Ignition energy is seen to have minimal effect on P_{max} and K_{St} values for all four samples. It can be noted that P_{max} value decreases by at most 4% as ignition energy is decreased from 10 kJ to 5 kJ and then 2.5 kJ. The K_{St} values either remains virtually unchanged with respect to fine and coarse polyethylene, or increases in the case of lycopodium, or decreases for niacin by 7%, with the same range of decreasing ignition energy. Given the recommendations on reproducibility found in ASTM E1226-12a [28], it can be concluded from the results that the values of P_{max} and K_{St} for a specific test material were statistically the same for all three ignition energies. The reason could be that, once combustion of the cloud had started, the intensity of the burning cloud exceeded that of the ignitor.

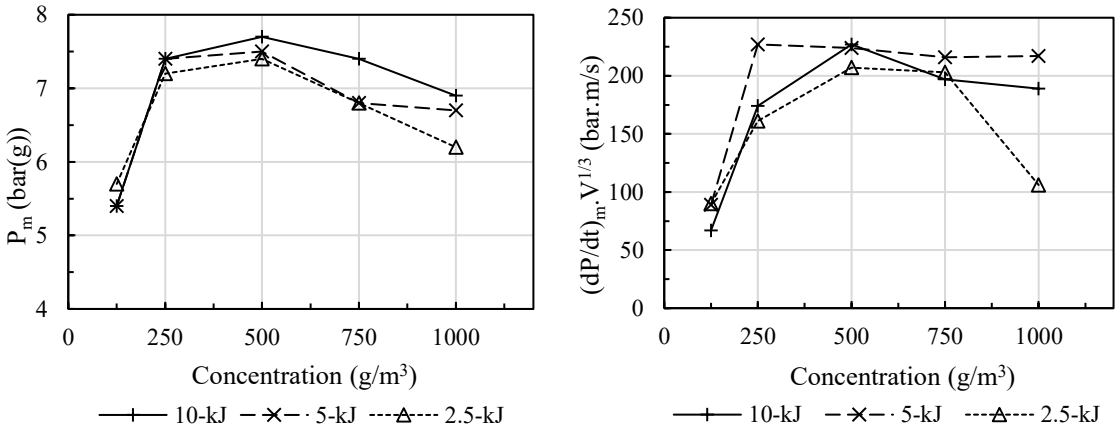

Figure 5.2: Plots of explosion pressure (P_m) and size-normalised rate of pressure rise ($(dP/dt)_m \cdot V^{1/3}$) of niacin at different ignition energies in the 20-L

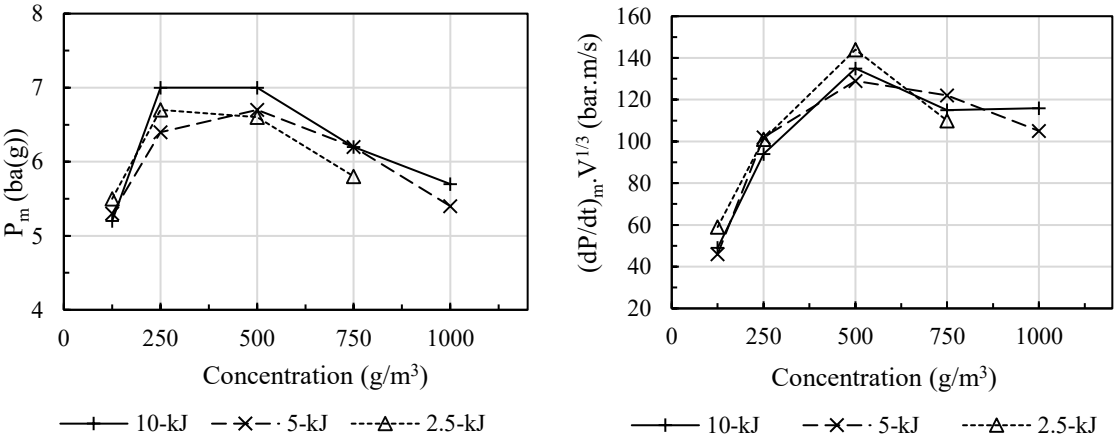

Figure 5.3: Plots of explosion pressure (P_m) and size-normalised rate of pressure rise ($(dP/dt)_m \cdot V^{1/3}$) of lycopodium at different ignition energies in the 20-L vessel

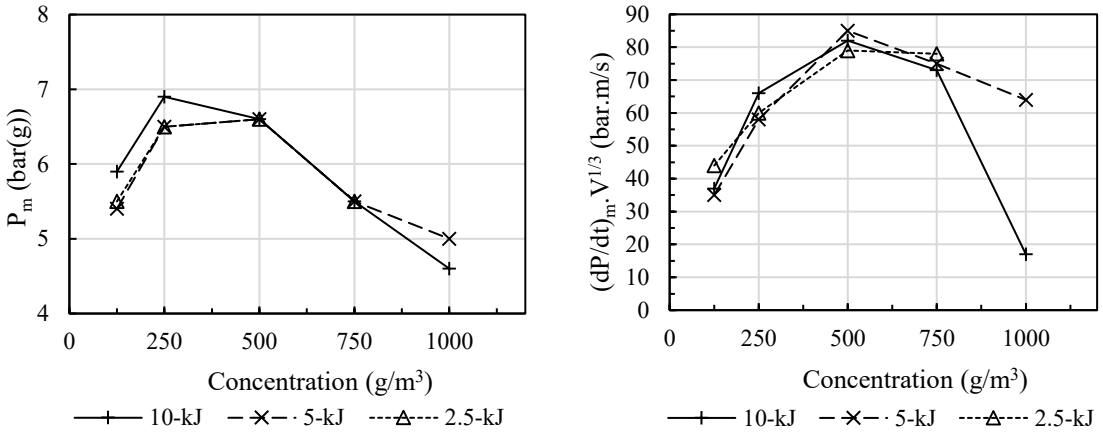

Figure 5.4: Plots of explosion pressure (P_m) and size-normalised rate of pressure rise ($(dP/dt)_m.V^{1/3}$) of fine polyethylene at different ignition energies in the 20-L vessel

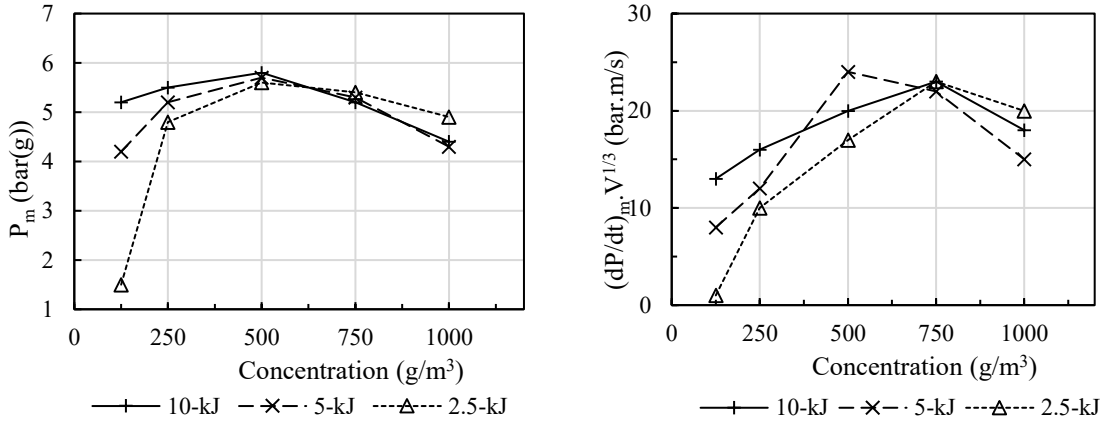

Figure 5.5: Plots of explosion pressure (P_m) and size-normalised rate of pressure rise ($(dP/dt)_m.V^{1/3}$) of coarse polyethylene at different ignition energies in the 20-L vessel

5.1.2 Explosion severity (P_{max}, $(dP/dt)_{max}$ and K_{St}) in the 1-m^3 chamber

P_{max} and K_{St} values were also obtained from the 1-m^3. Figure 5.6 gives the summary results (of Figures 4.25 to 4.28) of P_{max} and K_{St} respectively for all four dust samples. On this scale, determinations were made using an ignition energy of 10 kJ. Similar to the behaviour seen in the 20-L chamber, it can be noticed that the 1-m^3 results display the same expected trends in terms of material composition and particle size. For instance, the niacin dust (which is a refined dust) and polyethylene dusts recorded the highest and lowest P_{max} and K_{St} values respectively. In the case of the particle size, P_{max} and K_{St} of the polyethylene sample decreases as the median size (D_{50}) increases from 42 µm to 131 µm.

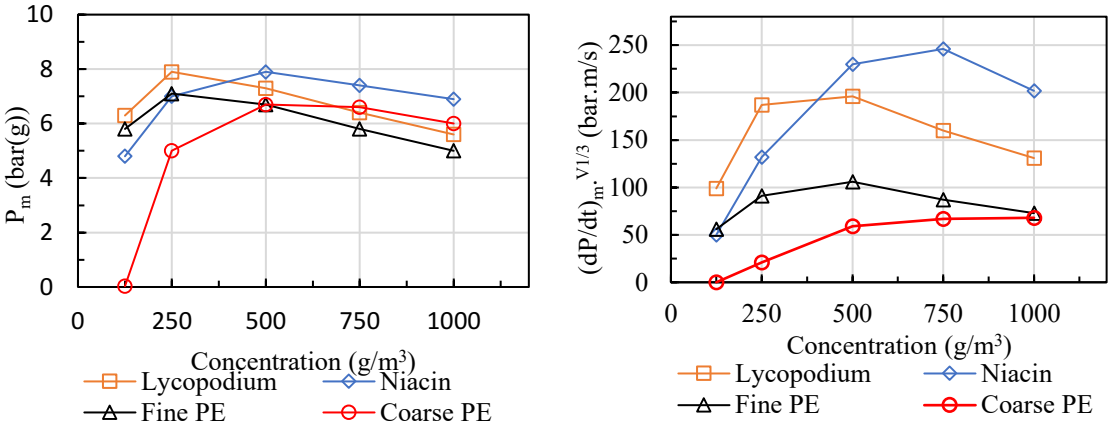

Figure 5.6: Summary of explosion parameters (P_m and $(dP/dt)_m.V^{1/3}$) in the 1-m^3 chamber using 10-kJ ignition energy at ignition delay time of 550 ms

Two different ignition delay times (at 550 and 600 ms) were used for P_{max} and K_{St} determinations (except for coarse polyethylene which was only determined at 550 ms) as seen in Table 5.1. A dash in the table means testing was not conducted at the indicated conditions. The ignition delay time influences turbulence in the chamber prior to ignition. Shorter times indicate higher turbulence and vice versa.

Table 5.1: Summary of explosion severity test results.

Materials	**Ignition Energy [kJ]**	**20 L 60 ms**		**1 m^3 550 ms**		**1 m^3 600 ms**	
		P_{max} [bar(g)]	**K_{St} [bar·m/s]**	**P_{max} [bar(g)]**	**K_{St} [bar·m/s]**	**P_{max} [bar(g)]**	**K_{St} [bar·m/s]**
Niacin	2.5	7.4	211	–	–	–	–
	5	7.5	233	–	–	–	–
	10	7.7	227	7.9	246	7.8	185
Lycopodium	2.5	6.8	144	–	–	–	–
	5	6.7	136	–	–	–	–
	10	7.1	135	7.9	204	7.4	165
Fine PE	2.5	6.7	80	–	–	–	–
	5	6.6	85	–	–	–	–
	10	7.0	82	7.1	106	7.0	101
Coarse PE	2.5	5.6	23	–	–	–	–
	5	5.7	27	–	–	–	–
	10	5.7	23	6.8	72	–	–

It can be observed from Table 5.1 that P_{max} values of the three dusts decreases with increasing ignition delay time. However, this decrease is statically insignificant. This behavior is as expected as turbulence in the chamber is reduced by increasing the time delay prior to ignition. The P_{max} value did not vary significantly at both time delays with lycopodium showing the highest decrease of about 6%. Furthermore, considering both P_{max} and K_{St}, it was seen that an ignition delay time of 550 ms was appropriate (compared to reference values [51]) for the niacin sample, while 600 ms was appropriate for lycopodium (compared to reference values [28]). This can be attributed to the relatively low density of lycopodium (as seen in Table 3.1) which enhances dispersity. The fine polyethylene showed slight difference in both P_{max} and K_{St} between the two delay times. According to Taveau [52], "there could be perfect agreement for an ignition delay greater than 600 ms in the case of lycopodium whereas the same can be achieved for niacin for an ignition delay comprised between 550 and 600 ms".

5.1.3 Effect of scale

Comparison of the 20-L results and 1-m^3 results (using 550-ms delay time) shown in Figure 5.7 to Figure 5.10 indicates that the values of P_{max} and K_{St} are within the reproducibility limits of ASTM E1226-12a [28] for niacin, lycopodium, and FPE except for the coarse polyethylene results which reveal a different trend. While the P_{max} values in both chambers are just within the 10% reproducibility limit given in ASTM E1226-12a [28], the K_{St} values do not agree within 30% of each other as stipulated in the ASTM standard [28]. Thus, it can be suggested that for explosibility tests involving highly explosible dusts (such as niacin, lycopodium and fine polyethylene) there is good agreement between the 20-L and 1-m^3 chambers without contradiction.

The difference in K_{St} values of coarse polyethylene as determined in the different sized chambers is due to its larger particle size. It needs more time for volatiles to be liberated, and to reach its nominal or stabilized combustion regime. The 1-m^3 provides enough time and volume for these processes. Another reason for the difference could be the fast settling of particles due to their larger sizes. It can therefore be suggested that scaling 20-L results for some class of dusts may not be as straight-forward and the difference should therefore be interpreted as real.

Testing of the coarse polyethylene in the 1-m^3 chamber at an ignition delay time of 600 ms would have provided further insight but was not done due to the unavailability of the 1-m^3 chamber. Even without the test at 600 ms, the current results presented in the study, however, permits a definitive conclusion as to whether the coarse polyethylene should be considered to be marginally explosible based solely on a 20-L K_{St} < 45 bar·m/s (as per the characteristics of marginal explosibility outlined in Section 2.5). With the 1-m^3 results indicating an explosion with higher P_{max} and K_{St} values of 6.8 bar(g) and 72 bar·m/s, the answer is clearly *no* (i.e., the coarse PE is not a marginally explosible dust).

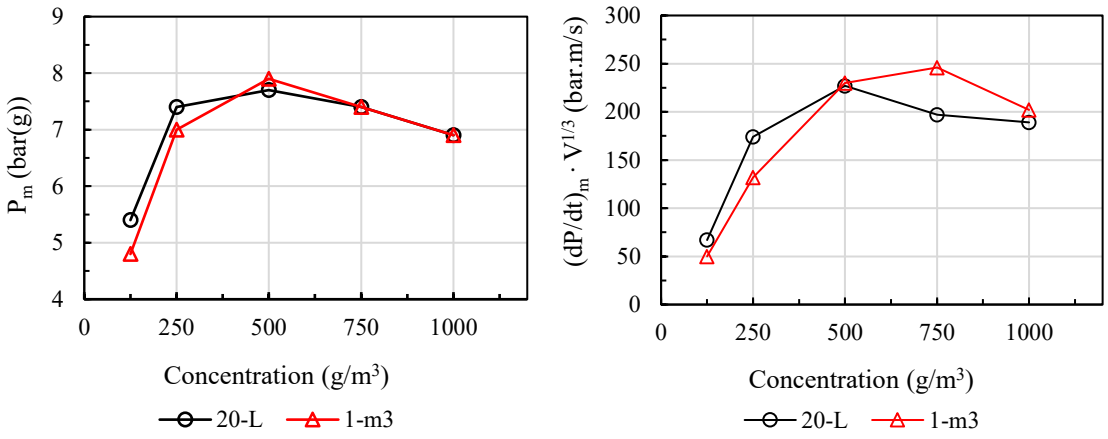

Figure 5.7: Comparison of explosion severity of niacin in the 20-L vessel and 1-m^3 chambers at ignition delay times of 550 ms

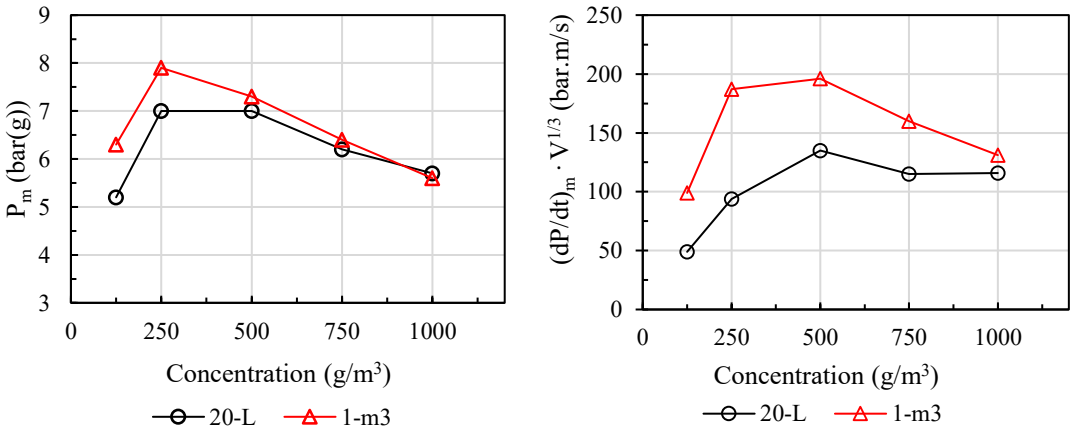

Figure 5.8: Comparison of explosion severity of lycopodium in the 20-L vessel and 1-m^3 chamber at ignition delay times of 550 ms

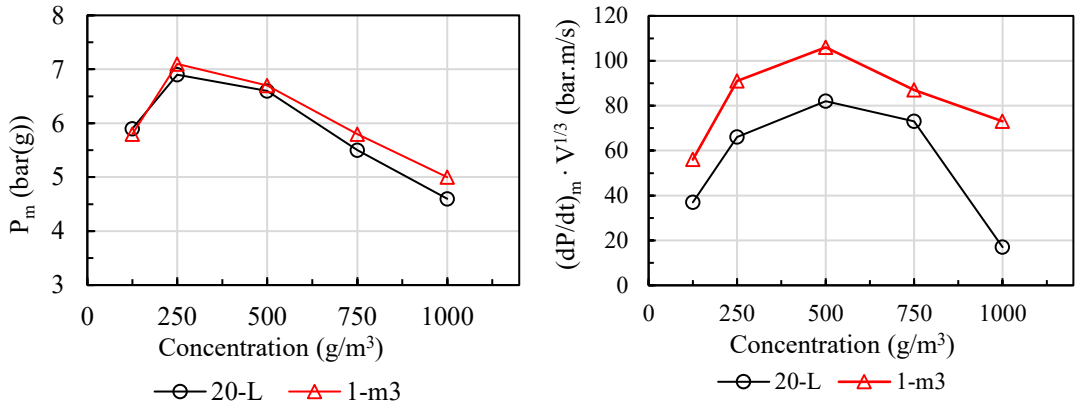

Figure 5.9: Comparison of explosion severity of fine polyethylene in the 20-L and 1-m^3 chambers at ignition delay times of 550 ms

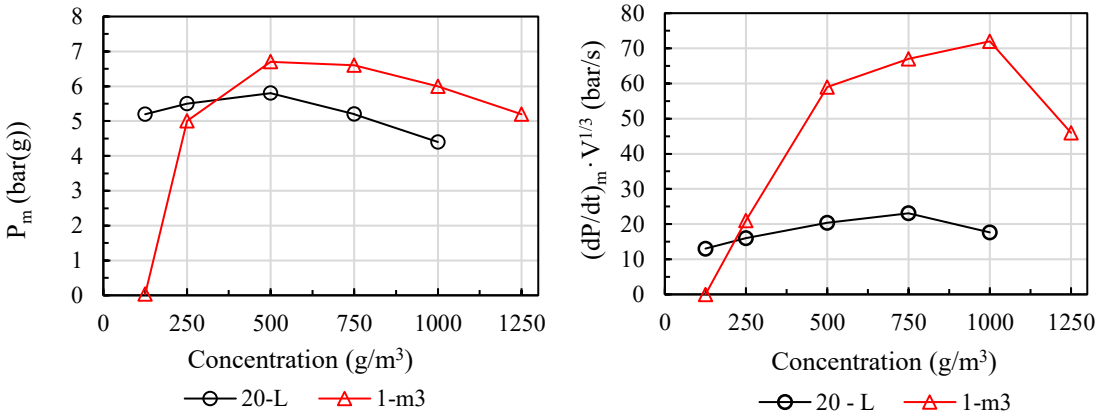

Figure 5.10: Comparison of explosion severity of coarse polyethylene in the 20-L and 1-m^3 chambers at ignition delay time of 550 ms

5.2 Relationship Between Experimentally Determined Material Properties and Explosion Severity Parameters

This section discusses the results of each material property or characterization determined experimentally in this work and how they related to the explosion severity parameters.

5.2.1 Effect of particle size

The effect of particle size on the explosibility of dust materials are well established in the literature. In this work, the trend seen between the particle size and the explosibility parameters demonstrates good agreement (especially for the two different size

polyethylene samples). The effect of particle size in this work has already been included in preceding sections related to each explosibility parameter.

5.2.2 Effect of specific surface area

Specific surface area (SSA) of all dust samples in this study was determined based on the Brunauer-Emmett-Teller (BET) multilayer gas adsorption theory using single point, multi-point, and Langmuir models. All three models produced comparable results as shown in Table 3.1. However, for microporous samples such as the materials used in this work, the Langmuir model was preferred. This is because both multi-point and single point BET were determined at relatively higher adsorbate gas pressure (P/Po = 0.1-0.3 Pa) and at this pressure, the nitrogen gas condenses (which is undesirable) into the micropores thus, resulting in erroneous determinations. This condensation does not occur in the Langmuir method due to the low gas pressure (0.04-0.06 Pa) used. The combustion of particles are strongly influenced by the available surface area of the particles. Generally, dusts with finer particle size have larger specific surface areas and produce higher explosion violence and vice versa. This is because a larger specific surface area increases the effective reaction area and allows the flame front to travel at a faster rate thus resulting in higher rate of pressure rise $(dP/dt)_m$ and deflagration index (K_{St} or $(dP/dt)_{max}.V^{1/3}$).

The results obtained from the specific surface area analysis in this work indicates that coarse polyethylene (D_{50} = 131 μm) had the largest surface area while niacin (D_{50} = 20 μm) shows the smallest specific surface area. This behaviour could be attributed to the degree of porosity of the dust samples. Figure 5.11 shows the desorption curves (or isotherms) for each dust. It can be realized from the graph that the coarse polyethylene sample is most porous and has the largest pore volumes while niacin has the smallest pore volumes.

Porosity plays a very significant role in the measurement of specific surface area using the BET apparatus. The method measures the SSA taking into consideration the pore volumes as well. The effect is that samples with higher porosities tend to record the largest surface areas regardless of particle size and vice versa. It can therefore be concluded that the pore sizes for the tested dusts did not play any role in determining the severity of the sample. The combustion event occurs so fast that the developing

flame front is not able to penetrate each pore to release volatiles. Thus, only the "truly exposed" surface area contributed. This means that not all the surface area measured by the BET apparatus would be available for the combustion reaction.

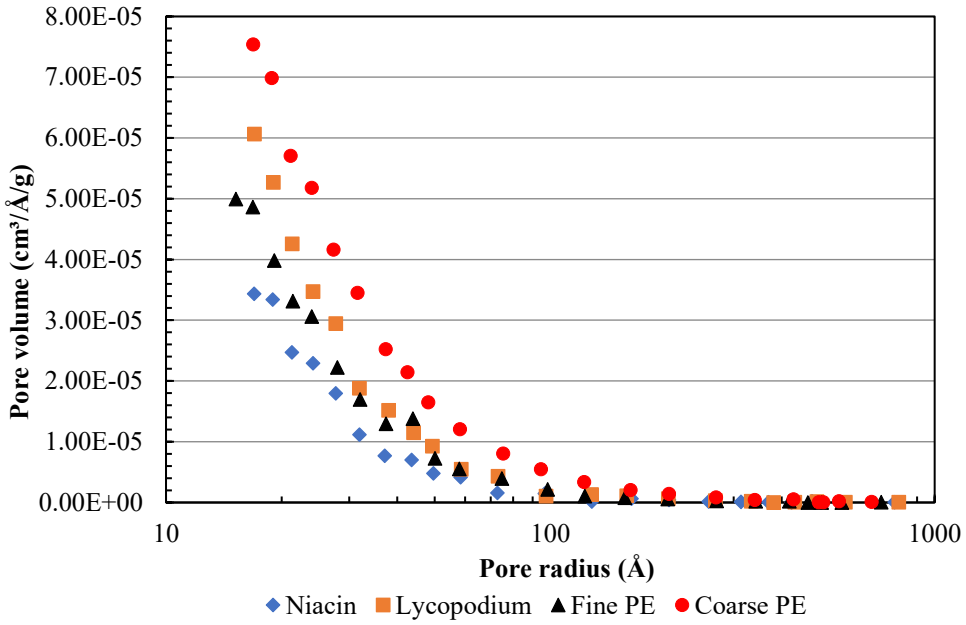

Figure 5.11: Isotherm showing coarse polyethylene with the largest pore volumes

5.2.3 Effect of heat of combustion (HOC)

The heat of combustion (HOC) of a dust material is strongly related to the maximum explosion pressure (P_{max}) generated during an explosion. The values obtained were as expected for organic dusts (i.e., organic dusts generally have high HOCs). The HOC is dependent on the chemical composition of the dust material. The HOC test was performed in pure oxygen and at 30 bar(g) pressure given a long reaction time which allowed full combustion development to release the material's calorific value. In the 20-L chamber, the short reaction time did not allow full combustion to be achieved and the rate of reaction was driven by other factors such as the particle size. This could be the reason for higher P_{max} values for fine PE than course PE. However, in the 1-m^3 chamber, the P_{max} values of the two PE samples were similar due to the relatively large volume and longer reaction time which allowed a better developed combustion. Thus, the components of the HOC test may be better suited to larger combustion volumes, and to make the HOC test a better predictor of the P_{max} values in the 20-L chamber, some modifications must be made.

5.2.4 Effect of moisture content

The moisture content of dust materials can have a significant impact on its explosion severity (P_{max} and K_{St}). Generally, higher moisture content results in a reduction of the explosion severity of the material. This is because prior to combustion, the moisture within the material absorbs the heat during evaporation slowing down the rate of the combustion reaction and hence, making it more difficult to burn. The moisture acts as a heat sink when present in high amounts. In view of the effect of moisture, the ASTM standards [28], [43] directs that explosibility testing be performed with materials having a moisture content not more than 5 wt% . In this study, all the dusts tested had a moisture content below 5 wt% (ranging from polyethylene, 0.2, to lycopodium, 4.3 wt%).

5.2.5 Effect of density

The densities of dust materials are important in understanding dust cloud ignition and explosion. Density influences the ability of dust materials to be dispersed into space (a property termed as dustiness [53]) and the period that these particles will stay airborne as a dust/air mixture. Denser materials collapse to the bottom of the test chamber at shorter periods, and this may decrease the concentration of dust that finally undergoes ignition and subsequent flame propagation. This explains why fixing a single ignition time delay in larger chambers such as the 1-m^3 may not be entirely accurate. An example can be seen for testing of lycopodium and niacin in the larger chamber where an ignition delay time of 600 ms was appropriate for lycopodium and 550 ms appropriate for niacin. Although the density values in Table 3.1 do not show significant differences, lycopodium has slightly lower density than niacin.

5.3 Explosion Likelihood

The likelihood of explosion gives an indication of the sensitivity of the dust materials to ignition and further to propagation into an explosion when required conditions are met. This study determined likelihood parameters such as the minimum explosible concentration (MEC), minimum ignition energy (MIE), and minimum ignition

temperature (MIT) of all organic dusts using well calibrated apparatus in accordance with applicable standards.

5.3.1 Minimum explosible concentration (MEC)

The minimum explosible concentration of combustible dusts is the lowest concentration of dust-air mixture below which the dust cloud is unable to self-propagate a flame at given conditions. This likelihood parameter is very important in prescribing explosion prevention strategies.

5.3.2 Minimum Explosible Concentration in the standard Siwek 20-L sphere

The MEC of individual dusts were experimentally determined in the 20-L chamber using 2.5-kJ Sobbe chemical ignitors as suggested in the study by Britton et al. [54]. The results obtained are summarized in Figure 5.12. Detailed results for each sample can be seen in Figures 4.32 to 4.35 (in chapter 4). It can be observed from the results that all MEC values are less than 100 g/m^3. This means that thin layers of all the dust materials tested, when deposited on surfaces, could readily form an explosible dust cloud if dispersed in air.

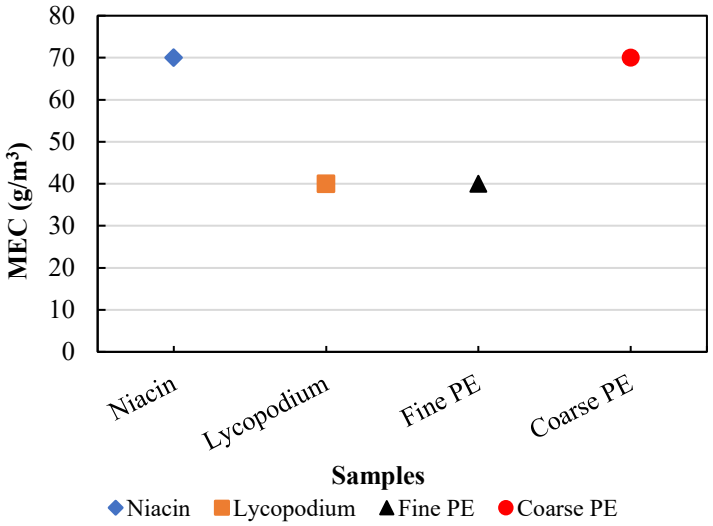

Figure 5.12: Summary of MEC of organic samples in 20-L chamber

It can also be seen that both lycopodium and fine polyethylene dusts recorded the lowest MEC with niacin and coarse polyethylene dusts both recording the highest MEC at 70 g/m^3. With respect to the two different particle size distributions of polyethylene

(PE) dusts, the trend realized is as expected, and can be attributed to the significant increase of particle size from the fine to coarse. The MEC of dust materials is strongly influenced by dust particle size. Increasing the particle size of dusts decreases the surface area and the effective reaction area for the combustion reaction to take place and subsequently for flame propagation.

Furthermore, increasing particle size decreases the number of particles involved in the combustion reaction therefore slowing the devolatilization process (which is the rate determining step) in the flame propagation process and is strongly influenced by particle size. Thus, it can be suggested that with continuous increase of the particle size, the polyethylene dusts (and other dusts) may exhibit an explosion trend moving from; explosible → marginally explosible → non-explosible. This means that as particle size increase from fine PE through coarse PE to larger particle, a point may be reached where the PE sample will exhibit marginal explosibility and a further increase will cause the dust to exhibit non-explosibility (at which point a MEC will not exist).

5.3.3 MEC in the 1-m^3 Explosion Chamber

Companion testing of all organic dusts were conducted in the larger 1-m^3 chamber. The 1-m^3 chamber is the internationally accepted test apparatus for assessing the MEC of combustible dust materials. Figure 5.13 shows the summary results obtained for the MEC of all organic dusts tested using an ignition energy of 10 kJ (2×5 kJ) (as specified in the standard ASTM E1515 [43]) from Sobbe chemical ignitors. Detailed results for each dust sample can be seen in Figure 4.36 to Figure 4.39.

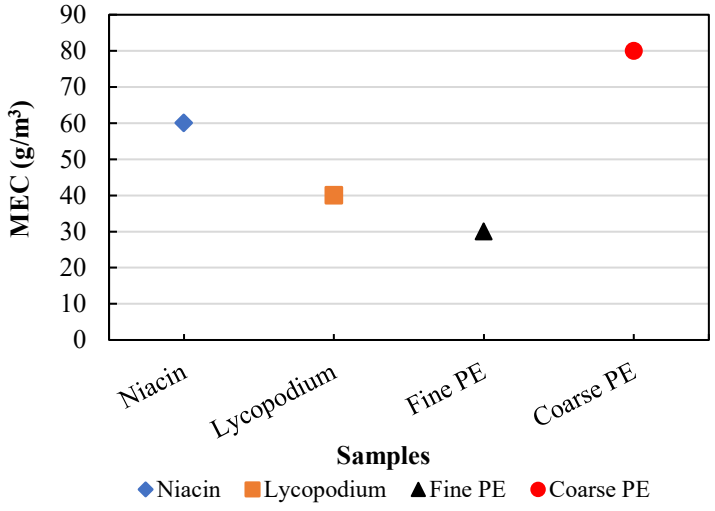

Figure 5.13: Summary of MEC of organic samples in 1-m^3 chamber

It is observed that the coarse polyethylene recorded the highest MEC followed by niacin, with fine polyethylene recording the lowest MEC. The lycopodium MEC is the same as recorded in the 20-L chamber at 40 g/m^3. Similar to the MEC values obtained in the small 20-L chamber, all MEC values obtained from the 1-m^3 chamber are all below 100 g/m^3. The lowest MEC of the fine polyethylene dust could be attributed to its small particle size as can be seen in Table 3.1. MEC decreases with decreasing particle size due to the increase of the effective surface area and reaction area of dust particles for the combustion and flame propagation processes. On the other hand, the increase in particle size (as seen in the case of coarse polyethylene) leads to the reduction of the particles' total surface area, therefore resulting in a decrease of the effective heating and reaction area of particles.

5.3.4 Comparing MECs on both testing scales (20-L and 1-m^3 chambers)

Comparing the MEC results from both chambers, it can be seen that there is good agreement for most of the dusts tested with a maximum difference of 10 g/m^3 as in the cases for niacin, fine polyethylene, and coarse polyethylene. For lycopodium there is perfect agreement between both testing scales as MEC recorded was the same at 40 g/m^3. Testing on the larger scale confirmed that all the dusts tested in this work have MECs and are all less than 100 g/m^3 thus indicating that thin layers of these dusts deposited on surfaces could readily form combustible dust clouds if dispersed in air.

5.3.5 Minimum Ignition Energy (MIE)

The minimum ignition energy (MIE) is determined as the lowest amount of electrical energy stored in a capacitor which when released as a high voltage spark, is just sufficient to ignite a fuel (dust) at its most easily ignitable concentration in air [44]. Knowledge of this parameter is very important in order to prevent or mitigate any hazard that might result from electrical discharge to cause ignition of the materials being handled or processed in the facility. In this project, the MIE was determined using the MIKE-3 apparatus according to standard procedures in the ASTM E2019-06 [44]. The MIEs of four organic dusts have been investigated and the discussions presented in this section. For this study, MIE of dusts were determined both with and without

inductance in the spark discharge circuitry. The statistical energy (E_s) value is only used here for simplicity and the ease of comparison.

5.3.6 Minimum ignition energy (MIE) of dusts without inductance

Figure 5.14 presents the summary results obtained for the minimum ignition energy of all dusts tested without inductance. Figures 4.40 to 4.43 show detailed results for each dust sample. It can be seen from Figure 5.14 that niacin recorded the lowest value with 1.7 mJ while coarse polyethylene did not ignite (as indicated by unfilled data point) at the maximum ignition energy that can be measured by the apparatus (i.e., MIE > 1000 mJ or 1 J). The reason for the high MIE of coarse polyethylene could be attributed to its relatively large particle size (D_{50}) compared to the other dusts as presented in Table 3.1.

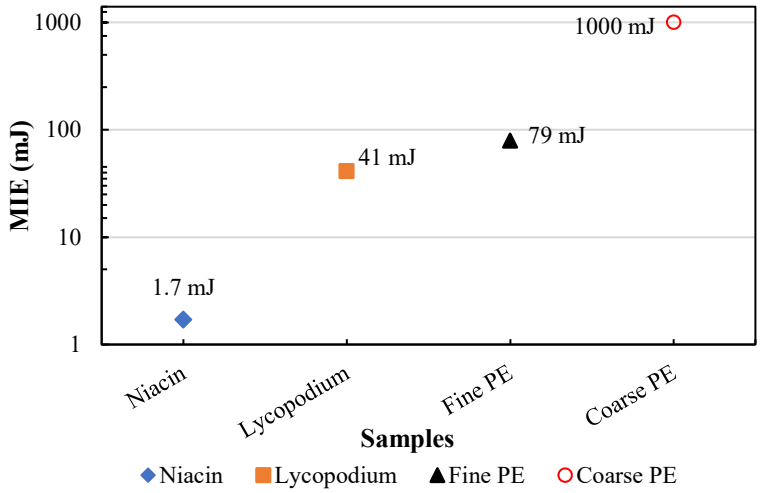

Figure 5.14: MIE of organic samples in MIKE-3 apparatus without inductance

Generally, the minimum ignition energy of dusts is strongly dependent on the size of the dust particles (and the ability to form a combustible dust cloud – a property termed as the dustiness of the dust material). An increase of the dust particle size decreases the surface area available for the ignition to prevail and consequently, largely increases minimum ignition energy. Thus, dust particles with smaller particle size may be easily dispersed and ignited as compared to the ones with coarser sizes. Smaller particles remain in suspension for longer periods compared to coarser particle due to the action of gravity which increases with increased particle size (for materials with similar densities such as fine PE and coarse PE). This means that at a given period of time,

more of the fine PE will be available in the dust-air cloud for flame propagation than for coarse PE when both are dispersed at under similar conditions. Moreover, decreasing particle size will greatly increase the number of particles under the same dust concentration, which will also increase the effective reaction surface of the dusts.

5.3.7 Minimum ignition energy with 1-mH inductance

The minimum ignition energy of each dust sample was also determined with 1-mH inductance in the spark discharge circuitry and the results presented in Figure 5.15. The trend realized was as expected. It could be seen that there was a general decrease in MIE of dusts when sparks with inductance was applied. For instance, the MIE of niacin decreased by 0.5 mJ, lycopodium by 29 mJ and fine PE by 67 mJ. Coarse PE which did not ignite at spark ignition energy of 1000 mJ, showed ignition at an ignition energy below 1000 mJ (i.e., E_s = 840 mJ) when inductance was applied. The results for niacin indicate that it is highly sensitive to low energy electric sparks regardless of the inclusion or exclusion of inductance.

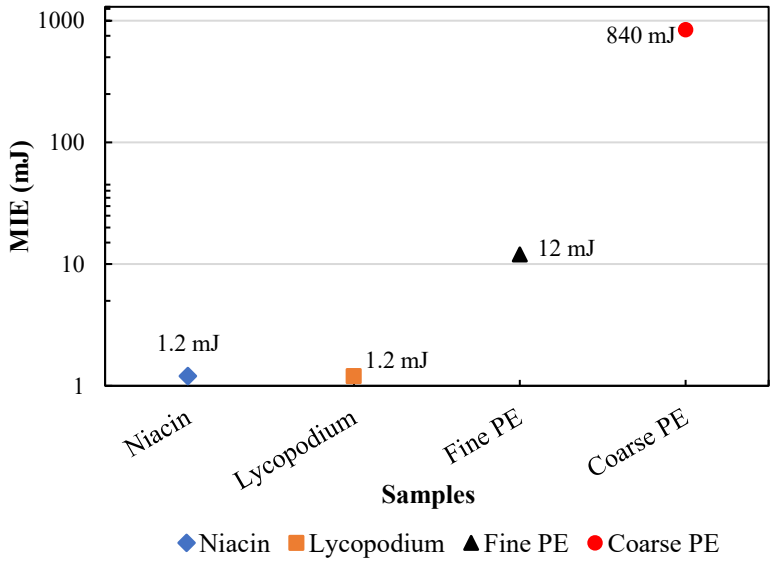

Figure 5.15: MIE of organic samples in MIKE-3 apparatus with 1-mH inductance

von Pidoll [55] explains that the presence of inductance in the spark discharge circuitry results in lingering capacitor discharges which has higher ignition probability than purely capacitive discharges. Application of MIE results with inductance to operational

conditions which are generally more is only possible if the capacitors present in dust handling facilities are also discharged with inductance. Therefore, to assess the ignition ability of electrical discharges with respect to dust-air mixtures, the MIE must also be measured without the influence of inductance in the discharge circuit [14].

Similar to the trend observed in the case of MIE measured without inductance, lower MIE values were measured for the finer size polyethylene compared to the coarser size polyethylene. This can be attributed to the increase in particle surface area brought about by a significant decrease in the particle median diameter. The coarse PE was found to be relatively insensitive to spark ignition (and a further increase in particle size may result in a corresponding increase in MIE or non-ignition with spark discharges).

5.3.8 Minimum ignition temperature (MIT) of dust clouds

The minimum ignition temperature (MIT) is an important explosion likelihood parameter when conducting hazard assessment for processes involving dust-air mixtures as well as other fuel mixtures, when a hot surface is considered as an ignition source. It is the lowest temperature of a hot surface that has the potential to ignite a fuel-oxidizer mixture within the explosible range. There are several situations in industry where hot surfaces capable of igniting dust-air mixture exist. Examples are the surface of furnaces, burners, dryers, etc. of different kinds and configurations. Also, unplanned situations such as overheated bearings and other rotating or sliding mechanical parts have the potential to generate hot surfaces.

5.3.9 Minimum ignition temperature in the BAM Oven

Figure 5.16 shows the summary of minimum ignition temperature (MIT) results of all tested dusts. The summary was obtained from detailed results as presented in Figures 4.44 to 4.47 (presented earlier in chapter 4). It could be observed that all four samples were determined to have approximately the same MIT (with niacin recording the highest at 440 ^{o}C and the fine polyethylene recording the lowest) with the difference between the highest and lowest MIT (i.e., for FPE) being 30 ^{o}C. The 5-seconds ignition criterion for the BAM oven could lead to sample material emitting sufficient volatiles for combustion as it sits on the bottom surface of the heated furnace. This likely

explains why there is only a 10 °C difference in MIT values for the two sizes of polyethylene.

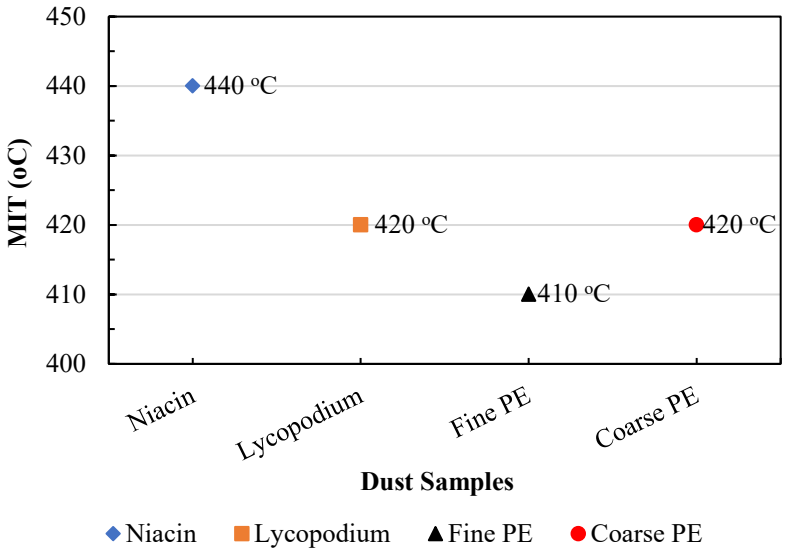

Figure 5.16: Summary of MIT results of organic samples in BAM Oven

The minimum ignition temperature is influenced by factors such as the material composition, volatile content, particle size, moisture content, thermal conductivity, etc. For instance, with similar material composition such as for the polyethylene samples, the minimum ignition temperature did not differ significantly; the temperatures recorded were 410 and 420 °C for fine polyethylene and coarse polyethylene respectively. This phenomenon could be attributed to the combustion behavior of the molten polyethylene particles. The slight difference of 10 °C could be due to the increase of particle size from fine (42 µm) to coarse (131 µm). Similar observations were made by Mittal and Guha [18] and recent works by Gan et al. [56],[57]. As stated previously, the presence of volatiles (such as ethylene - C_2H_2, methane - CH_4) emitted plays an important role in the MIT values [56]. This justifies the slightly low MIT values of the polyethylene samples (with approximately 99.9 wt% volatile content [58]) compared to the smaller size (31 µm) lycopodium (91.06 wt% [40]). The MIT results showed that all four dusts could undergo surface ignition at temperatures around 400 °C.

5.4 Correlation of Explosion Likelihood with Explosion Severity

Tables 5.1 and 5.2 show the summary of explosion severity and explosion likelihood results respectively for all four samples tested. The severity results determined in the 20-L chamber and those determined at both delay times of 550 and 600 ms in the 1-m^3 chamber were compared with the results of the explosion likelihood parameters obtained from their respective apparatus.

Table 5.2: Summary Table for explosion likelihood parameters

Samples	**Explosion Likelihood**				
	20-L	**1-m^3**	**MIKE-3**		**BAM**
	MEC [g/m^3]	**MEC [g/m^3]**	**MIE (1 mH) [mJ]**	**MIE (0 mH) [mJ]**	**MIT [^oC]**
Niacin	70	60	1-3 Es = 1.2	1-3 Es = 1.7	440
Lycopodium	40	40	10-30 Es = 12	30-100 Es = 41	420
Fine PE	40	30	10-30 Es = 12	30-100 Es = 79	410
Coarse PE	70	80	300-1000 Es = 840	> 1000	420

Comparison of both sets of results (likelihood and severity) reveal no apparent correlation between MIT and explosion severity as represented by P_{max} and K_{St}. The same holds true for MEC with the niacin and coarse polyethylene – which are at opposite ends of the severity scale – having comparable values of minimum explosible concentration. However, the MIE is seen to correlate well with explosion severity; niacin has by far the lowest MIE and highest P_{max} and K_{St} while coarse polyethylene easily has the highest MIE and lowest P_{max} and K_{St}. This finding is not unexpected, given that dusts yielding the most severe consequences often (not always) have very low minimum ignition energies.

CHAPTER 6: CONCLUSIONS

Combustible dusts that have been referred to as marginally explosible continue to present difficulties during hazard identification due to the discrepancies they present on the smaller laboratory scale and the intermediate testing scale. The problem therefore is whether to classify them as explosible or not, although they certainly pose a flash fire hazard. This uncertainty may also present in designing dust explosion risk reduction measures. This burden is extended to the partners on this project (Fauske and Associates, FIKE Corporation, and Professional Loss Control) who are in the business of testing and advising clients on the explosibility of their dust materials. In order to understand the explosibility behaviour these dusts, various explosion parameters need to be known. In view of this, the current work has provided a comprehensive set of explosibility data for four well-characterized organic samples: niacin, lycopodium and two size fractions of polyethylene. Measurements were made for the following dust explosion parameters: maximum explosion pressure (P_{max}), volume-normalized maximum rate of pressure rise (K_{St}), minimum explosible concentration (MEC), minimum ignition energy (MIE) and minimum ignition temperature (MIT), with P_{max}, K_{St} and MEC being determined at both 20-L and 1-m^3 scales. P_{max}, and K_{St} are parameters that measure the explosion severity while MEC, MIE and MIT measure the likelihood of an explosion.

P_{max} and K_{St} results in both 20-L and 1-m^3 chambers demonstrated expected trends with respect to composition and particle size. Niacin which is a refined chemical and also has the smallest particle size (D_{50}) recorded the highest severity while coarse polyethylene, which was found on the opposite side of the particle size scale and approached a reactivity limit, showed the lowest values for P_{max} and K_{St}. Coarse polyethylene was found to have the largest surface area because of its high porosity, but records the lowest severity due to its large (D_{50}). This is because not the entire surface area measured by the BET apparatus may be available for combustion, but only the truly exposed surface area. The porosity however, did not play a role in determining the explosibility of the samples due to the short reaction time. It can also be concluded that dust material density plays an important role in explosibility determinations and fixing a single ignition time delay for all dusts may not be the best.

All MEC values were < 100 g/m^3, indicating that thin layers of these materials deposited on surfaces could readily form a combustible dust cloud if dispersed in air. Agreement between MEC values measured in the two chambers was excellent. The influence of inductance in generating sparks with longer duration had the expected effect of lowering the MIE of a given sample. The lone exception was niacin which was highly sensitive to low-energy electric sparks. Lower MIE values were recorded for the finer size of polyethylene, again because of the increase in particle surface area brought about by a decrease in particle diameter. The coarse polyethylene was relatively insensitive to spark ignition. All four samples were determined to have approximately the same MIT. This is a reflection of the fact that hot-surface ignition processes involve different physical and chemical phenomena than those in spark ignition scenarios. Also, the 5-second ignition criterion for the BAM oven can lead to sample material emitting sufficient volatiles for combustion.

Comparison of the severity and likelihood results showed no apparent correlation between MIT and explosion severity as represented by P_{max} and K_{St}. The same can be said for MEC with the niacin and coarse polyethylene having comparable values of minimum explosible concentration. MIE did, however, correlate well with explosion severity; niacin had by far the lowest MIE and highest P_{max}/K_{St} while coarse polyethylene easily had the highest MIE and lowest P_{max}/K_{St}.

This work has demonstrated that with thorough equipment calibration and standard test protocols, it is possible to obtain good agreement of explosion severity (P_{max} and K_{St}) and explosion likelihood (MEC) data measured at different testing scales. This conclusion is valid for three of the samples tested: niacin, lycopodium and fine polyethylene. P_{max} for these materials lies in the approximate range of 7 – 8 bar(g) for both chambers used here; K_{St} values are in the approximate range of 80 – 230 bar·m/s for the 20-L chamber and 100 – 250 bar·m/s for the 1-m^3 chamber.

The exception to the above conclusion was for samples that were approaching a reactivity limit – in the work here, a limit brought about by a large particle size as in the case of the coarse polyethylene. Testing for this sample has shown a higher K_{St} measured in the 1-m^3 than in the 20-L chamber. The low 20-L K_{St} of 23 bar·m/s was therefore not indicative of a false positive in the smaller chamber. The coarse polyethylene, though was relatively insensitive to spark ignition, is clearly ***not*** a

marginally explosible dust. It has a measurable P_{max}, K_{St} and MEC in both size vessels, and can undergo surface ignition at temperatures around 400 °C.

This study has therefore shown that basing the definition of so-called marginal explosibility on a K_{St} value in the 20-L chamber may not be entirely accurate since explosibility behaviour differ from material to material.

6.1 Recommendations

Clearly, it can be seen that the issue of establishing the explosibility regime of so-called marginally explosible dusts is a complex one and cannot be exhausted in a single study. Therefore, it is recommended that dust explosion research should continue with regard to this class of dusts in order to provide further understanding of their behaviour in the different sized test scales, and to determine without ambiguity whether they are explosible or not.

Also, more dust materials should be considered for experimental investigation. The current work considered four dust samples (with niacin and lycopodium selected to represent dusts with known explosibility, and two different sizes of polyethylene selected to explore the possibility of marginal explosibility for the coarse size). In future work, more dust materials with low P_{max} and K_{St} values should be tested. A good reference to select candidate dust is the NFPA 652 [59].

Additionally, it is recommended that testing of the coarse polyethylene in the 1-m^3 at time delay of 600 ms be undertaken to further understand the difference (i.e., increase) in K_{St} values as determined in the two different sized chambers. Furthermore, work should be done to investigate the explosion dynamics including modelling the explosion probability and behaviour of these dusts in both chambers. This will give a better understanding of how flame development in each chamber proceeds with respect to these dusts.

Finally, more work is required in the area of detailed reaction mechanism to determine exact combustion intermediates and products. Overall, regardless of whether these dusts are explosible or not, process industries should prioritize good house-keeping practices to ensure that there is not enough dust for the occurrence of dust flash fires or explosions.

REFERENCES

[1] H. C. Verakis and J. Nagy. A Brief History of Dust Explosion. *Industrial Dust Explosions: Symposium on Industrial Dust*, pages 342–350, 1987.

[2] G. S. Rice, J. C. W. Frazer, A. Larsen, F. Haas, and C. Scholz. *The Explosibility of Coal Dust*. Washington: US Goverment Printing Office, 1910.

[3] US Chemical Safety and Hazard Investigation Board. *Investigation Report: Combustible Dust Hazard Study*. Report No. 2006-H-1, 2006.

[4] K. P. Richard. *The Westray story - A Predictable Path to Disaster*. Report of the Westray Mine Public Inquiry. Province of Nova Scotia, Canada, 1997.

[5] C. T. Cloney. Mydustexplosionresearch. [Online]. Available: http://www.mydustexplosionresearch.com/explosion-incidents/ [Accessed: 08-Jun-2018].

[6] U.S. Chemical Safety Board. *Metal Dust Flash Fires and Hydrogen Explosion*. Hoeganaes Corporation, Gallatin, TN, pages 1–31, 2011.

[7] R. K. Eckhoff. *Dust Explosions in the Process Industries*. Gulf Professional Publishing, Amsterdam, 3rd ed, 2003.

[8] D. A. Crowl. *Understanding Explosions*, 2003.

[9] D. Bjerketvedt, J. R. Bakke and K. Van Wingerden. Gas explosion handbook, *Journal of Hazardous Materials*, 52:1–150, 1997.

[10] F. A. William and E. S. Oran. The physics, chemistry and dynamics of explosions, 370:534–543, 2012.

[11] NFPA 68. *Standard on the Fundamentals of Combustible Dust*. National Fire Protection Agency, Quincy, MA, 2018.

[12] NFPA 654. *Standard on the Prevention of Fire and Dust Explosions from the Manufacturing, Processing, and Handling of Combustible Particulate Solids.* National Fire Protection Agency, Quincy, MA, 2017.

[13] P. R. Amyotte. *An Introduction to Dust Explosions: Understanding the Myths and Realities of Dust Explosions for a Safer Workplace*. Elsevier Inc., Oxford, UK, 2013.

[14] M. F. Ivanov, A. D. Kiverin, and M. A. Liberman. Ignition of deflagration and detonation ahead of the flame due to radiative preheating of suspended micro particles. *Combustion and Flame*, 162:1-47, 2014.

[15] P. R. Amyotte and R. K. Eckhoff. Dust explosion causation, prevention and mitigation: An overview. *Journal of Chemical, Health and Safety*, 17:15–28, 2010.

[16] K. L. Cashdollar. Overview of dust explosibility characteristics. *Journal of Loss Prevention in the Process Industry*, 13:183–199, 2000.

[17] T. Abbasi and S. A. Abbasi. Dust explosions: Cases, causes, consequences, and control. *Journal of Hazardous Materials*, 140:7–44, 2007.

[18] M. Mittal and B. K. Guha. Study of Ignition Temperature of a Polyethylene Dust Cloud. *Fire Materials*, 20:97–105, 1996.

[19] R. Pilão, E. Ramalho, and C. Pinho. Influence of initial pressure on the explosibility of cork dust/air mixtures. *Journal of Loss Preventions in the Process Industries*, 17:87–96, 2004.

[20] K. N. Palmer and P.S. Tonkin, Explosibility of dusts in small-scale tests and large-scale industrial plant, pages 66–75, 1967.

[21] C. Proust, A. Accorsi, and L. Dupont. Measuring the violence of dust explosions with the 20-L sphere' and with the standard 'ISO 1-m^3 vessel. Systematic comparison and analysis of the discrepancies. *Journal of Loss Prevention in the. Process Industries*, 20:599–606, 2007.

[22] S. A. Rodgers and E. A. Ural. Practical issues with marginally explosible dusts: Evaluating the real Hazard. *Process Safety Progress*, 30:266–279, 2011.

[23] C. T. Cloney, R. C. Ripley, P. R. Amyotte, and F. I. Khan. Quantifying the effect of strong ignition sources on particle preconditioning and distribution in the 20-L chamber. *Journal of Loss Prevention in the Process Industries*, 26:1574–1582, 2013.

[24] N. Kuai, J. Li, Z. Chen, W. Huang, J. Yuan and W. Xu. Experiment-based investigations on the effect of ignition energy on dust explosion behaviors. *Journal of Loss Prevention in the Process Industries*, 26:869–877, 2013.

[25] N. Kuai, J. Li, Z. Chen, W. Huang, J. Yuan, and W. Xu. Experiment-based investigations of magnesium dust explosion characteristics. *Journal of Loss Prevention in the Process Industries*, 24:302–313, 2011.

[26] W. Gao, S. Zhong, N. Miao, and H. Li. Effect of ignition on the explosion behavior of 1-Octadecanol / air mixtures. *Powder Technology*, 241:105–114, 2013.

[27] J. K. Thomas, D. C. Kirby, and J. E. Going. Explosibility of a urea dust sample. *Process Saety Progress*, 32:189–192, 2013.

[28] ASTM E1226-12a. *Standard test method for explosibility of dust clouds*. ASTM International, West Conshohocken, PA, United States, 2018.

[29] K. L. Cashdollar and K. Chatrathi. Minimum explosible dust concentrations measured in 20-L and 1-m^3 chambers. *Combustion. Science Technology*, 87:157–171, 1993.

[30] J. E. Going, K. Chatrathi, and K. L. Cashdollar, Flammability limit measurements for dusts in 20-L and 1-m^3 vessels. *Journal of Loss Prevention in the Process Industries*, 13:209–219, 2000.

[31] J. Bucher, A. Ibarreta, K. Marr, and T. Myers. Mary Kay O ' Connor Process Safety Center - 15th Annual International Symposium Testing of Marginally Explosible Dusts : Evaluation of Overdriving and Realistic Ignition Sources in Process Facilities, 2012.

[32] T. J. Myers, A. F. Ibarreta, J. Bucher, and K. Marr. Assessing the hazard of marginally explosible dusts. In *American Institute of Chemical Engineers, Spring Meeting, 9th Global Congress on Process Safety*, San Antonio, Texas, 2013.

[33] ISO 6184-1(en). *Explosion protection systems — Part 1: Determination of explosion indices of combustible dusts in air*. ISO, Geneva, Switzerland, 1985.

[34] L. Marmo, D. Riccio, and E. Danzi, Explosibility of metallic waste dusts. *Process Safety and Environmental Protection*, 1:69–80, 2017.

[35] C. T. Cloney, P. R. Amyotte, F. I. Khan and R. C. Ripley. Development of an organizational framework for studying dust explosion phenomena. *Journal of Loss Prevention in the Process Industries*, 30:228–235, 2014.

[36] R. A. Ogle. *Dust Explosion Dynamics*. Elsevier Inc., Cambridge, MA, 2017.

[37] Wikipedia, FlashFire. [Online]. Available:https://en.wikipedia.org/wiki/Flash_fire. [Accessed: 10-Jun-2018].

[38] T. A. Kletz and P. R. Amyotte. *Process plants: A handbook for inherently safer design.* CRC Press., 2nd ed. Boca Raton, FL, 2010.

[39] Wikipedia, Niacin. [Online]. Available: https://en.wikipedia.org/wiki/Niacin. [Accessed: 08-Jun-2018].

[40] E. K. Addai, D. Gabel, and U. Krause. Experimental investigation on the minimum ignition temperature of hybrid mixtures of dusts and gases or solvents. *Journal of Hazardous Materials*, 301:314-326, 2016.

[41] Wikipedia, Ultra-high-molecular weight_polyethylene. [Online]. Available: https://en.wikipedia.org/wiki/Ultra-high-molecular-weight_polyethylene. [Accessed: 08-Jun-2018].

[42] ASTM D4464. *Standard Test Method for Particle Size Distribution of Catalytic Materials by Laser Light Scattering*. ASTM International, West Conshohocken, PA, United States, 2015.

[43] ASTM E1515-07. *Standard test method for minimum explosible concentration of combustible dusts*. ASTM International, West Conshohocken, PA, United States, 2018.

[44] ASTM E2019-03. *Standard test method for minimum ignition energy of a dust cloud in air*. ASTM International, West Conshohocken, PA, United States, 2018.

[45] ASTM E1491-06. *Standard test method for minimum autoignition temperature of dust clouds*. ASTM International, West Conshohocken, PA, United States, 2018.

[46] ASTM D3173. *Standard test method for moisture in the analysis sample of coal and coke*. ASTM International, West Conshohocken, PA, United States, 2007.

[47] ASTM D5865 – 13. *Standard Test Method for Gross Calorific Value of Coal and Coke*. ASTM International, West Conshohocken, PA, United States, 2013.

[48] ASTM D6556-16. *Standard Test Method for Carbon Black — Total and External Surface Area by Nitrogen*. West Conshohocken, PA, United States. 2017.

[49] J. E. Going, K. Chatrathi, and K. L. Cashdollar. Flammability limit measurements for dusts in 20-L and 1-m^3 vessels. *Journal of Loss Prevention in the Process Industry*, 13:209–219, 2000.

[50] F. & A. LLC, Blog | Fauske and Associates, LLC | 1 cubic meter chamber.

[51] Cesana-AG, Calibration Round-Robin for the determination of the explosion characteristics of dusts, pages 1–2, 2018. http://www.cesana-ag.ch/Calibration.shtml [Accessed: June 20, 2018].

[52] J. R. Taveau. (2018): Personal communication.

[53] A. Klippel, M. Scheid, and U. Krause. Investigations into the influence of dustiness on dust explosions, *Journal of Loss Prevention in the Process Industries*, 26:1616–1626, 2013.

[54] V. Babrauskas and L. G. Britton. Errors in the compilations of minimum explosible concentration values for dust clouds. *Fire Technology*, 54:37–55, 2018.

[55] U. von Pidoll, The ignition of clouds of sprays, powders and fibers by flames and electric sparks. *Journal of Loss Prevention in the Process Industries*, 14:103–9, 2001.

[56] B. Gan, Wei Gao; Haipeng, Jiang; Yanchao, Q. Zhang, and M. Bi. Flame propagation behaviors and temperature characteristics in polyethylene dust explosions. *Powder Technology*, 328:345–357, 2018.

[57] B. Gan, B. Li, H. Jiang, D. Zhang, M. Bi, and W. Gao. Ethylene / polyethylene hybrid explosions : Part 1: Effects of ethylene concentrations on flame propagations. *Journal of Loss Prevention in the Process Industries*, 54:93–102, 2018.

[58] R. Zevenhoven, M. Karlsson, M. Hupa, and M. Frankenhaeuser. Combustion and Gasification Properties of Plastics Particles. *Journal of Air Waste Managment Association*, 47:861–870, 1997.

[59] NFPA 652. *Standard on the Fundamentals of Combustible Dust*. National Fire Protection Agency, Quincy, MA. 2016.

APPENDIX A: Equipment Calibration Data in Tabular Form

Table A.1: Results of niacin explosion with IE of 10 kJ in the 20-L vessel

Test Series	Concentration (g/m^3)	P_m (bar(g))	$(dP/dt)_m$ (bar/s)	$(dP/dt)_m.V^{1/3}$ (bar·m/s)
1	60	3.3	54	15
1	125	5.4	246	67
1	250	7.3	494	134
1	500	7.7	820	223
1	750	7.4	728	198
1	1000	6.9	652	177
2	250	7.5	739	201
2	500	7.7	910	247
2	750	7.3	710	193
2	1000	6.8	690	187
3	250	7.5	694	188
3	500	7.7	778	211
3	750	7.4	735	200
3	1000	6.9	750	204

Table A.2: Maxima values for each test series with IE of 10 kJ in 20-L vessel

Test Series	Max. P_m of each series (bar(g))	Max. $(^{dP}/_{dt})_m$ of each series (bar/s)
1	7.7	820
2	7.7	910
3	7.7	778

Table A.3: Summary of explosion severity parameters of niacin dust at 10-kJ IE

Test IE (kJ)	Observed Severity Parameters			Reference Values (E1226-13)		
	P_{max} (bar (g))	$(dP/dt)_{max}$ (bar/s)	K_{St} (bar·m/s)	P_{max} (bar(g))	$(dP/dt)_{max}$ (bar/s)	K_{St} (bar·m/s)
10	7.7	836	227	8.2	880	243

Table A.4: MEC of niacin with IE of 2.5 kJ in the 20-L vessel

Test Series	**Concentration (g/m^3)**	**P_m of each series (bar(g))**	**$(^{dP}/_{dt})_m$ of each series (bar/s)**
1	80	2.7	26
1	**70**	**1.9**	22
1	60	0.5	9
2	60	0.4	7
2	50	0.2	6

MEC = 70 g/m^3

Table A.5: Calibration of MIKE-3 apparatus with niacin dust without the application of inductance

Series	**Conc. [mg]**	**I.E [mJ]**	**tv set [ms]**	**tv eff [ms]**	**Ind. [mH]**	**Ign.at (NI)**
1	900	100	120	121	0	1
2	900	30	120	122	0	5
3	900	10	120	121	0	1
4	900	3	120	117	0	1
5	900	1	120	119	0	(10)
6	1200	3	120	117	0	3
7	1200	1	120	120	0	(10)
8	1500	3	120	117	0	9
9	1500	1	120	120	0	(10)
10	600	3	120	117	0	(10)
11	300	3	120	118	0	(10)
12	900	3	90	87	0	(10)
13	1200	3	90	87	0	1
14	1200	1	90	88	0	(10)
15	1500	3	90	87	0	(10)
16	600	3	90	89	0	(10)
17	1800	3	90	87	0	(10)
18	900	3	150	147	0	1
19	900	1	150	148	0	(10)
20	1200	3	150	147	0	3
21	1200	1	150	149	0	(10)
22	1500	3	150	149	0	(10)
23	1800	3	150	147	0	(10)
24	600	3	150	148	0	(10)

Obtained results: 1 mJ < MIE < 3 mJ; Es = 1.7 mJ

Table A.6: Calibration of MIKE-3 apparatus with niacin dust with the application of inductance

Series	Conc. [mg]	I.E [mJ]	tv set [ms]	tv eff [ms]	Ind. [mH]	Ign.at (NI)
1	900	100	120	122	1	1
2	900	30	120	122	1	2
3	900	10	120	121	1	2
4	900	3	120	118	1	8
5	900	1	120	118	1	(10)
6	1200	3	120	119	1	8
7	1200	1	120	118	1	(10)
8	1500	1	120	118	1	(10)
9	1500	3	120	118	1	(10)
10	600	3	120	117	1	1
11	600	1	120	118	1	(10)
12	300	3	120	117	1	(10)
13	300	1	120	117	1	(10)
14	900	3	90	87	1	9
15	900	1	90	88	1	(10)
16	1200	1	90	87	1	(10)
17	1200	3	90	90	1	2
18	600	3	90	87	1	1
19	600	1	90	88	1	(10)
20	300	3	90	87	1	1
21	300	1	90	89	1	(10)
22	1500	3	90	87	1	4
23	1500	1	90	89	1	(10)
24	900	3	150	147	1	1
25	900	1	150	147	1	(10)
26	600	3	150	147	1	1
27	600	1	150	148	1	(10)
28	1200	3	150	147	1	1
29	1200	1	150	147	1	(10)
30	1500	3	150	147	1	2
31	1500	1	150	147	1	(10)
32	300	3	150	147	1	1
33	300	1	150	148	1	(10)

Reference (E2019-03) value = 1 mJ < MIE < 3 mJ

Obtained result: 1 mJ < MIE < 3 mJ; Es = 1.2 mJ

Table A.7: Calibration of the BAM oven with niacin dust

Temperature (°C)	Dust Volume (ml)		
	0.5	**1**	**2**
590	-	Ignition	-
570	-	Ignition	-
550	-	Ignition	-
530	-	Ignition	-
510	-	Ignition	-
490	-	Ignition	-
470	-	Ignition	-
460	-	Ignition	-
450	-	Ignition	-
440	**No Ignition**	**No Ignition**	**Ignition**
430	No Ignition	No Ignition	No Ignition
420	No Ignition	No Ignition	No Ignition

Reference (E1491-06) value = N/A

Table A.8: Results of lycopodium explosion with 10 kJ in the 20-L vessel

Test Series	Concentration (g/m^3)	P_m (bar(g))	$(dP/dt)_m$ (bar/s)	$(dP/dt)_m.V^{1/3}$ (bar·m/s)
1	125	5.2	180	49
1	250	6.8	373	101
1	500	6.9	461	125
1	750	6.2	410	111
2	250	7.0	287	78
2	500	7.2	515	140
2	750	6.2	441	120
3	250	7.1	380	103
3	500	7.0	512	139
3	750	6.3	420	114
3	1000	5.7	426	116

Table A.9: Maxima values for each test series with IE of 10 kJ in 20-L vessel

Test Series	Max. P_m of each series (bar(g))	Max. $(^{dP}/_{dt})_m$ of each series (bar/s)
1	6.9	461
2	7.2	515
3	7.1	512

Table A.10: Summary of explosion severity of lycopodium at 10-kJ IE

Test IE (kJ)	Observed Severity Parameters			Reference Values (E1226-13)		
	P_{max} (bar(g))	$(dP/dt)_{max}$ (bar/s)	K_{St} (bar·m/s)	P_{max} (bar(g))	$(dP/dt)_{max}$ (bar/s)	K_{St} (bar·m/s)
10	7.1	496	135	7.0	555	151

MEC of lycopodium with IE of 2.5 kJ in the 20-L vessel

Test Series	Concentration (g/m^3)	P_m of each series (bar(g))	$(^{dP}/_{dt})_m$ of each series (bar/s)
1	100	4.2	105
1	90	4.1	70
1	80	3.8	102
1	70	3.1	44
1	60	2.8	28
1	50	2.0	22
1	**40**	**1.3**	17
1	30	0.4	7
1	30	0.5	8

Reference (E1515-07) value = 30 g/m^3

MEC = 40 g/m^3

Table A.11: Calibration MIKE-3 apparatus using lycopodium and without the application of inductance

Series	Conc. [mg]	I.E [mJ]	tv set [ms]	tv eff [ms]	Ind. [mH]	Ign.at (NI)
32	900	30	120	121	0	(10)
33	900	100	120	120	0	1
34	600	100	120	120	0	4
35	600	30	120	121	0	(10)
36	1200	100	120	119	0	1
37	1200	30	120	120	0	(10)
38	900	30	90	90	0	(10)
39	900	100	90	90	0	1
40	600	100	90	91	0	1
41	600	30	90	91	0	(10)
42	1200	30	90	90	0	(10)
43	1500	30	150	150	0	(10)
44	1500	100	150	150	0	1
45	1200	30	150	150	0	(10)
46	300	100	150	150	0	7
47	300	30	150	150	0	(10)
48	600	30	150	150	0	(10)

Observed result: 30 < MIE < 100 mJ; Es = 41 mJ

Table A.12: Calibration of the MIKE-3 apparatus using lycopodium and with the application of inductance

Series	Conc. [mg]	I.E [mJ]	tv set [ms]	tv eff [ms]	Ind. [mH]	Ign.at (NI)
1	900	100	120	119	1	1
2	900	30	120	119	1	1
3	900	10	120	120	1	(10)
4	600	30	120	120	1	1
5	600	10	120	120	1	(10)
6	300	30	120	120	1	1
7	300	10	120	121	1	(10)
8	1200	30	120	119	1	1
9	1200	10	120	121	1	(10)
10	1500	30	120	120	1	2
11	1500	10	120	121	1	(10)
12	900	30	90	90	1	2
13	900	10	90	91	1	(10)
14	600	30	90	91	1	1
15	600	10	90	91	1	(10)
16	1200	30	90	90	1	1
17	1200	10	90	91	1	(10)
18	300	30	90	92	1	1
19	300	10	90	91	1	(10)
20	1500	30	90	90	1	2
21	1500	10	90	91	1	(10)
22	900	30	150	151	1	1
23	900	10	150	151	1	(10)
24	600	30	150	150	1	1
25	600	10	150	150	1	(10)
26	1200	30	150	147	1	1
27	1200	10	150	150	1	(10)
28	1500	30	150	148	1	1
29	1500	10	150	150	1	(10)
30	300	30	150	151	1	1
31	300	10	150	152	1	(10)

Reference (E2019-03) value = 10 mJ < MIE < 30 mJ

Obtained results: 10 mJ < MIE < 30 mJ; Es = 12 mJ

Table A.13: Calibration of the BAM oven with lycopodium dust

Temperature (°C)	**Dust Volume (ml)**		
	0.5	**1**	**2**
590	-	Ignition	-
570	-	Ignition	-
550	-	Ignition	-
530	-	Ignition	-
510	-	Ignition	-
490	-	Ignition	-
470	-	Ignition	-
450	No Ignition	No Ignition	Ignition
430	No Ignition	No Ignition	Ignition
420	**No Ignition**	**No Ignition**	**Ignition**
410	No Ignition	No Ignition	No Ignition
400	No Ignition	No Ignition	No Ignition

Reference (E1491-06) value = 410 °C

MIT = 420 °C

Table A.14: Results of Pittsburgh coal explosion with IE of 10 kJ in the 20-L vessel

Test Series	**Concentration (g/m^3)**	**P_m (bar(g))**	**$(dP/dt)_m$ (bar/s)**	**$(dP/dt)_m.V^{1/3}$ (bar·m/s)**
1	60	2.8	30	8
1	125	5.9	112	30
1	250	7.0	247	67
1	500	7.4	411	112
1	750	6.8	384	104
1	1000	6.3	297	81
2	250	7.6	332	90
2	500	7.3	464	126
2	750	6.8	371	101
3	250	7.6	246	67
3	500	7.6	454	123
3	750	7.0	283	77

Table A.15: Maxima values for each test series with IE of 10 kJ in 20-L vessel

Test Series	**Max. P_m of each series (bar(g))**	**Max. $(^{dP}/_{dt})_m$ of each series (bar/s)**
1	7.4	411
2	7.6	464
3	7.6	454

Table A.16: Summary of explosion severity of Pittsburgh coal with IE of 10 kJ

Test IE (kJ)	**Observed Severity Parameters**			**Reference Values (E1226-13)**		
	P_{max} (bar(g))	**$(dP/dt)_{max}$ (bar/s)**	**K_{St} (bar·m/s)**	**P_{max} (bar(g))**	**$(dP/dt)_{max}$ (bar/s)**	**K_{St} (bar·m/s)**
10	7.5	443	120	7.0	431	117

Table A.17: MEC of Pittsburgh coal dust with 2.5-kJ IE

Test Series	**Concentration (g/m^3)**	**P_m of each series (bar(g))**	**$(^{dP}/_{dt})_m$ of each series (bar/s)**
1	90	4.1	46
1	80	2.0	27
1	**70**	**1.9**	20
1	60	0.2	6
2	60	0.5	8

MEC = 70 g/m^3

Table A.18: Calibration of the MIKE-3 apparatus using Pittsburgh coal and without the application of inductance

Series	Conc. [mg]	I.E [mJ]	tv set [ms]	tv eff [ms]	Ind. [mH]	Ign.at (NI)
1	900	300	120	122	0	(10)
2	900	1000	120	122	0	2
3	1200	1000	120	122	0	3
4	1200	300	120	122	0	(10)
5	1500	1000	120	122	0	2
6	1500	300	120	122	0	7
7	1500	100	120	122	0	(10)
8	1800	300	120	122	0	(10)
9	2400	300	120	122	0	(10)
10	900	300	90	92	0	(10)
11	900	1000	90	93	0	2
12	1500	300	90	92	0	(10)
13	1200	300	150	152	0	(10)
14	1800	300	150	152	0	(10)
15	2400	300	150	152	0	(10)
16	2400	1000	150	152	0	4
17	1500	300	150	152	0	(10)

Obtained result: 100 mJ < MIE < 300 mJ; Es = 240 mJ

Table A.19: Calibration of the MIKE-3 apparatus using Pittsburgh coal and with the application of inductance

Series	Conc. [mg]	I.E [mJ]	tv set [ms]	tv eff [ms]	Ind. [mH]	Ign.at (NI)
1	900	100	120	120	1	(10)
2	900	300	120	121	1	6
3	1200	300	120	122	1	3
4	1200	100	120	122	1	7
5	1200	30	120	122	1	(10)
6	1500	100	120	122	1	5
7	1500	30	120	122	1	(10)
8	1800	100	120	122	1	9
9	1800	30	120	123	1	(10)
10	2400	100	120	121	1	(10)
11	900	300	90	92	1	(10)
12	1200	300	90	92	1	3
13	1200	100	90	92	1	8
14	1200	30	90	92	1	(10)
15	1500	100	90	92	1	2
16	1500	30	90	92	1	(10)
17	1800	100	90	92	1	(10)
18	2400	100	90	92	1	(10)
19	900	300	150	152	1	8
20	900	100	150	152	1	2
21	900	30	150	152	1	(10)
22	1200	100	150	152	1	(10)
23	1500	100	150	152	1	6
24	1500	30	150	152	1	(10)
25	1800	100	150	152	1	(10)
26	2400	100	150	152	1	(10)
27	600	100	90	92	1	(10)

Obtained result: 30 mJ < MIE < 100 mJ; Es = 55

Table A.20: Calibration MIT of Pittsburgh coal in the BAM oven

Temperature (ºC)	**Dust Volume (ml)**		
	0.5	**1**	**2**
590	**-**	Ignition	**-**
580	**-**	Ignition	**-**
570	**-**	Ignition	**-**
560	**-**	**Ignition**	**-**
550	No ignition	No ignition	No ignition
540	No ignition	No ignition	No ignition
530	No ignition	**-**	No ignition

MIT = 560 ºC

APPENDIX B: Experimental data for P_{max} and K_{St} in the 20-L vessel with 10-, 5- and 2.5-kJ ignition energies

Table B.1: Results of niacin explosion with IE of 10-kJ ignition energy in the 20-L vessel

Test Series	Concentration (g/m^3)	P_m (bar(g))	$(dP/dt)_m$ (bar/s)	$(dP/dt)_m.V^{1/3}$ (bar·m/s)
1	60	3.3	54	15
1	125	5.4	246	67
1	250	7.3	494	134
1	500	7.7	820	223
1	750	7.4	728	198
1	1000	6.9	652	177
2	250	7.5	739	201
2	500	7.7	910	247
2	750	7.3	710	193
2	1000	6.8	690	187
3	250	7.5	694	188
3	500	7.7	778	211
3	750	7.4	735	200
3	1000	6.9	750	204

Table B.2: Maxima values for each test series with IE of 10 kJ in the 20-L vessel

Test Series	Max. P_m of each series (bar(g))	Max. $(^{dP}/_{dt})_m$ of each series (bar/s)
1	7.7	820
2	7.7	910
3	7.7	778

Table B.3: Results of niacin explosion with IE of 5-kJ in the 20-L vessel

Test Series	**Concentration (g/m^3)**	**P_m (bar(g))**	**$(dP/dt)_m$ (bar/s)**	**$(dP/dt)_m.V^{1/3}$ (bar·m/s)**
1	60	2.7	40	11
1	125	5.4	334	91
1	250	7.4	853	232
1	500	7.5	777	211
1	750	6.8	777	211
1	1000	6.7	801	217
2	125	5.4	319	87
2	250	7.2	793	215
2	500	7.4	858	233
2	750	6.8	819	222
3	125	5.4	325	88
3	250	7.5	860	233
3	500	7.5	836	227
3	750	6.9	792	215

Table B.4: Maxima values for each test series with IE of 10 kJ in the 20-L vessel

Test Series	**Max. P_m of each series (bar(g))**	**Max. $(^{dP}/_{dt})_m$ of each series (bar/s)**
1	7.5	853
2	7.4	858
3	7.5	860

Table B.5: Results of niacin explosion with IE of 2.5 kJ in the 20-L vessel

Test Series	Concentration (g/m^3)	P_m (bar(g))	$(dP/dt)_m$ (bar/s)	$(dP/dt)_m.V^{1/3}$ (bar·m/s)
1	60	1.5	20	5
1	125	5.3	289	78
1	250	7.3	596	162
1	500	7.5	793	215
1	750	6.9	806	219
1	1000	6.2	590	160
2	125	5.8	320	87
2	250	7.2	522	142
2	500	7.3	712	193
2	750	6.8	735	200
2	1000	6.2	578	157
3	125	5.9	383	104
3	250	7.1	662	180
3	500	7.3	788	214
3	750	6.6	696	189

Table B.6: Maxima values for each test series with IE of 10 kJ in 20-L vessel

Test Series	Max. P_m of each series (bar(g))	Max. $(^{dP}/_{dt})_m$ of each series (bar/s)
1	7.5	806
2	7.3	735
3	7.3	788

Table B.7: Summary of explosion severity parameters of niacin dust at 10-, 5-, and 2.5-kJ IEs

Test IE (kJ)	Observed Severity Parameters			Reference Values (E1226-13)		
	P_{max} (bar(g))	$(dP/dt)_{max}$ (bar/s)	K_{St} (bar·m/s)	P_{max} (bar(g))	$(dP/dt)_{max}$ (bar/s)	K_{St} (bar·m/s)
10	7.7	836	227	8.2	880	243
5	7.5	857	233	-	-	-
2.5	7.4	776	221	-	-	-

Table B.8: Results of lycopodium explosion with IE of 10 kJ in 20-L vessel

Test Series	Concentration (g/m^3)	P_m (bar(g))	$(dP/dt)_m$ (bar/s)	$(dP/dt)_m.V^{1/3}$ (bar·m/s)
1	125	5.2	180	49
1	250	6.8	373	101
1	500	6.9	461	125
1	750	6.2	410	111
2	250	7.0	287	78
2	500	7.2	515	140
2	750	6.2	441	120
3	250	7.1	380	103
3	500	7.0	512	139
3	750	6.3	420	114
3	1000	5.7	426	116

Table B.9: Maxima values for each test series with IE of 10 kJ in 20-L vessel

Test Series	Max. P_m of each series (bar(g))	Max. $(^{dP}/_{dt})_m$ of each series (bar/s)
1	6.9	461
2	7.2	515
3	7.1	512

Table B.10: Results of lycopodium explosion with IE of 5 kJ in 20-L vessel

Test Series	Concentration (g/m^3)	P_m (bar(g))	$(dP/dt)_m$ (bar/s)	$(dP/dt)_m.V^{1/3}$ (bar·m/s)
1	125	4.8	160	43
1	250	5.9	269	73
1	500	6.5	440	119
1	750	6.2	496	135
1	1000	5.4	385	105
2	250	6.5	411	112
2	500	6.8	456	124
2	750	6.1	470	128
2	1000	5.4	383	104
3	250	6.9	449	122
3	500	6.7	536	145
3	750	6.2	376	102
3	125	5.8	179	49

Table B.11: Maxima values for each test series with IE of 5 kJ in 20-L vessel

Test Series	**Max. P_m of each series (bar(g))**	**Max. $(^{dP}/_{dt})_m$ of each series (bar/s)**
1	6.5	496
2	6.8	470
3	6.9	536

Table B.12: Results of lycopodium explosion with IE of 2.5 kJ in 20-L vessel

Test Series	**Concentration (g/m^3)**	**P_m (bar(g))**	**$(dP/dt)_m$ (bar/s)**	**$(dP/dt)_m.V^{1/3}$ (bar·m/s)**
1	60	3.3	50	14
1	125	5.0	165	45
1	250	6.9	377	102
1	500	6.5	529	144
1	750	5.6	369	100
2	125	6.1	252	68
2	250	6.7	343	93
2	500	6.6	530	144
2	750	5.9	443	120
2	125	5.4	233	63
3	250	6.5	395	107
3	500	6.6	529	144
3	750	6.0	410	111

Table B.13: Maxima values for each test series with IE of 2.5 kJ in 20-L vessel

Test Series	**Max. P_m of each series (bar(g))**	**Max. $(^{dP}/_{dt})_m$ of each series (bar/s)**
1	6.9	529
2	6.7	530
3	6.6	529

Table B.14: Summary of explosion severity parameters of lycopodium at 10-, 5- and 2.5-kJ IE's

Test IE (kJ)	Observed Severity Parameters			Reference Values (E1226-13)		
	P_{max} (bar(g))	$(dP/dt)_{max}$ (bar/s)	K_{St} (bar·m/s)	P_{max} (bar(g))	$(dP/dt)_{max}$ (bar/s)	K_{St} (bar·m/s)
10	7.1	496	135	7.0	555	151
5	6.7	501	136	-	-	-
2.5	6.8	529	144	-	-	-

Table B.15: Results of fine polyethylene dust explosion with IE of 10 kJ in the 20-L vessel

Test Series	Concentration (g/m^3)	P_m (bar(g))	$(dP/dt)_m$ (bar/s)	$(dP/dt)_m.V^{1/3}$ (bar·m/s)
1	125	5.4	96	26
1	250	6.7	223	61
1	500	6.7	312	85
1	750	5.4	260	71
2	125	6.3	178	48
2	250	7.0	230	62
2	500	6.6	265	72
2	750	5.5	259	70
3	250	7.1	281	76
3	500	6.6	329	89
3	750	5.6	285	77
3	1000	4.6	63	17

Table B.16: Maxima values for each test series with IE of 10 kJ in 20-L vessel

Test Series	Max. P_m of each series (bar(g))	Max. $(^{dP}/_{dt})_m$ of each series (bar/s)
1	6.7	312
2	7.0	265
3	7.1	329

Table B.17: Results of fine PE dust explosion with IE of 5 kJ in the 20-L vessel

Test Series	Concentration (g/m^3)	P_m (bar(g))	$(dP/dt)_m$ (bar/s)	$(dP/dt)_m.V^{1/3}$ (bar·m/s)
1	125	4.6	66	18
1	250	6.5	200	54
1	500	6.5	281	76
1	750	5.3	270	73
2	250	6.6	231	63
2	500	6.8	338	92
2	750	5.7	289	78
2	125	6.1	191	52
3	250	6.5	214	58
3	500	6.5	323	88
3	750	5.4	271	74
3	1000	5.0	237	64

Table B.18: Maxima values for each test series with IE of 5 kJ in 20-L vessel

Test Series	Max. P_m of each series (bar(g))	Max. $(^{dP}/_{dt})_m$ of each series (bar/s)
1	6.5	281
2	6.8	338
3	6.5	323

Table B.19: Results of fine polyethylene dust explosion with 2.5-kJ IE in the 20-L vessel

Test Series	Concentration (g/m^3)	P_m (bar(g))	$(dP/dt)_m$ (bar/s)	$(dP/dt)_m.V^{1/3}$ (bar·m/s)
1	125	4.5	57	15
1	250	6.6	172	47
1	500	6.6	321	87
1	750	5.5	311	84
2	250	6.8	272	74
2	500	6.6	262	71
2	750	5.3	269	73
2	125	6.4	214	58
3	250	6.2	218	59
3	500	6.6	286	78
3	750	5.6	284	77

Table B.20: Maxima values for each test series with IE of 2.5 kJ in 20-L vessel

Test Series	**Max. P_m of each series (bar(g))**	**Max. $(^{dP}/_{dt})_m$ of each series (bar/s)**
1	6.6	321
2	6.8	272
3	6.6	286

Table B.21: Summary of explosion severity parameters of fine polyethylene at 10-, 5- and 2.5-kJ ignition energies

Test (IE) (kJ)	**Explosion Severity Parameters**		
	P_{max} (bar(g))	**$(dP/dt)_{max}$ (bar/s)**	**K_{St} (bar·m/s)**
10	7.0	302	82
5	6.6	314	85
2.5	6.7	293	80

Table B.22: Results of coarse polyethylene dust explosion with IE of 10 kJ in the 20-L vessel

Test Series	**Concentration (g/m^3)**	**P_m (bar(g))**	**$(dP/dt)_m$ (bar/s)**	**$(dP/dt)_m.V^{1/3}$ (bar·m/s)**
1	125	5.2	48	13
1	250	5.6	68	18
1	500	5.9	80	22
1	750	5.4	101	27
1	1000	4.2	60	16
2	250	5.4	54	15
2	500	5.7	82	22
2	750	4.8	77	21
3	250	5.5	55	15
3	500	5.7	64	17
3	750	5.4	76	21
3	1000	4.5	69	19

Table B.23: Maxima values for each test series with IE of 10 kJ in 20-L vessel

Test Series	Max. P_m of each series (bar(g))	Max. $(^{dP}/_{dt})_m$ of each series (bar/s)
1	5.9	101
2	5.7	82
3	5.7	76

Table B.24: Results of coarse polyethylene dust explosion with 5-kJ IE in the 20-L vessel

Test Series	Concentration (g/m^3)	P_m (bar(g))	$(dP/dt)_m$ (bar/s)	$(dP/dt)_m.V^{1/3}$ (bar·m/s)
1	125	4.2	30	8
1	250	5.0	41	11
1	500	5.4	62	17
1	750	5.2	92	25
1	1000	4.3	54	15
2	250	5.5	56	15
2	500	5.8	101	27
2	750	5.3	68	18
3	250	5.1	38	10
3	500	5.9	102	28
3	750	5.4	88	24

Table B.25: Maxima values for each test series with IE of 5 kJ in the 20-L vessel

Test Series	Max. P_m of each series (bar(g))	Max. $(^{dP}/_{dt})_m$ of each series (bar/s)
1	5.4	92
2	5.8	101
3	5.9	102

Table B.26: Results of coarse polyethylene dust explosion with 2.5-kJ IE in the 20-L vessel

Test Series	Concentration (g/m^3)	P_m (bar(g))	$(dP/dt)_m$ (bar/s)	$(dP/dt)_m.V^{1/3}$ (bar·m/s)
1	125	1.5	5	1
1	250	3.9	22	6
1	500	5.4	68	18
1	750	5.3	81	22
2	1000	5.0	70	19
2	250	5.1	38	10
2	500	5.6	53	14
2	750	5.4	90	24
2	1000	5.1	83	23
3	250	5.3	56	15
3	500	5.9	70	19
3	750	5.5	80	22
3	1000	4.5	68	18

Table B.27: Maxima values for each test series with IE of 2.5 kJ in the 20-L vessel

Test Series	Max. P_m of each series (bar(g))	Max. $(^{dP}/_{dt})_m$ of each series (bar/s)
1	5.4	81
2	5.6	90
3	5.9	80

Table B.28: Summary of explosion severity parameters of coarse polyethylene at 10-,5- and 2.5-kJ ignition energies in the 20-L vessel

Test IE (kJ)	Explosion Severity Parameters		
	P_{max} (bar(g))	$(dP/dt)_{max}$ (bar/s)	K_{St} (bar·m/s)
10	5.7	86	23
5	5.7	98	27
2.5	5.6	84	23

APPENDIX C: Experimental data for P_{max} and $(^{dP}/_{dt})_m$ in 1-m^3 at ignition delay times of 550 and 600 ms with 10-kJ ignition energy

Table C.1: Results of niacin explosion with 10-kJ ignition energy in the 1-m^3 chamber at 550 ms

Test Series	Concentration (g/m^3)	P_m of each series (bar(g))	$(^{dP}/_{dt})_m$ of each series (bar/s)
1	125	4.8	50
1	250	6.9	126
1	500	8.0	217
1	750	7.5	235
1	1000	6.8	200
1	1250	6.4	181
2	250	7.1	146
2	500	7.9	245
2	750	7.4	257
2	1000	6.8	195
3	250	7.0	126
3	500	7.9	227
3	750	7.4	246
3	1000	7.0	212

Table C.2: Results of niacin explosion with 10-kJ ignition energy in the 1-m^3 chamber at 600 ms

Test Series	Concentration (g/m^3)	P_m of each series (bar(g))	$(^{dP}/_{dt})_m$ of each series (bar/s)
1	125	5.1	48
1	250	7.0	109
1	500	7.8	143
1	750	7.6	184
1	1000	7.0	147

Table C.3: Results of lycopodium explosion with 10-kJ ignition energy in the 1-m^3 chamber at 550 ms

Test Series	**Concentration (g/m^3)**	**P_m of each series (bar(g))**	**$(^{dP}/_{dt})_m$ of each series (bar/s)**
1	125	6.0	97
1	250	7.9	175
1	500	7.3	191
1	750	6.4	156
1	1000	5.6	131
2	125	6.4	100
2	250	7.8	198
2	500	7.3	174
2	750	6.5	165
3	125	6.4	99
3	250	7.9	188
3	500	7.4	223
3	750	6.3	158

Table C.4: Results of lycopodium explosion with 10-kJ ignition energy in the 1-m^3 chamber at 600 ms

Test Series	**Concentration (g/m^3)**	**P_m of each series (bar(g))**	**$(^{dP}/_{dt})_m$ of each series (bar/s)**
1	125	6.2	94
1	250	7.4	150
1	500	7.0	165
1	750	6.0	120

Table C.5: Results of fine polyethylene explosion with 10-kJ ignition energy in the 1-m^3 chamber at 550 ms

Test Series	**Concentration (g/m^3)**	**P_m of each series (bar(g))**	**$(^{dP}/_{dt})_m$ of each series (bar/s)**
1	125	5.9	53
1	250	7.2	93
1	500	6.7	104
1	750	5.6	77
1	1000	5.0	73
2	125	5.8	61
2	250	6.9	86
2	500	6.8	108
2	750	5.8	88
3	125	5.8	54
3	250	7.3	95
3	500	6.7	105
3	750	5.9	95

Table C.6: Results of fine polyethylene explosion with 10-kJ ignition energy in the 1-m^3 chamber at 600 ms

Test Series	**Concentration (g/m^3)**	**P_m of each series (bar(g))**	**$(^{dP}/_{dt})_m$ of each series (bar/s)**
1	125	5.5	45
1	250	7.0	73
1	500	6.9	90
1	750	6.0	95
1	1000	5.5	81
2	125	5.6	41
2	250	7.3	101
2	500	6.6	106
2	750	5.7	89
3	125	6.9	81
3	250	7.7	99
3	500	6.9	101
3	750	5.8	94

Table C.7: Results of coarse polyethylene explosion with 10 kJ IE in the 1-m^3 at 550 ms

Test Series	**Concentration (g/m^3)**	**P_m of each series (bar(g))**	**$(^{dP}/_{dt})_m$ of each test (bar/s)**
1	125	0.03	0
1	250	5.0	21
1	500	6.6	55
1	750	6.8	73
1	1000	6.3	68
1	1250	5.7	50
2	500	6.8	60
2	750	6.6	60
2	1000	6.0	74
2	1250	4.7	41
3	500	6.7	62
3	750	6.5	68
3	1000	5.7	61

Table C.8: Average maxima values of coarse polyethylene in 1-m^3 at 550 ms

Test IE (kJ)	**Explosion Severity Parameters**		
	P_{max} (bar(g))	**$(dP/dt)_{max}$ (bar/s)**	**K_{St} (bar·m/s)**
10	6.8	72	72

Table C.9: Average maxima values of fine polyethylene in 1-m^3 at 550 ms

Test IE (kJ)	**Explosion Severity Parameters**		
	P_{max} (bar(g))	**$(dP/dt)_{max}$ (bar/s)**	**P_{max} (bar(g))**
10	7.1	106	106

Table C.10: Average maxima values of fine polyethylene in 1-m^3 at 600 ms

Test IE (kJ)	**Explosion Severity Parameters**		
	P_{max} (bar(g))	**$(dP/dt)_{max}$ (bar/s)**	**P_{max} (bar(g))**
10	7.3	101	101

APPENDIX D: MEC Data for dust samples in the 20-L vessel using 2.5-kJ IE

Table D.1: MEC of niacin with IE of 2.5 kJ in the 20-L vessel

Test Series	Concentration (g/m^3)	P_m of each series (bar(g))	$(^{dP}/_{dt})_m$ of each series (bar/s)
1	80	2.7	26
1	**70**	**1.9**	22
1	60	0.5	9
2	60	0.4	7
2	50	0.2	6

MEC = 70 g/m^3

Table D.2: MEC of lycopodium with IE of 2.5 kJ in the 20-L vessel

Test Series	Concentration (g/m^3)	P_m of each series (bar(g))	$(^{dP}/_{dt})_m$ of each series (bar/s)
1	100	4.2	105
1	90	4.1	70
1	80	3.8	102
1	70	3.1	44
1	60	2.8	28
1	50	2.0	22
1	**40**	**1.3**	17
1	30	0.4	7
1	30	0.5	8

MEC = 40 g/m^3 Reference (E1515-07) value = 30 g/m^3

Table D.3: MEC of fine polyethylene with IE of 2.5 kJ in the 20-L vessel

Test Series	Concentration (g/m^3)	P_m of each series (bar(g))	$(^{dP}/_{dt})_m$ of each series (bar/s)
1	100	4.3	81
1	90	4.3	60
1	80	4.0	47
1	70	3.2	22
1	60	2.8	22
1	50	1.9	14
1	**40**	**1.3**	12
2	30	0.9	8
2	30	0.4	7

MEC = 40 g/m^3

Table D.4: MEC of coarse polyethylene with IE of 2.5 kJ in the 20-L vessel

Test Series	**Concentration (g/m^3)**	**P_m of each series (bar(g))**	**$(^{dP}/_{dt})_m$ of each series (bar/s)**
1	100	3.5	19
1	90	3.3	18
1	80	3.0	20
1	**70**	**1.8**	8
1	60	0.4	3
1	60	0.3	3

MEC = 70 g/m^3

APPENDIX E: MEC results for dust samples in the 1-m^3 chamber with IE of 10 kJ at delay time of 550 ms

Table E.1: MEC of niacin in the 1-m^3 chamber with IE of 10 kJ at 550 ms

Test Series	Concentration (g/m^3)	P_m of each series (bar(g))	$(^{dP}/_{dt})_m$ of each series (bar/s)
1	60	0.9	2.9
1	**60**	**1.6**	5.6
1	50	0.3	3.1
1	50	0.5	2.6
1	50	0.4	3
1	40	0.1	0

MEC = 60 g/m^3

Table E.2: MEC of lycopodium in the 1-m^3 chamber with IE of 10 kJ at 550 ms

Test Series	Concentration (g/m^3)	P_m of each series (bar(g))	$(^{dP}/_{dt})_m$ of each series (bar/s)
1	50	3.0	14
1	**40**	**1.5**	4
1	30	0.2	0.3
2	30	0.1	0
3	30	0.2	0

MEC = 40 g/m^3

Table E.3: MEC of fine polyethylene in the 1-m^3 chamber with IE of 10 kJ at 550 ms

Test Series	Concentration (g/m^3)	P_m of each series (bar(g))	$(^{dP}/_{dt})_m$ of each series (bar/s)
1	50	3.8	21
1	**30**	**1.2**	4
1	25	0.2	0.2
1	25	0.3	0.2
1	25	0.3	0.2
1	20	0.2	0.1

MEC = 30 g/m^3

Table E.4: MEC of coarse polyethylene in the 1-m^3 chamber with IE of 10 kJ at 550 ms

Test Series	**Concentration (g/m^3)**	**P_m of each series (bar(g))**	**$(^{dP}/_{dt})_m$ of each series (bar/s)**
1	125	4.3	17
1	100	2.8	7
1	90	1.5	4
1	**80**	**3.1**	11
1	70	0.3	2.3
2	70	0.03	0
3	70	0.03	0
3	60	0.6	2.0

MEC = 80 g/m^3

APPENDIX F: MIE data for organic and metallic dusts in MIKE-3 apparatus

Table F.1: MIE of niacin dust in the MIKE-3 apparatus without inductance

Series	Conc. [mg]	IE [mJ]	tv set [ms]	tv eff [ms]	Ind. [mH]	Ign.at (NI)
1	900	100	120	121	0	1
2	900	30	120	122	0	5
3	900	10	120	121	0	1
4	900	3	120	117	0	1
5	900	1	120	119	0	(10)
6	1200	3	120	117	0	3
7	1200	1	120	120	0	(10)
8	1500	3	120	117	0	9
9	1500	1	120	120	0	(10)
10	600	3	120	117	0	(10)
11	300	3	120	118	0	(10)
12	900	3	90	87	0	(10)
13	1200	3	90	87	0	1
14	1200	1	90	88	0	(10)
15	1500	3	90	87	0	(10)
16	600	3	90	89	0	(10)
17	1800	3	90	87	0	(10)
18	900	3	150	147	0	1
19	900	1	150	148	0	(10)
20	1200	3	150	147	0	3
21	1200	1	150	149	0	(10)
22	1500	3	150	149	0	(10)
23	1800	3	150	147	0	(10)
24	600	3	150	148	0	(10)

Obtained results: 1 mJ < MIE < 3 mJ; Es = 1.7 mJ

Table F.2: MIE of niacin dust in the MIKE-3 apparatus with inductance

Series	Conc. [mg]	IE [mJ]	tv set [ms]	tv eff [ms]	Ind. [mH]	Ign.at (NI)
1	900	100	120	122	1	1
2	900	30	120	122	1	2
3	900	10	120	121	1	2
4	900	3	120	118	1	8
5	900	1	120	118	1	(10)
6	1200	3	120	119	1	8
7	1200	1	120	118	1	(10)
8	1500	1	120	118	1	(10)
9	1500	3	120	118	1	(10)
10	600	3	120	117	1	1
11	600	1	120	118	1	(10)
12	300	3	120	117	1	(10)
13	300	1	120	117	1	(10)
14	900	3	90	87	1	9
15	900	1	90	88	1	(10)
16	1200	1	90	87	1	(10)
17	1200	3	90	90	1	2
18	600	3	90	87	1	1
19	600	1	90	88	1	(10)
20	300	3	90	87	1	1
21	300	1	90	89	1	(10)
22	1500	3	90	87	1	4
23	1500	1	90	89	1	(10)
24	900	3	150	147	1	1
25	900	1	150	147	1	(10)
26	600	3	150	147	1	1
27	600	1	150	148	1	(10)
28	1200	3	150	147	1	1
29	1200	1	150	147	1	(10)
30	1500	3	150	147	1	2
31	1500	1	150	147	1	(10)
32	300	3	150	147	1	1
33	300	1	150	148	1	(10)

Reference (E2019-03) value = 1 mJ < MIE < 3 mJ

Obtained result: 1 mJ < MIE < 3 mJ; Es = 1.2 mJ

Table F.3: MIE of lycopodium in the MIKE-3 apparatus without inductance

Series	Conc. [mg]	IE [mJ]	tv set [ms]	tv eff [ms]	Ind. [mH]	Ign.at (NI)
32	900	30	120	121	0	(10)
33	900	100	120	120	0	1
34	600	100	120	120	0	4
35	600	30	120	121	0	(10)
36	1200	100	120	119	0	1
37	1200	30	120	120	0	(10)
38	900	30	90	90	0	(10)
39	900	100	90	90	0	1
40	600	100	90	91	0	1
41	600	30	90	91	0	(10)
42	1200	30	90	90	0	(10)
43	1500	30	150	150	0	(10)
44	1500	100	150	150	0	1
45	1200	30	150	150	0	(10)
46	300	100	150	150	0	7
47	300	30	150	150	0	(10)
48	600	30	150	150	0	(10)

Obtained result: 30 < MIE < 100 mJ; Es = 41 mJ

Table F.4: MIE of lycopodium using MIKE-3 apparatus with inductance

Series	Conc. [mg]	IE [mJ]	tv set [ms]	tv eff [ms]	Ind. [mH]	Ign.at (NI)
1	900	100	120	119	1	1
2	900	30	120	119	1	1
3	900	10	120	120	1	(10)
4	600	30	120	120	1	1
5	600	10	120	120	1	(10)
6	300	30	120	120	1	1
7	300	10	120	121	1	(10)
8	1200	30	120	119	1	1
9	1200	10	120	121	1	(10)
10	1500	30	120	120	1	2
11	1500	10	120	121	1	(10)
12	900	30	90	90	1	2
13	900	10	90	91	1	(10)
14	600	30	90	91	1	1
15	600	10	90	91	1	(10)
16	1200	30	90	90	1	1
17	1200	10	90	91	1	(10)
18	300	30	90	92	1	1
19	300	10	90	91	1	(10)
20	1500	30	90	90	1	2
21	1500	10	90	91	1	(10)
22	900	30	150	151	1	1
23	900	10	150	151	1	(10)
24	600	30	150	150	1	1
25	600	10	150	150	1	(10)
26	1200	30	150	147	1	1
27	1200	10	150	150	1	(10)
28	1500	30	150	148	1	1
29	1500	10	150	150	1	(10)
30	300	30	150	151	1	1
31	300	10	150	152	1	(10)

Reference (E2019-03) value = 10 mJ < MIE < 30 mJ

Obtained results: 10 mJ < MIE < 30 mJ; E_s = 12 mJ

Table F.5: MIE of fine PE dust using MIKE-3 apparatus without inductance

Series	Conc. [mg]	IE [mJ]	tv set [ms]	tv eff [ms]	Ind. [mH]	Ign.at (NI)
36	900	100	120	122	0	(10)
37	900	300	120	122	0	(10)
38	900	1000	120	122	0	1
39	1200	300	120	122	0	10
40	1200	100	120	122	0	(10)
41	1500	300	120	122	0	4
42	1500	100	120	122	0	(10)
43	1800	300	120	122	0	(10)
44	2400	300	120	123	0	1
45	2400	100	120	122	0	(10)
46	3000	300	120	122	0	8
47	3000	100	120	122	0	(10)
48	1200	300	150	152	0	1
49	1200	100	150	152	0	(10)
50	1800	300	150	152	0	(10)
51	3000	300	150	152	0	10
52	3000	100	150	152	0	2
53	3000	30	150	152	0	(10)
54	3600	100	150	152	0	(10)
55	2400	100	150	152	0	(10)
56	2400	100	90	92	0	(10)
57	3000	100	90	92	0	(10)
58	3600	100	90	92	0	(10)
59	3600	100	120	122	0	(10)

Obtained result = 30 mJ < MIE < 100 mJ; E_s = 79 mJ

Table F.6: MIE of fine PE dust using MIKE-3 apparatus with inductance

Series	Conc. [mg]	IE [mJ]	tv set [ms]	tv eff [ms]	Ind. [mH]	Ign.at (NI)
1	900	100	120	121	1	1
2	900	30	120	121	1	3
3	900	10	120	121	1	(10)
4	600	30	120	122	1	(10)
5	1200	30	120	122	1	7
6	1200	10	120	121	1	(10)
7	1500	30	120	122	1	7
8	1500	10	120	121	1	(10)
9	1800	30	120	122	1	10
10	1800	10	120	121	1	(10)
11	2400	30	120	122	1	10
12	2400	10	120	121	1	(10)
13	3000	30	120	121	1	6
14	3000	10	120	121	1	(10)
15	900	30	150	151	1	5
16	900	10	150	151	1	(10)
17	1200	30	150	152	1	1
18	1200	10	150	151	1	(10)
19	1500	30	150	152	1	2
20	1500	10	150	151	1	(10)
21	600	30	150	152	1	(10)
22	1800	30	150	151	1	1
23	1800	10	150	151	1	(10)
24	3000	30	150	152	1	6
25	3000	10	150	151	1	(10)
26	900	30	90	92	1	7
27	900	10	90	91	1	(10)
28	600	30	90	92	1	8
29	600	10	90	91	1	(10)
30	1200	30	90	92	1	3
31	1200	10	90	92	1	(10)
32	1500	10	90	92	1	(10)
33	2400	30	90	92	1	4
34	2400	10	90	91	1	(10)
35	3000	10	90	91	1	(10)

Obtained result = 10 mJ < MIE < 30 mJ; E_s = 12 mJ

Table F.7: MIE of coarse PE dust using MIKE-3 apparatus without inductance

Series	Conc. [mg]	IE [mJ]	tv set [ms]	tv eff [ms]	Ind. [mH]	Ign.at (NI)
1	1500	1000	120	120	0	(10)
2	1800	1000	120	121	0	(10)
3	2400	1000	120	122	0	(10)
4	3000	1000	120	122	0	(10)
5	3600	1000	150	151	0	(10)
6	1800	1000	150	151	0	(10)
7	2400	1000	150	151	0	(10)
8	3000	1000	90	91	0	(10)
9	1200	1000	90	92	0	(10)
10	2400	1000	90	92	0	(10)

Obtained result = MIE > 1000 mJ

Table F.8: MIE of coarse PE dust in the MIKE-3 apparatus with inductance

Series	Conc. [mg]	IE [mJ]	tv set [ms]	tv eff [ms]	Ind. [mH]	Ign.at (NI)
11	900	1000	120	121	1	(10)
12	1200	1000	120	120	1	(10)
13	1500	1000	120	120	1	(10)
14	1800	1000	120	120	1	9
15	1800	300	120	122	1	(10)
16	2400	1000	120	122	1	(10)
17	3000	1000	120	122	1	(10)
18	3600	1000	120	121	1	(10)
19	1800	1000	150	150	1	(10)
20	2400	1000	150	150	1	(10)
21	1500	1000	150	152	1	(10)
22	1200	1000	150	150	1	(10)
23	3000	1000	150	150	1	6
24	3000	300	150	150	1	(10)
25	3600	1000	150	151	1	(10)
26	1800	1000	90	90	1	(10)
27	2400	1000	90	91	1	(10)
28	3000	1000	90	91	1	(10)
29	1500	1000	90	90	1	(10)
30	1800	300	150	150	1	(10)
31	3000	300	90	90	1	(10)

Obtained result = 300 mJ < MIE < 1000 mJ; E_s = 840 mJ

Table F.9: MIE of Fe-101 dust in the MIKE-3 apparatus without inductance

Series	Conc. [mg]	IE [mJ]	tv set [ms]	tv eff [ms]	Ind. [mH]	Ign.at (NI)
1	900	1000	120	120	0	(10)
2	1200	1000	120	120	0	(10)
3	1500	1000	120	121	0	(10)
4	1800	1000	120	120	0	(10)
5	2400	1000	120	121	0	(10)
6	3000	1000	120	122	0	2
7	3000	300	120	120	0	(10)
8	3600	1000	120	120	0	4
9	3600	300	120	121	0	(10)

Obtained result: 300 mJ < MIE < 1000 mJ; Es = 740 mJ

Table F.10: MIE of Fe-101 dust in the MIKE-3 apparatus with inductance

Series	Conc. [mg]	IE [mJ]	tv set [ms]	tv eff [ms]	Ind. [mH]	Ign.at (NI)
10	900	300	120	120	1	(10)
11	900	1000	120	121	1	8
12	1200	1000	120	121	1	1
13	1200	300	120	120	1	6
14	1200	100	120	120	1	(10)
15	1500	300	120	120	1	6
16	1500	100	120	121	1	(10)
17	1800	300	120	120	1	(10)
18	600	300	120	121	1	(10)
19	2400	300	120	121	1	1
20	2400	100	120	121	1	(10)
21	3000	300	120	121	1	1
22	3000	100	120	120	1	(10)
23	900	300	90	90	1	(10)
24	1200	300	90	90	1	4
25	1200	100	90	90	1	(10)
26	1500	300	90	90	1	1
27	1500	100	90	90	1	(10)
28	1800	300	90	91	1	5
29	1800	100	90	90	1	(10)
30	2400	300	90	91	1	7
31	2400	100	90	91	1	(10)
32	3000	300	90	91	1	7
33	3000	100	90	90	1	(10)
34	900	300	150	150	1	(10)
35	1200	300	150	150	1	(10)
36	1500	300	150	150	1	(10)
37	1800	300	150	151	1	2
38	1800	100	150	151	1	(10)
39	2400	300	150	150	1	4
40	2400	100	150	150	1	(10)
41	3000	300	150	151	1	6
42	3000	100	150	150	1	(10)

Obtained result: 100 mJ < MIE < 300 mJ; Es = 130 mJ

Table F.11: MIE of Fe-102 dust in the MIKE-3 apparatus without inductance

Series	Conc. [mg]	IE [mJ]	tv set [ms]	tv eff [ms]	Ind. [mH]	Ign.at (NI)
1	900	300	120	122	0	(10)
2	1200	300	120	123	0	(10)
3	1200	1000	120	122	0	(10)
4	1500	1000	120	122	0	(10)
5	1800	1000	120	122	0	(10)
6	2400	1000	120	122	0	6
7	2400	300	120	122	0	(10)
8	3000	1000	120	122	0	10
9	3000	300	120	122	0	(10)
10	3600	1000	120	123	0	8
11	3600	300	120	122	0	(10)
12	1500	1000	90	93	0	6
13	1500	300	90	92	0	(10)
14	1800	1000	90	92	0	(10)
15	2400	1000	90	92	0	(10)
16	3000	1000	90	92	0	5
17	3000	300	90	92	0	(10)
18	3600	1000	90	92	0	5
19	3600	300	90	92	0	(10)
20	1200	1000	150	151	0	(10)
21	1500	1000	150	152	0	(10)
22	1800	1000	150	152	0	9
23	1800	300	150	152	0	(10)
24	2400	1000	150	153	0	(10)
25	3000	1000	150	153	0	1
26	3000	300	150	151	0	(10)
27	3600	300	150	152	0	1
28	3600	100	150	152	0	(10)
29	4200	300	150	152	0	(10)

Obtained result: 100 mJ < MIE < 300 mJ; Es = 220 mJ

Table F.12: MIE of Fe-102 dust in the MIKE-3 apparatus with inductance

Series	Conc. [mg]	IE [mJ]	tv set [ms]	tv eff [ms]	Ind. [mH]	Ign.at (NI)
30	900	100	120	121	1	(10)
31	900	300	120	122	1	5
32	1200	100	120	121	1	1
33	1200	30	120	121	1	(10)
34	1500	100	120	121	1	(10)
35	1800	100	120	120	1	(10)
36	2400	100	120	120	1	(10)
37	3000	100	120	121	1	(10)
38	3600	100	120	121	1	1
39	3600	30	120	121	1	(10)
40	900	100	150	151	1	(10)
41	1200	100	150	151	1	(10)
42	1500	100	150	151	1	(10)
43	1800	100	150	151	1	(10)
44	2400	100	150	151	1	5
45	2400	30	150	151	1	(10)
46	3000	100	150	151	1	(10)
47	3600	100	150	151	1	(10)
48	900	100	90	90	1	(10)
49	1200	100	90	91	1	(10)
50	1500	100	90	91	1	6
51	1500	30	90	91	1	(10)
52	1800	100	90	91	1	6
53	1800	30	90	91	1	(10)
54	2400	100	90	91	1	7
55	2400	30	90	91	1	(10)
56	3000	100	90	91	1	(10)
57	3600	100	90	91	1	(10)

Obtained result: 30 mJ < MIE < 100 mJ; Es = 64 mJ

Table F.13: MIE of Fe-103 dust in the MIKE-3 apparatus without inductance

Series	**Conc. [mg]**	**IE [mJ]**	**tv set [ms]**	**tv eff [ms]**	**Ind. [mH]**	**Ign.at (NI)**
1	1500	1000	120	121	0	(10)
2	1800	1000	120	121	0	(10)
3	2400	1000	90	91	0	(10)
4	3000	1000	90	91	0	(10)
5	3000	1000	150	151	0	(10)
6	3600	1000	150	151	0	(10)

Obtained result: MIE > 1000 mJ

Table F.14: MIE of Fe-103 dust in the MIKE-3 apparatus with inductance

Series	Conc. [mg]	IE [mJ]	tv set [ms]	tv eff [ms]	Ind. [mH]	Ign.at (NI)
7	900	1000	120	122	1	(10)
8	1200	1000	120	122	1	(10)
9	1500	1000	120	122	1	(10)
10	1800	1000	120	122	1	(10)
11	2400	1000	120	122	1	(10)
12	3000	1000	120	122	1	(10)
13	3600	1000	120	122	1	(10)
14	1200	1000	90	92	1	(10)
15	1500	1000	90	92	1	(10)
16	3000	1000	90	92	1	(10)
17	1800	1000	150	151	1	(10)
18	2400	1000	150	152	1	(10)
19	3600	1000	150	151	1	(10)

Obtained result: MIE > 1000 mJ

Table F.15: MIE of Al-100 dust in the MIKE-3 apparatus without inductance

Series	Conc. [mg]	IE [mJ]	tv set [ms]	tv eff [ms]	Ind. [mH]	Ign.at (NI)
1	900	10	120	122	0	(10)
2	900	30	120	120	0	2
3	1200	10	120	121	0	(10)
4	1500	10	120	121	0	(10)
5	1800	10	120	122	0	8
6	1800	3	120	117	0	(10)
7	2400	10	120	122	0	(10)
8	900	10	90	92	0	(10)
9	1200	10	90	92	0	(10)
10	1500	10	90	92	0	(10)
11	1800	10	90	91	0	9
12	1800	3	90	87	0	(10)
13	2400	10	90	91	0	(10)
14	900	10	150	150	0	(10)
15	1200	10	150	151	0	(10)
16	1500	10	150	151	0	7
17	1500	3	150	147	0	(10)
18	1800	10	150	151	0	(10)
19	2400	10	150	151	0	(10)

Obtained result: 3 mJ < MIE < 10 mJ; Es = 8 mJ

Table F.16: MIE of Al-100 dust in the MIKE-3 apparatus with inductance

Series	**Conc. [mg]**	**IE [mJ]**	**tv set [ms]**	**tv eff [ms]**	**Ind. [mH]**	**Ign.at (NI)**
20	900	10	120	121	1	2
21	900	1	120	117	1	(10)
22	900	3	120	117	1	(10)
23	1200	3	120	117	1	(10)
24	1500	3	120	117	1	(10)
25	600	3	120	117	1	(10)
26	1800	3	120	117	1	(10)
27	600	3	90	87	1	(10)
28	900	3	90	87	1	(10)
29	1200	3	90	87	1	(10)
30	1500	3	90	87	1	(10)
31	1800	3	90	87	1	(10)
32	600	10	90	92	1	(10)
33	1200	10	90	92	1	1
34	900	10	150	152	1	4
35	900	3	150	147	1	(10)
36	1200	3	150	147	1	(10)
37	1500	3	150	147	1	(10)
38	1800	3	150	147	1	(10)
39	2400	3	150	147	1	(10)

Obtained result: 3 mJ < MIE < 10 mJ; Es = 5 mJ

Table F.17: MIE of Al-101 dust in the MIKE-3 apparatus without inductance

Series	Conc. [mg]	IE [mJ]	tv set [ms]	tv eff [ms]	Ind. [mH]	Ign.at (NI)
1	900	300	120	123	0	(10)
2	1200	300	120	123	0	(10)
3	900	1000	120	123	0	1
4	1500	300	120	122	0	2
5	1500	100	120	122	0	(10)
6	1800	300	120	123	0	(10)
7	2400	300	120	124	0	(10)
8	3000	300	120	124	0	4
9	3000	100	120	124	0	(10)
10	1200	300	90	94	0	(10)
11	1500	300	90	94	0	(10)
12	1800	300	90	94	0	(10)
13	3000	300	90	94	0	1
14	3000	100	90	94	0	(10)
15	1200	300	150	154	0	(10)
16	1500	300	150	153	0	2
17	1500	100	150	154	0	(10)
18	1800	300	150	153	0	(10)
19	2400	300	150	152	0	2
20	2400	100	150	152	0	(10)
21	3000	300	150	153	0	(10)
22	1200	100	150	153	0	(10)
23	1800	100	90	94	0	(10)
24	3600	300	150	153	0	(10)

Obtained result: 100 mJ < MIE < 300 mJ; E_s = 210 mJ

Table F.18: MIE of Al-101 dust in the MIKE-3 apparatus with inductance

Series	Conc. [mg]	IE [mJ]	tv set [ms]	tv eff [ms]	Ind. [mH]	Ign.at (NI)
25	900	100	120	122	1	1
26	900	30	120	122	1	(10)
27	1200	30	120	122	1	(10)
28	1500	30	120	122	1	(10)
29	1800	30	120	122	1	(10)
30	600	30	120	122	1	(10)
31	1200	100	120	122	1	1
32	600	100	120	122	1	1
33	300	100	120	122	1	(10)
34	1500	100	120	122	1	9
35	900	100	150	152	1	(10)
36	1200	100	150	152	1	6
37	1200	30	150	153	1	(10)
38	1500	100	150	152	1	1
39	1500	30	150	153	1	(10)
40	1800	100	150	153	1	1
41	1800	30	150	153	1	(10)
42	600	100	150	153	1	(10)
43	900	100	90	93	1	4
44	900	30	90	93	1	(10)
45	1200	100	90	93	1	2
46	1200	30	90	93	1	(10)
47	600	100	90	93	1	5
48	600	30	90	93	1	(10)
49	1500	100	90	93	1	3
50	1500	30	90	93	1	(10)

Obtained result: 30 mJ < MIE < 100 mJ; Es = 38 mJ

Table F.19: MIE of Al-103 dust in the MIKE-3 apparatus without inductance

Series	Conc. [mg]	IE [mJ]	tv set [ms]	tv eff [ms]	Ind. [mH]	Ign.at (NI)
1	1200	1000	120	120	0	(10)
2	1500	1000	120	121	0	(10)
3	1800	1000	90	90	0	(10)
4	3000	1000	90	90	0	(10)
5	2400	1000	150	150	0	(10)
6	3600	1000	150	151	0	(10)

Obtained result: MIE > 1000 mJ

Table F.20: MIE of Al-103 dust in the MIKE-3 apparatus with inductance

Series	Conc. [mg]	IE [mJ]	tv set [ms]	tv eff [ms]	Ind. [mH]	Ign.at (NI)
7	900	1000	120	120	1	(10)
8	1200	1000	120	121	1	(10)
9	1500	1000	120	121	1	(10)
10	1800	1000	120	120	1	(10)
11	2400	1000	120	121	1	(10)
12	3000	1000	120	121	1	(10)
13	3600	1000	90	91	1	(10)
14	1200	1000	90	91	1	(10)
15	1500	1000	90	90	1	(10)
16	2400	1000	90	91	1	(10)
17	1800	1000	150	151	1	(10)
18	3000	1000	150	151	1	(10)
19	3600	1000	150	152	1	(10)

Obtained result: MIE > 1000 mJ

APPENDIX G: MIT Data for Organic and Metallic Dusts in BAM oven

Table G.1: MIT of niacin dust using BAM oven

Temperature (ºC)	Dust Volume (ml)		
	0.5	**1**	**2**
590	-	Ignition	-
570	-	Ignition	-
550	-	Ignition	-
530	-	Ignition	-
510	-	Ignition	-
490	-	Ignition	-
470	-	Ignition	-
460	-	Ignition	-
450	-	Ignition	-
440	**No Ignition**	**No Ignition**	**Ignition**
430	No Ignition	No Ignition	No Ignition
420	No Ignition	No Ignition	No Ignition

Reference (E1491-06) value = N/A

Obtained result: 440 ºC

Table G.2: MIT of lycopodium using BAM oven

Temperature (ºC)	Dust Volume (ml)		
	0.5	**1**	**0.5**
590	-	Ignition	-
570	-	Ignition	-
550	-	Ignition	-
530	-	Ignition	-
510	-	Ignition	-
490	-	Ignition	-
470	-	Ignition	-
450	No Ignition	No Ignition	Ignition
430	No Ignition	No Ignition	Ignition
420	**No Ignition**	**No Ignition**	**Ignition**
410	No Ignition	No Ignition	No Ignition
400	No Ignition	No Ignition	No Ignition

Reference (E1491-06) value = 410 ºC

Obtained result: 420 ºC

Table G.3: MIT of fine polyethylene dust using BAM oven

Temperature (ºC)	**Dust Volume (ml)**		
	0.5	1	**0.5**
590	-	Ignition	-
570	-	Ignition	-
550	-	Ignition	-
530	-	Ignition	-
510	-	Ignition	-
490	-	Ignition	-
470	-	Ignition	-
450	-	Ignition	-
430	-	Ignition	-
420	-	Ignition	-
410	**No Ignition**	**Ignition**	**No Ignition**
400	No Ignition	No Ignition	No Ignition
390	No Ignition	No Ignition	No Ignition

Obtained result: 410 ºC

Table G.4: MIT of coarse polyethylene dust using BAM oven

Temperature (ºC)	**Dust Volume (ml)**		
	0.5	**1**	**2**
590	-	Ignition	-
570	-	Ignition	-
550	-	Ignition	-
530	-	Ignition	-
510	-	Ignition	-
490	-	Ignition	-
470	-	Ignition	-
450	-	Ignition	-
430	-	Ignition	-
420	**No Ignition**	**No Ignition**	**Ignition**
410	No Ignition	No Ignition	No Ignition
400	No Ignition	No Ignition	No Ignition

Obtained result: 420 ºC

MIT of Metallic Dusts

Table G.5: MIT of Fe-101 dust using BAM oven

Temperature (ºC)	Dust Volume (ml)		
	0.5	**1**	**2**
590	-	Ignition	-
570	-	Ignition	-
550	-	Ignition	-
530	-	Ignition	-
510	-	Ignition	-
490	-	Ignition	-
470	-	Ignition	-
450	-	Ignition	-
430	-	Ignition	-
420	-	Ignition	-
410	-	Ignition	-
400	-	Ignition	-
390	**No Ignition**	**Ignition**	**No Ignition**
380	No Ignition	No Ignition	No Ignition
370	No Ignition	No Ignition	No Ignition

Table G.6: MIT of Fe-102 dust using BAM oven

Temperature (ºC)	Dust Volume (ml)		
	0.5	**1**	**2**
590	-	Ignition	-
570	-	Ignition	-
550	-	Ignition	-
530	-	Ignition	-
510	-	Ignition	-
490	-	Ignition	-
470	-	Ignition	-
450	-	Ignition	-
430	-	Ignition	-
420	**No Ignition**	**No Ignition**	**Ignition**
410	No Ignition	No Ignition	No Ignition
400	No Ignition	No Ignition	No Ignition

Table G.7: MIT of Fe-103 dust using BAM oven

Temperature (ºC)	Dust Volume (ml)		
	0.5	1	2
590	No Ignition	No Ignition	No Ignition
600	No Ignition	No Ignition	No Ignition

Observation: Sparks were seen exiting the flap end of the oven

Table G.8: MIT of Al-100 dust using BAM oven

Temperature (ºC)	Dust Volume (ml)		
	0.5	1	2
590	No Ignition	No Ignition	No Ignition
600	No Ignition	No Ignition	No Ignition

Table G.9: MIT of Al-101 dust using BAM oven

Temperature (ºC)	Dust Volume (ml)		
	0.5	1	2
590	No Ignition	No Ignition	No Ignition
600	No Ignition	No Ignition	No Ignition

Table G.10: MIT of Al-103 dust using BAM oven

Temperature (ºC)	Dust Volume (ml)		
	0.5	1	2
590	No Ignition	No Ignition	No Ignition
600	No Ignition	No Ignition	No Ignition

APPENDIX H: Particle size distribution for organic samples

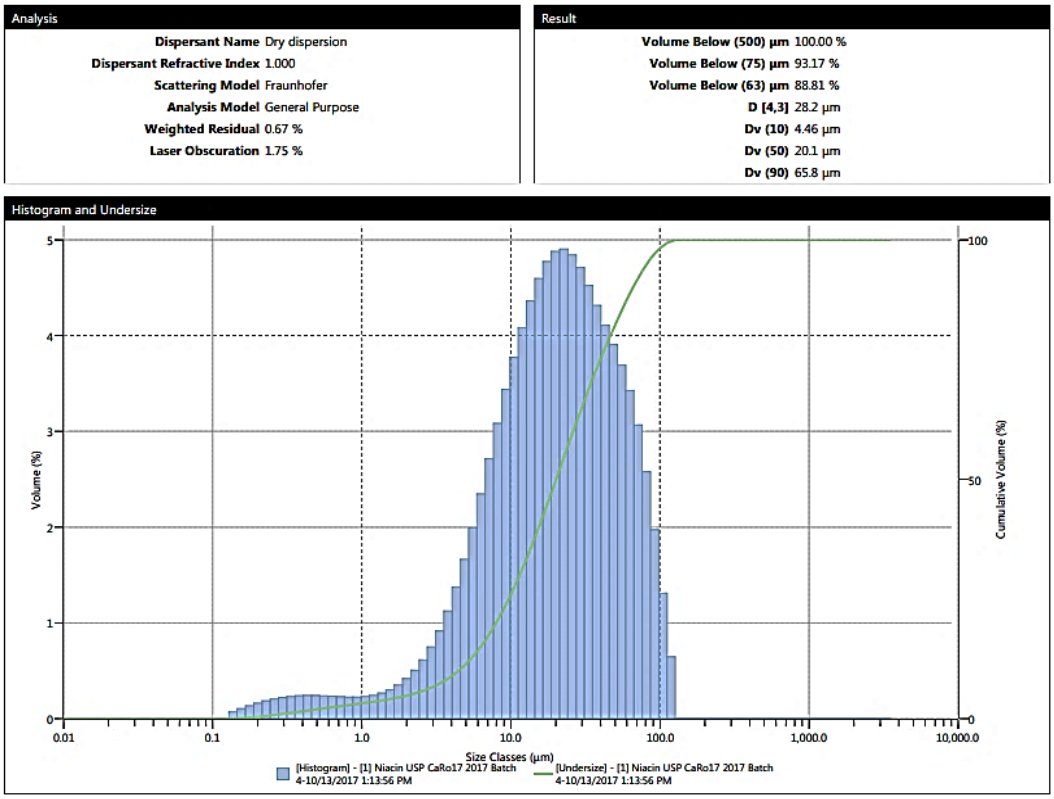

Figure H.1: Particle size distribution of niacin dust

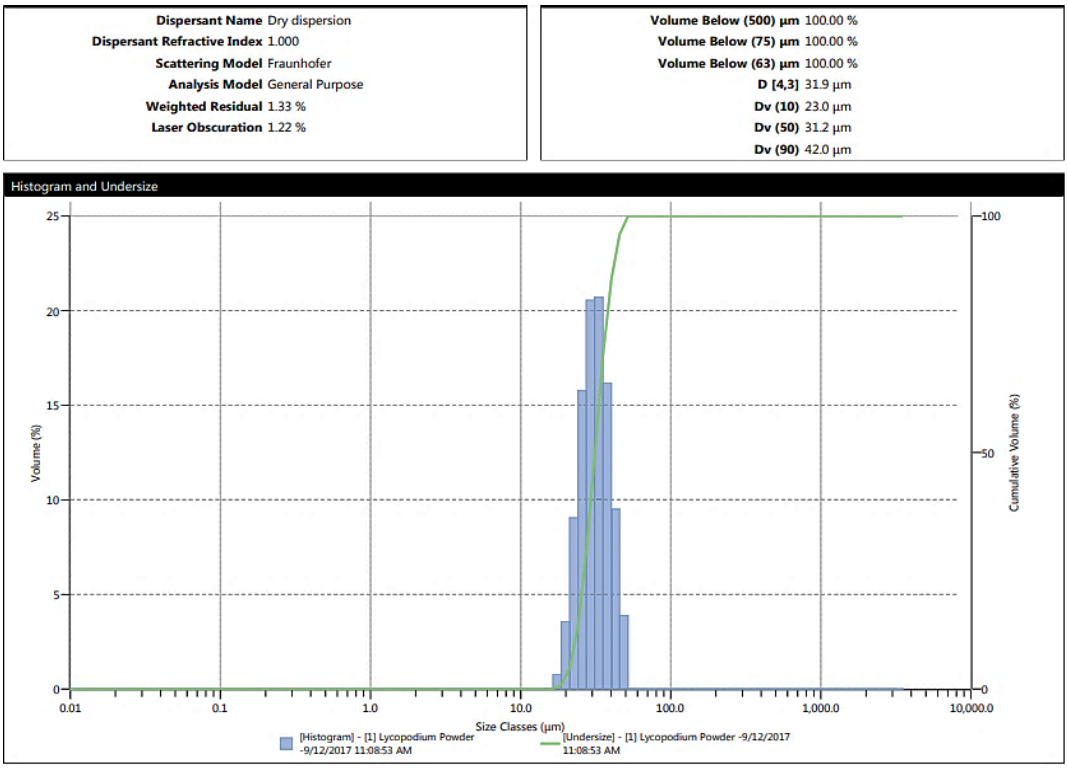

Figure H.2: Particle size distribution of lycopodium dust

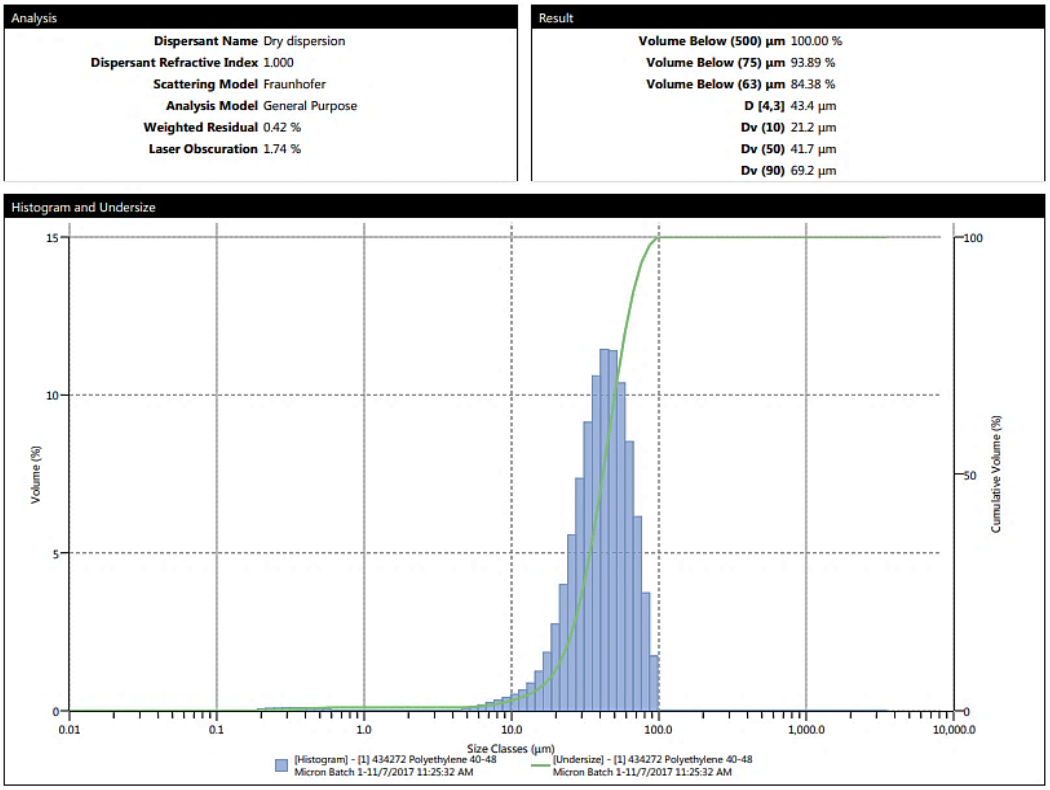

Figure H.3: Particle size distribution of fine polyethylene

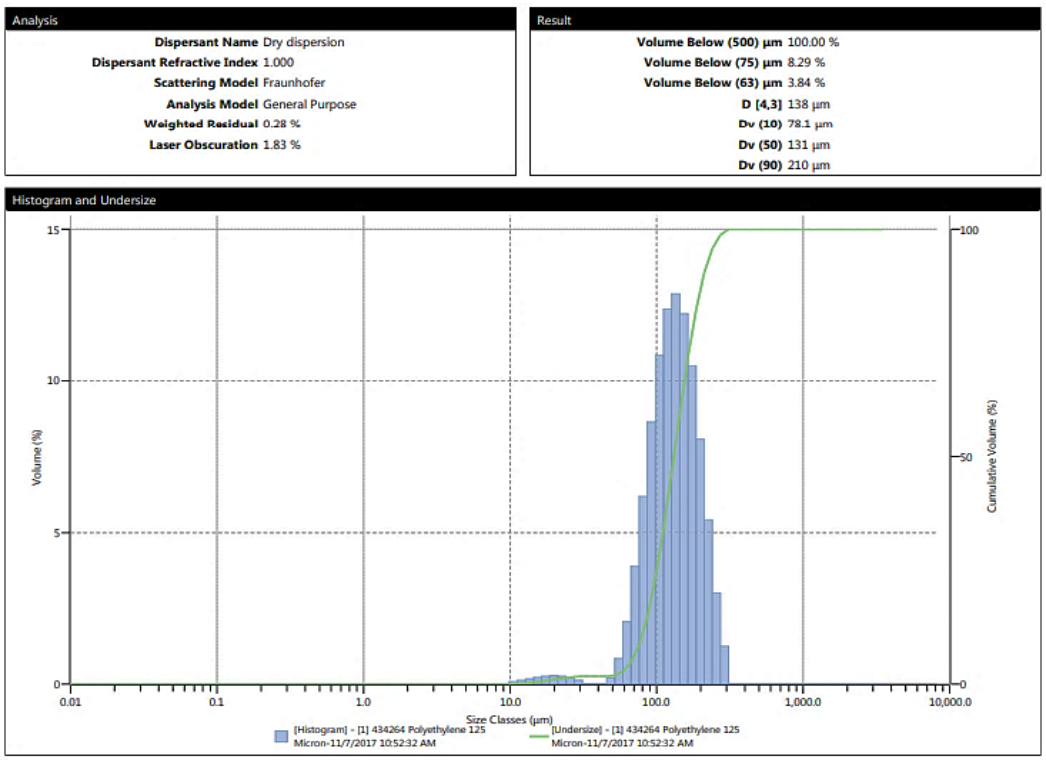

Figure H.4: Particle size distribution of coarse polyethylene